Pharmacological characterization of fish melanocortin-4 and melanocortin-5 receptors

By

Ting Liu

A dissertation submitted to the Graduate Faculty of
Auburn University
in partial fulfillment of the
requirements for the Degree of
Doctor of Philosophy

Auburn, Alabama
August 7, 2021

Keywords: G protein-coupled receptor, Melanocortin-4 receptor, Melanocortin-5 receptor, Energy homeostasis, Fish

Approved by

Ya-Xiong Tao, Chair, Professor of Anatomy, Physiology and Pharmacology
Ramesh B. Jeganathan, Professor of Nutrition
Miranda Reed, Associate Professor of Drug Discovery and Development
Chad Foradori, Associate Professor of Anatomy, Physiology and Pharmacology
Chen-Che Jeff Huang, Assistant Professor of Anatomy, Physiology and Pharmacology

Abstract

The melanocortin-4 receptor (MC4R) plays an important role in the regulation of food intake and energy expenditure. The melanocortin-5 receptor (MC5R) has been implicated in the regulation of exocrine gland secretion, immune regulation, and muscle fatty acid oxidation in mammals. Melanocortin-2 receptor accessory protein 2 (MRAP2) modulates trafficking, ligand binding, and signaling of melanocortin receptors. To explore pharmacological properties of MCRs and their modulation by MRAP2 in teleosts, we conducted experiments on snakehead MC4R/MRAP2 and ricefield eel MC5R/MRAP2.

The Northern snakehead (*Channa argus*) is an economically important freshwater fish native to East Asia. To explore potential interaction between snakehead MC4R and MRAP2, herein we cloned snakehead *mc4r* and *mrap2*. The snakehead *mc4r* consisted of a 984 bp open reading frame encoding a protein of 327 amino acids, while snakehead *mrap2* contained a 693 bp open reading frame encoding a protein of 230 amino acids. Synteny analysis indicated that *mc4r* was highly conserved with similar gene arrangement, while *mrap2* contained two isoforms in teleost with different gene orders. Snakehead *mc4r* was primarily expressed in the brain, whereas *mrap2* was expressed in the brain and intestine. Snakehead *mc4r* and *mrap2* expression was modulated by fasting and refeeding. Further pharmacological experiments showed that the cloned snakehead MC4R was functional, capable of binding to peptide agonists and increasing intracellular cyclic AMP (cAMP) production in a dose-dependent manner. Snakehead MC4R exhibited high constitutive activity. MRAP2 significantly decreased basal and agonist-stimulated cAMP signaling. These findings suggest that snakehead MC4R might be involved in energy balance regulation by interacting with MRAP2. Further studies are needed to

elucidate MC4R in regulating diverse physiological processes in snakehead.

The ricefield eel (*Monopterus albus*) has significant economic and research value. To explore potential interaction between ricefield eel MC5R and MRAP2s (maMC5R, maMRAP2X1, and maMRAP2X2), herein we studied the pharmacological characteristics of maMC5R and its modulation by maMRAP2s. Three agonists, a-melanocyte stimulating hormone (α-MSH), ACTH (1-24), and [Nle^4, D-Phe^7]-α-MSH, could bind to maMC5R and induce intracellular cAMP production dose-dependently. Compared with human MC5R (hMC5R), maMC5R displayed decreased maximal binding but higher binding affinity to α-MSH or ACTH (1-24). When stimulated with α-MSH or ACTH (1-24), maMC5R showed significantly lower EC_{50} and maximal response than hMC5R. Two maMRAP2s had no effect on cell surface expression of maMC5R, whereas they significantly increased maximal binding. Only maMRAP2X2 significantly decreased the binding affinity of ACTH (1-24). Both maMRAP2X1 and maMRAP2X2 significantly reduced maMC5R efficacy but did not affect ligand sensitivity. The availability of maMC5R pharmacological characteristics and modulation by maMRAP2s will assist the investigation of its roles in regulating diverse physiological processes in ricefield eel.

Acknowledgments

I would like to express my deepest appreciation to my mentor, Dr. Ya-Xiong Tao, for his great support, continuous guidance, and inexhaustible patience during my graduate study. Dr. Tao provided me with the opportunity to continue pursuing my PhD degree in his lab when I was faced with a difficulty in September 2017. Without his endless help, I would never finish my dissertation. It is really an honor for both me and my family.

I would like to sincerely appreciate my graduate committee members, Drs. Ramesh Jeganathan, Miranda Reed, Chad Foradori, and Chen-Che Jeff Huang for sharing their advice, expertise, experience, and wisdom throughout the years. I am thankful to my university reader Dr. Muralikrishnan Dhanasekaran for his careful review and valuable suggestions of my dissertation.

I would like to thank my lab colleagues and alumni, Ren-Lei Ji, Chuan-Ling Xu, Drs. Li-Kun Yang, Zhi-Shuai Hou, Min Tao, Qian Wang and Fan Yu, for their valuable contributions to my work. I would like to thank our collaborator, Zheng-Yong Wen, for his contribution in fish sampling, gene cloning and gene expression measurement of Chapter 2. I would like to thank all the faculty, staff members and students in the Department of Anatomy, Physiology and Pharmacology for their kind support. Specifically, I would like to acknowledge China Scholarship Council of the People's Republic of China for the financial support throughout these years.

I am whole-heartedly grateful to my parents for their endless love and encouragement. I owe my deepest gratitude to my husband, Rui Zhang, for his

unconditional love, support, and encouragement all the time.

Table of contents

List of Tables

List of Figures

List of Abbreviations

AC Adenylyl cyclase

ACTH, adrenocorticotropic hormone;

AgRP, Agouti-related peptide;

AMPK, 5'-AMP-activated protein kinase;

ARC, arcuate nucleus;

BSA, Bovine serum albumin;

cAMP, 3’,5’-cyclic adenosine monophosphate;

CNS, central nervous system;

DMH, dorsomedial nucleus of the hypothalamus;

EC_{50}, half maximal effective concentration;

ECL, extracellular loop;

ER, endoplasmic reticulum;

ERK1/2, extracellular signal-regulated kinases 1/2

Fig. S, supplementary figures;

GPCR, G protein-coupled receptor;

HEK 293T, human embryonic kidney 293T;

IC_{50}, half maximal inhibitory concentration;

i.c.v, intracerebroventricular;

ICL, intracellular loop;

IML, intermediolateral nucleus of the spinal cord;

JNK, c-Jun N-terminal kinases;

Kir7.1 channel, inward-rectifier potassium channel;

MCR, melanocortin receptor;

MSH, melanocyte-stimulating hormone;

MRAP, melanocortin-2 receptor accessory protein

NDP-MSH, [Nle^4, $D\text{-}Phe^7$]-α-MSH;

NPY, neuropeptide-Y;

ORF, open reading frame;

PI3K, phosphatidylinositol 3-kinase

PKA/C, protein kinase A/C;

PKB or AKT, protein kinase B;

POMC, proopiomelanocortin;

PVN, paraventricular nucleus;

Table S, supplementary tables;

TMD, transmembrane domain;

WT, wild-type;

Chapter 1: Literature review

1.1. Introduction

The G protein-coupled receptors (GPCRs), which comprise the largest family of membrane proteins, are widely exist in most eukaryotic cells, from yeast (Yun et al., 1997), plants (Josefsson and Rask, 1997), invertebrates (Hill et al., 2002), to vertebrates, including humans (Reviewed in (Tao, 2020)). They consist of seven transmembrane domains (TMDs) connected by the extracellular N-terminus, intracellular C-terminus, and alternating extracellular and intracellular loops (ECLs and ICLs) (Tao, 2008). GPCRs play the significant role in mediating diverse physiological functions since they relay a variety of extracellular signals, including chemical and sensory stimuli, into the interior (Bockaert and Pin, 1999). Mutations in GPCRs can cause diseases (Tao and Conn, 2014). Due to the substantial involvement in human pathophysiology, GPCRs are targeted to develop therapeutic drugs (Hauser et al., 2017).

Melanocortin receptors (MCRs), consisting of five members (MC1R to MC5R), belong to Family A (rhodopsin-like) GPCRs (Cone, 2006; Mountjoy et al., 1992; Tao, 2017). The MCRs are unique since they have both natural agonists, including α-melanocyte stimulating hormone (MSH), β-MSH, γ-MSH and ACTH, and antagonists, including agouti-signaling protein and agouti-related peptide (AGRP) (Ringholm et al., 2002). The agonists are the products of proopiomelanocortin (POMC) through tissue specific post-translational processing, whereas the antagonists are generated from separate precursors (Ringholm et al., 2002). After activation, MC1R mediates effects of MSH on pigmentation (Valverde et al., 1995), MC2R regulates the adrenal steroidogenesis (Mountjoy et al., 1992), MC3R and MC4R play crucial non-redundant

roles in energy homeostasis (Cone, 2006), MC5R is involved in regulating exocrine gland secretion (Chen et al., 1997) (Reviewed in (Cone, 2006; Tao, 2017)).

Of the five MCRs, only MC2R is difficult to reach the cell surface of heterologous cells except for adrenal cell lines (Noon et al., 2002). Several studies have revealed that the melanocortin-2 receptor accessory protein 1 (MRAP1), belongs to MRAP family, is required for cell surface expression and signaling of MC2R (Metherell et al., 2005; Sebag and Hinkle, 2007, 2009b). The second member of MRAP family, MRAP2, can also assist MC2R to reach the cell membrane (Gorrigan et al., 2011; Sebag and Hinkle, 2010). However, the affinity for ACTH of MC2R/MRAP2 complex is very low (Sebag and Hinkle, 2010). Both MRAP1 and MRAP2 are small single transmembrane proteins. In addition to MC2R, they can interact with other four human MCRs (Chan et al., 2009). Recently, several studies showed that MRAPs can interact with GPCRs beyond the MCRs, including orexin receptor 1, ghrelin receptor, and prokineticin receptor 1 (Chaly et al., 2016; Rouault et al., 2017a; Rouault et al., 2017b; Srisai et al., 2017) (Reviewed in (Tao, 2020)).

This chapter provides an overview of the melanocortin system including MC4R and MC5R and ligands. The diverse physiological functions and intracellular signaling pathways of MC4R and MC5R are also discussed. The effects of MRAPs on MC4R and MC5R are also highlighted.

1.2. Melanocortin system

1.2.1. Endogenous ligands

The agonists, including α-MSH, β-MSH, γ-MSH, and ACTH, as well as some less studied peptides such as γ_3-MSH and desacetyl-α-MSH, are all derived from tissue-specific posttranslational processing of POMC which is primarily produced by arcuate nucleus (ARC) in CNS and the anterior pituitary as well as the skin (Bertagna, 1994; Smith and Funder, 1988). The MSHs are produced in CNS (Pritchard et al., 2002). The two antagonists are Agouti and AgRP. Agouti selectively functions as endogenous antagonist of MC1R and MC4R (Fan et al., 1997; Lu et al., 1994), whereas AgRP specifically binds to MC3R and MC4R (Fong et al., 1997; Ollmann et al., 1997). AgRP also serves as an inverse agonist independent of antagonism, suppressing the constitutive (basal) activities of MC3R and MC4R (Haskell-Luevano and Monck, 2001; Nijenhuis et al., 2001; Tao, 2010). Additionally, two ancillary proteins, mahogany and syndecan-3, have been found that modulate the activity of the melanocortin peptides (Gantz and Fong, 2003).

1.2.2. Molecular cloning and tissue distribution of MC4R and MC5R

The human MC4R (hMC4R), independently cloned by groups of Gantz and Cone, is encoded by an intronless gene located at chromosome 18q21.3 and contains 332 amino acids (Gantz et al., 1993; Mountjoy et al., 1994). MC4R is highly expressed in brain, including the cortex, thalamus, hippocampus, hypothalamus, brain stem, and spinal cord areas (Gantz et al., 1993; Mountjoy et al., 1994). In hypothalamus, it is primarily expressed in the paraventricular nucleus (PVN), the supraoptic nucleus, and the nucleus basalis of Meynert (Siljee et al., 2013). MC4R, together with MC3R which is also highly expressed in the central nervous system (CNS), are named neural MCRs. In addition to its neuronal expression, the distribution of *MC4R* transcripts has also been reported in several peripheral tissues such as astrocytes (Caruso et al., 2007; Selkirk et al., 2007) and epidermal melanocytes (Spencer and Schallreuter, 2009). *MC4R* mRNA is also

detected in developing heart, lung, muscle, kidney, and testis during the fetal period (Mountjoy et al., 2003). In non-mammalian species, such as fish, MC4R is also abundantly distributed in brain. In most fish, MC4R expression can also be detected in pituitary gland as well as peripheral tissues, such as gonads, liver, intestine, heart, and kidney (Cerdá-Reverter et al., 2003b; Klovins et al., 2004; Li et al., 2016a; Li et al., 2017a; Rao et al., 2019; Ringholm et al., 2002; Sánchez et al., 2009b; Tao et al., 2020; Yi et al., 2018).

The human MC5R (hMC5R), first cloned by Chhajlani and colleagues, is a protein of 325-amino acids encoded by *MC5R* gene localized at chromosome 18p11.2 (Chhajlani et al., 1993; Chowdhary et al., 1995; Logan et al., 2003). MC5R has been identified in numerous peripheral tissues, including adrenal gland, kidney, lymph node, liver, lung, skeletal muscle, bone marrow, adipocyte, lymphocyte and exocrine glands (Chhajlani, 1996; Millington, 2006; Xu et al., 2020). Among these peripheral organs and tissues, *MC5R* is detected at extremely high levels in exocrine glands, such as lacrimal and harderian glands (Chen et al., 1997). It also has a limited expression in the brain (Gantz and Fong, 2003; Millington, 2006). In non-mammals, the cloning of two zebrafish MC5R orthologues (Ringholm et al., 2002) lay the foundation for a series of reports about the identification of fish MC5R. The piscine MC5Rs display similar tissue distribution as in mammals, in both brain areas and a multitude of peripheral tissues including heart, intestine, gill and many others (Cerdá-Reverter et al., 2003a; Klovins et al., 2004; Liao et al., 2019; Ringholm et al., 2002; Sánchez et al., 2009a).

1.3. Physiological functions of MC4R and MC5R

Following the cloning of MC4R, numerous studies demonstrated the critical

importance of the MC4R in mediating energy homeostasis. In vivo, intracerebroventricular (ICV) administration of α-MSH decreases food intake in rats (Poggioli et al., 1986), while ICV administration of AGRP can increase food intake and block the inhibitory effect of α-MSH (Rossi et al., 1998). Moreover, direct injection of melanotan II (MTII) and SHU9119 into the PVN of rats where MC4R is highly expressed results in extremely potent alterations in food intake, suggesting the PVN neurons to be the primary sites of action in melanocortin-induced feeding behavior regulation (Giraudo et al., 1998) (MTII is a superpotent analogue of α-MSH, and SHU9119 is a high-affinity antagonist of MC3R and MC4R). In addition, gene targeted inactivation of MC4R in mice causes weight gain in a gene-dosage dependent manner since heterozygous knockout mice have intermediate body weight compared with the wild type (WT) and homozygous knockout mice (Huszar et al., 1997). Changes in food intake accounts for 60% of MC4R effects on energy balance, the remaining 40% comes from energy expenditure alterations (Balthasar et al., 2005). The MC4R, expressed in other neurons located in the intermediolateral nucleus of the spinal cord (IML) (Rossi et al., 2011) and dorsomedial nucleus of the hypothalamus (DMH) (Chen et al., 2017), are involved in the energy expenditure (Balthasar et al., 2005; Chen et al., 2017; Rossi et al., 2011). In addition to its role in the regulation of energy homeostasis, MC4R has also been reported to be involved in multiple physiological functions such as glucose and lipid homeostasis, cardiovascular functions, reproductive and sexual behaviors, bone metabolism, and brain inflammation (Reviewed in (Tao, 2010)). The regulation role in energy balance of MC4R is also operational in non-mammalian species, such as fish. ICV injection of agonist, NDP-MSH or MTII, inhibits food intake, whereas the antagonist, HS024 or SHU9119, increases food intake in goldfish and rainbow trout (Cerdá-Reverter et al., 2003b; Cerdá-Reverter et al., 2003c; Schjolden et al., 2009). In transgenic zebrafish, overexpressing of AgRP leads to obesity with increased linear growth and adipocyte hypertrophy (Song and Cone, 2007), similar

to transgenic mice with AgRP overexpression (Reviewed in (Tao, 2010)).

The vital role of MC4R in regulating body weight has obtained increasing attention as mutations of this receptor cause up to 6% of early-onset obesity cases in some ethnic populations (Farooqi et al., 2003). Since the first *MC4R* frameshift mutation was reported (Vaisse et al., 1998; Yeo et al., 1998), a variety of *MC4R* mutations were identified in obese patients. The obese individuals are characterized by hyperphagia, increased linear growth, hyperinsulinemia, bone mineral density and bone mineral content, and final adult height (Branson et al., 2003; Dubern et al., 2007; Farooqi et al., 2003; Farooqi et al., 2000; Iepsen et al., 2020; Martinelli et al., 2011; Vollbach et al., 2017). However, the prevalence of hypertension is significantly lower in *MC4R* mutation carriers than in the control subjects who have normal *MC4R* sequence and similar body mass index (BMI) (Greenfield et al., 2009). Regarding the effects on energy expenditure in *MC4R* variants carriers, the results are controversial. Farooqi and colleagues demonstrated that *MC4R* mutations do not affect energy expenditure (Farooqi et al., 2003), whereas later studies showed that *MC4R* mutations are associated with altered energy expenditure (Cole et al., 2010; Krakoff et al., 2008). Except obesity, one of the *MC4R* mutation I269N is associated with type 2 diabetes (T2DM) in a sex/gender-dependent manner in one Mexican population (Vázquez-Moreno et al., 2020).

Since the extensive expression in numerous organs and tissues, MC5R mediates various physiological functions. The well-known functions of MC5R are regulation of exocrine gland secretion. The *Mc5r* knockout mice exhibit a severe dysfunction of exocrine secretion, resulting in reduced hair lipid content, defects in water repulsion, and impaired thermoregulatory function (Chen, 2000; Chen et al., 1997). This suggests that MC5R is centrally involved in sebogenesis in which sebum-specific lipids are produced,

released, and delivered to the hair and skin surface for protective coating and moisturization (Berg et al., 2006; Eisinger et al., 2011; Møller et al., 2015). Additionally, MC5R was revealed to be involved in the differentiation of murine adipocyte and act as a lipolysis stimulator as well as re-esterification repressor upon α-MSH stimulation (Boston and Cone, 1996; Rodrigues et al., 2013). Also An et al. demonstrated that MC5R plays important role in increasing fatty acid oxidation in skeletal muscles (An et al., 2007). Except for its role in lipid metabolism, MC5R was also shown to be associated with inflammatory response in adipocytes and eyes (Jun et al., 2010; Taylor et al., 2006). MC5R is also suggested to be involved in stress response by mediating protein secretion of lacrimal glands and stimulate tear secretion (Entwistle et al., 1990). In fish, MC5R is also speculated to be involved in the control of hepatic lipid metabolism, body color change, and stress response (Kobayashi et al., 2016; Liao et al., 2019; Sánchez et al., 2009a).

Considering the extensive range of functions, it is easy to understand that dysfunctions in MC5R will lead to various diseases. However, studies revealing correlation between *MC5R* variants and related traits are scarce. Up to now, only several variants (including F209L, A81A, D108D, S125S, T248T, L283L, and variants in PstI, PvuII) of the *MC5R* gene were identified to be related with some traits. They are associated with obesity (Chagnon et al., 1997; Valli-Jaakola et al., 2008), T2DM (Valli-Jaakola et al., 2008), as well as schizophrenia and bipolar disorder (Miller et al., 2009), but without effects on skin condition (acne vulgaris) (Hatta et al., 2001).

1.4. Multiple signaling pathways of MC4R and MC5R

The canonical signaling pathway for the MC4R is by coupling to the heterotrimeric

stimulatory G protein (Gs), then leading to increased cAMP production, and subsequently protein kinase A (PKA) activation. This signaling pathway is known to be required for MC4R to regulate energy balance, glucose metabolism and thermogenesis (Podyma et al., 2018). In addition to Gs, the MC4R can bind to other G proteins, such as Gq protein which activates phospholipase C/protein kinase C (PLC/PKC) to increase intracellular calcium (Newman et al., 2006), and Gi protein which inhibits adenylyl cyclase (AC) activity to decrease cAMP level (Büch et al., 2009). Recently, more and more studies have proved that MC4R is able to couple to Gi and Gq (Büch et al., 2009; Clément et al., 2018; Li et al., 2016b; Metzger et al., 2019). Additionally, Inoue and colleagues determined MC4R binds to G12/13 by systematically quantifying ligand-induced interactions between 148 GPCRs and all 11 unique Gα subunit C-termini (Inoue et al., 2019).

In addition to the G protein dependent signaling pathway, multiple in vivo and in vitro studies demonstrated that MC4R also activates extracellular signal-regulated kinases 1/2 (ERK1/2) pathway (Chai et al., 2006; Daniels et al., 2003; Sutton et al., 2005; Vongs et al., 2004). However, the underlying mechanism varies based on the cell types. In CHO cells expressing hMC4R, [Nle^4, D-Phe^7]-α-MSH (NDP-MSH)-induced ERK1/2 activation is mediated by phosphatidylinositol 3-kinase (PI3K) other than PKA (Vongs et al., 2004). However, ERK1/2 activation through MC4R induced by α-MSH is only PKA-dependent in GT1-7 cells (Damm et al., 2012). Another study reported that ERK1/2 activation through MC4R is mediated by Gi protein in HEK293 cells, but through calcium and PKC in GT1-1 cells (Chai et al., 2006). Recently, Lotta and colleagues indicated that β-arrestin recruitment results in enhanced ERK1/2 phosphorylation in gain-of-function *MC4R* mutants (Lotta et al., 2019).

In addition to ERK1/2 signaling, MC4R may activate other signaling pathways,

including c-Jun N-terminal kinases (JNK), 5'-AMP-activated protein kinase (AMPK), and protein kinase B (PKB or AKT) (Chai et al., 2009; Damm et al., 2012; Minokoshi et al., 2004; Yang and Tao, 2016). Additionally, MC4R regulates other downstream effectors via recruitment to β-arrestin (Gillyard et al., 2019; Shenoy and Lefkowitz, 2011). Moreover, the inward-rectifier potassium (Kir7.1) channel seems to be involved in MC4R-mediated regulation of energy homeostasis (Anderson et al., 2019; Ghamari-Langroudi et al., 2015).

Intracellular signaling of MC5R, compared to that of MC4R, is less extensively studied. As a typical GPCR, MC5R is able to trigger Gs-cAMP-PKA signaling pathway. In addition, MC5R may activate ERK1/2 signaling pathway through a PI3K-dependent mechanism (Rodrigues et al., 2009). MC5R may activate different cellular signaling pathways when bound to different agonists or when activated in different cell types, leading to different cellular effects and biological functions (Reviewed in (Xu et al., 2020)). In both murine Ba/F3 pro-B lymphocytes and human IM-9 lymphoblasts that express MC5R, α-MSH binding stimulates Janus kinase 2 (JAK2) and signal transducers and activators of transcription (STAT1) tyrosine phosphorylation (Buggy, 1998). In erythroid cells, PI3K/AKT/MLC2 is directly activated by an ACTH signal via MC5R pathway to regulate erythropoiesis (Simamura et al., 2015). Moreover, MC5R may act as a new target to treat high glucose-induced hypertrophy of the cardiac cells since MC5R-induced PI3K activation reduces GLUT1/GLUT4 glucose transporters ratios on cell membrane (Trotta et al., 2018).

1.5. Effects of MRAPs on MC4R and MC5R

MRAP family consists of MRAP1 and MRAP2. They are single pass transmembrane proteins. MRAP1 is encoded by a single gene with 6 exons located on chromosome

21q22.11 (Xu et al., 2002). There are two functional spliced variants: MRAP1-α comprises 172 amino acids derived from exon 1-5 and MRAP1-β contains 102 amino acids derived from exon 1-4 and 6 (Xu et al., 2002) (Reviewed in (Berruien and Smith, 2020)). These two variants are highly conserved at N-terminus but not C-terminus (Metherell et al., 2005; Xu et al., 2002). Little conservation of MRAP1 is shown between species (Webb and Clark, 2010). As a paralog to MRAP1, MRAP2 is a 205-amino acids protein encoded by a gene located at 6q14.3, and shows approximately 40% homology with MRAP1 (Chan et al., 2009). The expression of MRAP1 and MRAP2 have been reported to in multiple tissues including adrenal gland and brain (Chan et al., 2009; Gardiner et al., 2002; Metherell et al., 2005). Therefore, there is a great potential for MRAPs to interact with MC4R and MC5R.

MRAP1 is discovered to promote the maturation of hMC4R since MRAP1 increases proteins that are resistant to endoglycosidase H, proteins that have exited the endoplasmic reticulum (ER), or at the plasma membrane (Kay et al., 2013a, b). The MC4R is constitutively active (Tao, 2014). MRAP1 is able to increase hMC4R basal activity at the Gs-cAMP pathway (Kay et al., 2015). MRAP2 has been shown to interact with MC4R in multiple in vivo and in vitro experiments. For example, MRAP2 in paraventricular MC4R-expressing neurons potentiates MC4R activation at baseline conditions to regulate energy homeostasis (Bruschetta et al., 2018). MRAP2 converts MC4R into an ACTH receptor by increasing MC4R sensitivity to ACTH stimulation to that of MC2R (Josep Agulleiro et al., 2013; Soletto et al., 2019; Zhang et al., 2017). Mutations in *MRAP2* have been shown to be a potential cause for early-onset morbid obesity by regulating the MC4R (Schonnop et al., 2016).

The effect of MRAPs on MC5R is less studied. Coexpression with MRAP1 makes

the MC5R retained intracellularly (Chan et al., 2009; Sebag and Hinkle, 2009a). MRAP1 was found to act as a negative regulator of the MC5R in cAMP assays in response to NDP-MSH (Chan et al., 2009), which may be due to its action on the disruption of MC5R dimers (Sebag and Hinkle, 2009a). Like MRAP1, MRAP2 was also found to have a significant inhibitory role of MC5R (Chan et al., 2009). MRAP1 and MRAP2 have been described to express in the foetal adrenal gland indicating a role of MC2R/MRAPs in the adrenal development (Gorrigan et al., 2011). Intriguingly, MC5R was reported to play a role in foetal adrenal gland development since its expression in this tissue (Nimura et al., 2006). The heterodimerization happens among MCRs (Mandrika et al., 2005). Therefore, MRAP1 and MRAP2 may regulate adrenal differentiation and proliferation via interacting with either MC2R, MC5R or a heterodimer of both (Reviewed in (Berruien and Smith, 2020)).

Chapter 2: MRAP2 interaction with melanocortin-4 receptor in snakehead (*Channa argus*)

2.1. Introduction

The melanocortin-4 receptor (MC4R), a Family A G protein-coupled receptor (GPCR), plays a central role in energy homeostasis regulation in mammals (Cone, 2005; Tao, 2010). It consists of the hallmark seven transmembrane domains (TMDs) connected by alternating extracellular and intracellular loops, with an extracellular N-terminus and intracellular C-terminus (Gantz et al., 1993). Since the human MC4R (hMC4R) was first cloned in 1993 by degenerate PCR (Gantz et al., 1993), extensive studies have been done to elucidate the potential physiological and pathophysiological relevance of this receptor. Cone and colleagues showed that MC4R is highly expressed in neuroendocrine and autonomic control circuits in the brain (Mountjoy et al., 1994). In 1997, it was discovered that modulation of MC4R activation or genetic inactivation exerts a profound influence on food intake and energy expenditure (Fan et al., 1997; Huszar et al., 1997; Ollmann et al., 1997). Subsequent studies found that mutations in *MC4R* and common genetic variation near MC4R lead to a dominant form of obesity and insulin resistance (Chambers et al., 2008; Loos et al., 2008; Vaisse et al., 1998; Yeo et al., 1998). Moreover, several studies suggested that MC4R is also involved in modulating the reproductive function of animals (Irani et al., 2005; Sandrock et al., 2009; Van der Ploeg et al., 2002).

Activation of neurons expressing pro-opiomelanocortin (POMC) decreases food intake, whereas activation of neurons expressing neuropeptide-Y (NPY) and agouti-related peptide (AgRP) increases food intake (Tao, 2010). MC4R mediates the agonist signal provided by the POMC derived peptide α-melanocyte stimulating hormone (α-

MSH), and the antagonist signal provided by AgRP (Agosti et al., 2014; Cone, 2005). After ligand binding, MC4R is primarily coupled to Gs, which stimulates adenylyl cyclase activity and increases intracellular cAMP level. This classical Gs-cAMP signaling pathway is required for regulation of energy balance, thermogenesis, and glucose metabolism (Podyma et al., 2018). Moreover, the pharmacological properties of MC4R are modulated by melanocortin-2 receptor accessory proteins (MRAPs) (Cerdá-Reverter et al., 2013; Cortés et al., 2014).

MRAP family consists of two members, MRAP1 and MRAP2. These two small single transmembrane proteins have been identified to be involved in the regulation of MCR functions as MRAP1 is responsible for the formation of a functional MC2R, and MRAP2 is relevant for the regulation of energy balance (Rouault et al., 2017b). Nonsynonymous *MRAP2* variants have been detected in obese patients, but not in normal weight controls in a meta-analysis (Schonnop et al., 2016), and *Mrap2*-deletion leads to obesity in mice (Asai et al., 2013). One important mechanism is that MRAP2 exerts its effects on energy homeostasis through action on the MC4R. For classical Gs-cAMP signaling pathway, MRAP2 does not affect basal activity, but decreases agonist-stimulated cAMP production in human (h) MC4R (Chan et al., 2009), while MRAP2 suppresses basal signaling, but increases agonist-stimulated maximal response in mouse MC4R (Asai et al., 2013). MRAP2 also enhances MC4R-mediated cAMP production in feline (Habara et al., 2018). An in vivo experiment showed that MRAP2 potentiates mouse MC4R activation in regulating energy homeostasis at baseline conditions in paraventricular nucleus (PVN) MC4R-expressing neurons (Bruschetta et al., 2018).

MC4R has been investigated in several non-mammalian vertebrates including ectotherm fish, such as goldfish (Cerdá-Reverter et al., 2003b), rainbow trout (Haitina et

al., 2004), spotted scat (Li et al., 2016a), grass carp (Li et al., 2017a), ricefield eel (Yi et al., 2018), orange-spotted grouper (Rao et al., 2019), and topmouth culter (Tao et al., 2020). Similar to mammalian MC4Rs, teleost MC4R is also involved in regulating food intake and maintaining energy balance. In barfin flounder, food deprivation induces significantly higher *mc4r* expression in the liver (Kobayashi et al., 2008), and the same phenomenon was observed in the brain of Ya-fish (Wei et al., 2013). Meanwhile, intracerebroventricular administration of MC4R agonist melanotan II inhibits food intake, whereas intracerebroventricular injection of selective MC4R antagonist HS024 stimulates food intake in goldfish (Cerdá-Reverter et al., 2003b). In addition, nonsynonymous mutations in cavefish *mc4r* were found to play an important role in adapting to nutrient-poor condition (Aspiras et al., 2015).

MRAP2 and its modulatory role on MC4R have also been studied in several fishes. Different from mammals, some teleosts, such as zebrafish and topmouth culter, possess two isoforms of MRAP2 (Josep Agulleiro et al., 2013; Sebag et al., 2013; Tao, 2020), while other lower vertebrates including tilapia, sea lamprey, and grouper, have only one (Rao et al., 2019; Wang et al., 2019; Zhu et al., 2019b), suggesting that the phylogenetic process in fish may be more complex than in mammals. In addition, MRAP2 has different effects on MC4R expression, ligand binding, and signaling in different fishes. In sea lamprey, MRAP2 interacts with MCRa and MCRb, reducing their expressions on the cell surface, but increases α-MSH-induced signaling of receptors (Zhu et al., 2019b). In tilapia, MRAP2 decreases both cell surface expression and ligand-stimulated signaling at the Gs-cAMP pathway (Wang et al., 2019). In grouper, both basal and agonist-stimulated Gs-cAMP signaling of MC4R is decreased by MRAP2 (Rao et al., 2019). In zebrafish, MRAP2a decreases α-MSH binding affinity, whereas MRAP2b enhances ligand sensitivity of MC4R (Sebag et al., 2013). In topmouth culter, MRAP2a increases the

maximal binding (B_{max}) and decreases agonist-induced cAMP, but MRAP2b does not affect B_{max} and agonist-stimulated cAMP (Tao et al., 2020). Therefore, more studies about interactions between MRAP2 and MC4R are worth pursuing.

The northern snakehead (*Channa argus*) belongs to the family Channidae and the order Perciformes, and is an economically important freshwater fish native to East Asia (Wen et al., 2020c). Although the annual production has reached 510,000 tons per year in China, the genetic degradation caused by inbreeding of *C. argus* cultivation has led to higher susceptibility to diseases in recent years (Xu et al., 2017). As MC4R is functionally related to growth and reproduction in fish, studies on MC4R will undoubtedly be helpful for understanding the growth traits of *C. argus* and might also be of benefit for future breeding projects. We herein investigated the molecular cloning, tissue distribution, pharmacological characteristics of caMC4R and its regulation by caMRAP2, and a potential role in food intake regulation.

2.2. Materials and methods

2.2.1. Fish sampling

The northern snakehead, weight (71.3 ± 5.6 g) used in this study, were obtained from Neijiang Fish Farm (Neijiang, China) and transported to the experimental aquarium at the College of Life Sciences of Neijiang Normal University. The fish were kept in 100 L tanks under natural light-dark conditions (12 L/12 D) with a constant flow of filtered water and water temperature maintained at 18-20 °C. The fish were fed with fish meat (5-8% of body weight) at 19:00 every day. Fish were acclimated for 2 weeks before the experiment, showing a normal feeding pattern during this acclimation period.

Following acclimation, six fish were randomly selected for cloning and tissue distribution studies. The fish were anesthetized on ice and sacrificed by decapitation. Tissue samples including adipose, brain, eye, gill, gonad (ovary), heart, intestine, kidney, liver, muscle, and spleen, were collected and frozen in liquid nitrogen immediately. For a short-term food deprivation experiment, fish were sampled at 19:00 (after feeding, 0 h), 22:00 (3 h), 01:00 (6h), 07:00 (12 h), and 19:00 (24 h). Six fish were selected from each group, and their brains were sampled and stored. For a long-term food deprivation experiment, fish were assigned to 4 experimental tanks (with 20 fish per tank, 2 tanks of fish were fed, and the other 2 tanks were unfed) for two weeks. Five fish were chosen, and their brains were sampled from each group. Subsequently, the fasted group was refed and sampled. All samples were kept at −80 °C until further analysis.

All animal experiments were performed with the approval of the Neijiang Normal University Animal Care and Use Committee and in full compliance with its ethics guidelines.

2.2.2. Ligands and plasmids

NDP-MSH was purchased from Peptides International (Louisville, KY, USA), α- and β-MSHs were purchased from Pi Proteomics (Huntsville, AL, USA), and ACTH (1-24) was purchased from Phoenix Pharmaceuticals (Burlingame, CA, USA). Both [^{125}I]-NDP-MSH and [^{125}I]-cAMP were iodinated in our lab using chloramine T method (Mo et al., 2012; Steiner et al., 1969). The N terminal c-myc-tagged hMC4R subcloned into pcDNA3.1 vector was prepared as described in our previous study (Tao and Segaloff, 2003). The coding sequences of snakehead MC4R and MRAP2 were commercially synthesized and

subcloned into pcDNA3.1 vector by GenScript (Piscataway, NJ, USA) to generate the plasmids used for transfection.

2.2.3. Molecular cloning of snakehead *mc4r* and *mrap2* genes

Protein similarity-based blast was performed to search the target genes in the snakehead genome and transcriptome databases (Xu et al., 2017), using zebrafish *mc4r*, *mrap2a*, and *mrap2b* as references. After searching, we obtained the genomic and transcriptomic sequences of the snakehead *mc4r* and *mrap2* (single copy, showing close relationship with zebrafish *mrap2b*) genes. Two pairs of primers were designed to validate the two sequences, respectively. Total RNA was isolated from the whole brain with the Trizol reagent (Invitrogen, Carlsbad, CA, USA) according to manufacturer's protocol, and 1 μg of the RNA was reverse transcribed to cDNA using SuperScript™ II RT reverse transcriptase (Invitrogen, Carlsbad, CA, USA). The basic cycling conditions of the PCR were set as follows: A denaturing stage at 94 °C for 30 s, gene-specific annealing temperature for 45 s and an elongation stage at 72 °C for 60 s, a total of 34 cycles. The PCR products were purified from agarose gel using the Universal DNA Purification Kit (TIANGEN, Beijing, China), and then cloned into the pMD-19T vector (Takara, Dalian, China). The inserts were sequenced at BGI (Beijing, China), and the primers used to validate *mc4r* and *mrap2* genes were listed in Table S2.1.

2.2.4. Sequence analysis and data processing

The coding sequences (CDS) were determined using online software ORF finder (https://www.ncbi.nlm.nih.gov/gorf/gorf.html), and then the putative protein sequences were translated with Primer Premier 5.0 software. Moreover, the Bioedit software was

used to determine the isoelectric point (PI), the online tool TMHMM Server v. 2.0 (http://www.cbs.dtu.dk/services/TMHMM-2.0/) was used to identify the transmembrane domain, and the Expasy (http://www.expasy.org/tools/) was used to predict glycosylation and phosphorylation sites. Furthermore, multiple sequence alignments were done as described in our previous work (Wen et al., 2015), and the predicted secondary structure of snakehead MC4R was drawn according to two related studies (Aspiras et al., 2015; Tao, 2010). Additionally, three dimensional structures of several vertebrate MC4Rs were predicted with an online tool SWISS MODEL (https://www.swissmodel.expasy.org/) using human MC4R as reference (Yu et al., 2020). Finally, a comparative genomic survey was performed to investigate the gene synteny of *MC4R* and *MRAP2* in vertebrates as described previously (Wen et al., 2020b; Wen et al., 2019), based on a series of representative animal genomes.

2.2.5. Phylogenetic analysis

The predicted snakehead MC4R and MRAP2 protein sequences together with those of other vertebrates were aligned by CLUSTAL X2.1, respectively. The aligned protein datasets were used to construct the phylogenetic tree with Neighbor-Joining approach using Mega 6.0 software (Wen et al., 2020a). The best-fitting model was calculated by MrmodelTest 2.0 (Nylander, 2004) and ProtTest 2.4 (Abascal et al., 2005), and the JTT + G model was selected as the best model after evaluation. The phylogenetic trees were redrawn using Figtree software. The robustness of the tree topology was assessed by nonparametric bootstrap analysis with 1000 resampling replicates. IDs of the protein sequences used in present study are shown in Tables S2.2 and Table S2.3.

2.2.6. Quantitative real-time PCR

Extraction of total RNA from fish tissues and first strand cDNA synthesis were performed as described above. Then, real-time PCR was used to detect the mRNA expressions of *mc4r* and *mrap2* with LightCycler® Real-Time system. Reverse transcription product was used for real-time PCR in a final volume of 10 μL. The end products of PCR were verified with the melting curves that showing a single peak specific for the target gene. The relative expression levels were calculated according to the method described previously (Livak and Schmittgen, 2001), and *tubα1* was used as reference gene. Primers used to amplify *mc4r*, *mrap2*, and *tubα1* are shown in Table S2.1. Values are expressed as means ± SEM (n = 6).

2.2.7. Cell culture and transfection

Human Embryonic Kidney (HEK) 293T cells, purchased from American Type Culture Collection (Manassas, VA, USA), were cultured in Dulbecco's Modified Eagle's medium (DMEM) (Invitrogen, Carlsbad, CA, USA) containing 10% newborn calf serum (PAA Laboratories, Etobicoke, ON, Canada), 10 mM HEPES, 0.25 μg/mL of amphotericin B, 50 μg/mL of gentamicin, 100 IU/mL of penicillin, and 100 μg/mL of streptomycin at 37 °C in a 5% CO_2-humidified atmosphere. The cells were plated into 6-well or 24-well plates (Corning, NY, USA) pre- coated with 0.1% gelatin and transfected or co-transfected when cells reached at ~70% confluence using calcium phosphate precipitation method (Chen and Okayama, 1987).

2.2.8. Flow cytometry assay

To investigate the effect of snakehead MRAP2 on the cell surface and total expression levels of MC4R, cells were plated into 6-well plates and transfected with snakehead MC4R and MRAP2 plasmids in four ratios (1:0, 1:1, 1:3, and 1:5). Then, cells were incubated with mouse anti-myc 9E10 monoclonal antibody (Developmental Studies Hybridoma Bank, The University of Iowa, Iowa City, IA, USA) diluted 1:40 and Alexa Fluor 488-labeled goat anti-mouse antibody (Invitrogen) diluted 1:2000 for 1 h, respectively. Flow cytometry was carried out, and C6 Accuri Cytometer (Accuri Cytometers, Ann Arbor, MI, USA) was applied to collect fluorescence signals. The expression level of caMC4R (caMC4R fluorescence − pcDNA3.1 fluorescence) from 1:0 (caMC4R/caMRAP2) group was set as 100%, and the expression levels of other groups were calculated as a percentage of 1:0 group (Wang et al., 2008).

2.2.9. Ligand binding assays

To assess the ligand binding properties of the caMC4R, four ligands (NDP-MSH, ACTH (1-24), α-MSH, β-MSH) were used. Forty-eight hours after transfection, HEK293T cells were washed twice with warm DMEM containing 1 mg/mL bovine serum albumin (BSA, EMD Millipore Corporation, Billerica, MA, USA) (DMEM/BSA). To study the effects of caMRAP2 on the binding property of caMC4R, two ligands (α-MSH and ACTH (1-24)) were used. Forty-eight hours after transfection, HEK293T cells co-transfected with caMC4R and caMRAP2 at four ratios (1:0, 1:1, 1:3, and 1:5) were washed twice with warm DMEM/BSA. After 1-h incubation with ligands, the competitive binding reaction was terminated by washing cells twice with cold Hank's balanced salt solution containing 1 mg/mL BSA on ice. The cells were lysed with 0.5 M NaOH, collected with cotton swabs, and radioactivity detected with gamma counter (Cobra II Auto-Gamma, Packard Bioscience, Frankfurt, Germany).

2.2.10. cAMP assays

Forty-eight hours after transfection, HEK293T cells were washed twice with warm DMEM/BSA and then incubated with DMEM/BSA containing 0.5 mM isobutylmethylxanthine (Sigma–Aldrich, St. Louis, MO, USA) at 37 °C for another 15 min. Then, different concentrations of NDP-MSH, ACTH (1-24), α-MSH, or β-MSH were added to make the final concentration of ligands ranging from 10^{-12} to 10^{-6} M for NDP- MSH and ACTH (1-24) or from 10^{-11} to 10^{-5} M for α-MSH and β-MSH. After an hour's incubation at 37 °C, the reaction was terminated on ice and the intracellular cAMP was collected by adding 0.5 M perchloric acid containing 180 μg/mL theophylline (Sigma- Aldrich) and 0.72 M KOH/0.6 M $KHCO_3$ into each well. The cAMP levels were measured by radioimmunoassay (RIA) (Steiner et al., 1969).

To investigate the potential effect of caMRAP2 on caMC4R signaling, two ratios of caMC4R and caMRAP2 (1:0 and 1:5) were applied to co-transfect cells, and two ligands, α-MSH and ACTH (1-24), were used. To explore the dose-dependent effect of caMRAP2 on the maximal response (R_{max}) of cAMP levels to α-MSH and ACTH (1-24) stimulation, cells were co-transfected with caMC4R and caMRAP2 in four ratios (1:0, 1:1, 1:3, and 1:5). To study the constitutive activity of Gs cAMP, cells were transfected with different concentrations caMC4R plasmid (0, 0.007, 0.015, 0.030, 0.060, 0.125, and 0.250 μg/μL).

2.2.11. Statistical analysis

All data were expressed as the mean ± SEM. Statistical analysis of gene expression was performed with SPSS 19.0 software. Significant differences were calculated using

one-way analysis of variance (ANOVA), followed by the post hoc test (least significant difference test and Duncan's multiple range test), after confirming for data normality and homogeneity of variances. GraphPad Prism 6.0 software (San Diego, CA, USA) was used to calculate the parameters of ligand binding and cAMP signaling assays including B_{max}, IC_{50}, R_{max}, and EC_{50}. The significance of differences in ligand binding and signaling between caMC4R and hMC4R were determined by Student's t-test. Parameters in flow cytometry, ligand binding, and cAMP of caMC4R regulated by MRAP2s were analyzed for significance of differences by one-way ANOVA.

2.3. Results

2.3.1. Molecular cloning of snakehead *mc4r* and *mrap2* genes

The cDNA sequence of snakehead *mc4r* was 1515 bp in length, and contained a 984 bp open reading frame (ORF) encoding a putative 327-amino acid protein, and has been deposited into the GenBank database (accession number KU728167) (Fig. 2.1A). Similar to other teleost *mc4r*, the coding region of the snakehead *mc4r* was intronless. In addition, cysteine residues at positions 40, 84, 131, 178, 197, 258, 272, 278, 280, and 319 were highly conserved in all vertebrate MC4Rs (Fig. S2.1A). Alignment showed the deduced amino acid sequence of snakehead MC4R was 66% and 93% identical to human and seabass MC4Rs, respectively (Fig. S2.1A). The sequence identity was unevenly distributed, with the N-terminal extracellular domain displaying the lowest identity to other MC4Rs, including seabass MC4R (Fig. S2.1A).

The ORF of snakehead *mrap2* was 693 bp long, encoding a protein of 230 amino acids (Fig. 2.1B), and has been deposited into the GenBank database (accession number

MW118677). Consistent with other teleost MRAP2s, snakehead MRAP2 possessed a conserved motif (LKAHKYS) crucial for the formation of antiparallel homodimer, a single TMD, and a conserved motif (NIPNFVN) in C-terminus (Fig. 2.1B, Fig. S2.2), with a calculated PI and molecular weight of 4.73 and 25.79 kDa, respectively. Snakehead MRAP2 showed 40.0% and 38.3% similarity with its homologs from human and chicken, and shared 42.7%, 37.5%, 55.0%, and 77.5% identity with zebrafish (MRAP2a and MRAP2b), pufferfish, and grouper MRAP2s (Fig. S2.2).

2.3.2. Comparative synteny of *mc4r* and *mrap2* in various vertebrate genomes

In the present study, a comparative genomic analysis was performed to investigate the genetic diversity of *MC4R* and *MRAP2* in vertebrates (Fig. 2.2). As shown in Fig. 2.2A, a conserved gene cluster *RNF152-CDH20-MC4R-DROSHA-CDH6* was identified in genomes of nearly all representative species, implying that the synteny of *MC4R* was highly conserved across vertebrates (Fig. 2.2A).

Different from *MC4R*, *mrap2* possessed two isoforms in teleosts and only a single gene in tetrapods (Fig. 2.2B). Generally, a gene conserved cluster N*T5E-TBX18-CEP162 MRAP2-CYB5R4-RIPPLY2* was identified in tetrapods, and the core gene cluster *CEP162-MRAP2a-CYB5R4* was also found in teleosts (Fig. 2.2B), such as zebrafish (*D. rerio*) and a living fossil species reedfish (*E. calabaricus*). However, *mrap2a* was lost fishes including snakehead (*C. argus*), tilapia (*O. niloticus*), and pufferfish (*T. rubripes*). Interestingly, a different gene cluster *SOBPb-MRAP2b-RIPPLY2-SIM1b* was identified in almost all teleosts examined in the present study, except reedfish (Fig. 2.2B).

2.3.3. Phylogenetic analysis

Two phylogenetic trees were constructed using Neighbor-Joining (NJ) method based on a series of protein sequences of vertebrate MC4Rs and MRAP2s, and both trees were robust with high bootstrap values (Fig. 2.3). As shown in Fig. 2.3A, the phylogenetic tree was divided into two groups, teleost MC4Rs and higher vertebrate MC4Rs, and the teleost MC4R group could be further divided into four subgroups containing Cyprinodontiformes, Perciformes, Tetraodonformes, and Cypriniformes. Meanwhile, MC4R in Perciformes appeared posterior to Cypriniformes, but prior to Cyprinodontiformes in the evolutionary history of vertebrates (Fig. 2.3A). Moreover, the snakehead MC4R was grouped into Perciformes, and shared a close relationship with seabass (*Dicentrarchus labrax*) and large yellow croaker (*Larimichthys crocea*) MC4Rs (Fig. 2.3A). Additionally, the phylogenetic tree of MRAP2 was clustered into two groups of tetrapods and teleosts, and snakehead MRAP2 was grouped into the Perciforms with a close relationship with tilapia, orange-spotted grouper, and large yellow croaker (Fig. 2.3B). Notably, it is shown that zebrafish MRAP2b shared close relationship with MRAP2 from other teleosts, in comparison with its paralog MRAP2a (Fig. 2.3B).

2.3.4. Tissue distribution of snakehead *mc4r* and *mrap2* genes

The expression of snakehead *mc4r* and *mrap2* was determined using quantitative real time PCR. Similar to other fish, snakehead *mc4r* was found to be extensively expressed in central and peripheral tissues, including adipose, brain, eye, gill, gonad (ovary), heart, intestine, kidney, liver, muscle, and spleen (Fig. 2.4A), with the highest expression in the brain (Fig. 2.4A). Similarly, snakehead *mrap2* was also widely distributed in these tissues with the highest expression in brain (Fig. 2.4B).

2.3.5. Effects of fasting and refeeding on the expressions of snakehead *mc4r* and *mrap2* genes

To investigate the potential roles of snakehead MC4R and MRAP2 in energy balance, the mRNA expression levels of both genes in the brain were determined after food deprivation and refeeding. In the short-term trial, the *mc4r* mRNA level was significantly increased at 3 and 6 h while returned to basal level at 12 and 24 h after food deprivation (Fig. 2.5A). Meanwhile, the *mrap2* mRNA level was significantly increased at 3 h, and then maintained at relatively high mRNA levels at 6, 12, and 24 h (Fig. 2.5B). In the long-term trial, the expression level of *mc4r* was significantly increased after two-week fasting, and further increased after refeeding (Fig. 2.6A). Differently, the mRNA level of *mrap2* was dramatically decreased after fasting whereas recovered to the control level after refeeding (Fig. 2.6B).

2.3.6. Ligand binding properties of caMC4R

Ligand binding assays were performed to determine the binding properties of caMC4R with different MC4R ligands. Four unlabeled ligands (NDP-MSH, ACTH (1-24), α-MSH and β-MSH) were used to compete with ^{125}I-NDP-MSH. The maximal binding value of caMC4R was significantly lower than that of hMC4R (16.32 ± 2.46% of hMC4R) (Fig. 2.7 and Table 2.1). When NDP-MSH or α-MSH was used to displace the ^{125}I-NDP-MSH, caMC4R showed significantly decreased or increased IC_{50} values in comparison with hMC4R, whereas when the other two ligands were used as competitors, hMC4R and caMC4R exhibited similar IC_{50}s (Fig. 2.7 and Table 2.1).

2.3.7. Signaling properties of caMC4R

To investigate whether caMC4R could respond to ligand stimulation with increased cAMP level, RIA was carried out. As shown in Fig. 2.8, all ligands could increase the intracellular cAMP level in a dose-dependent manner. The EC_{50} of ACTH (1-24) for caMC4R was significantly lower than that of hMC4R, whereas the EC_{50}s of NDP-MSH, α-MSH, and β- MSH were comparable with those of hMC4R (Table 2.2). The caMC4R showed higher maximal responses than hMC4R when stimulated with ACTH (1-24), α-MSH, and β-MSH, and slightly decreased maximal response in response to NDP-MSH (Fig. 2.8 and Table 2.2).

The basal cAMP level of caMC4R was also measured. The results demonstrated caMC4R had significantly increased basal activity, which was 7.39 times that of hMC4R (Fig. 2.9A and Table 2.2). To confirm constitutive activity of caMC4R, different concentrations of caMC4R plasmids were transfected into HEK293T cells and basal cAMP levels were measured. The high basal intracellular cAMP level was detected at only 0.03 μg/μL caMC4R plasmid transfected (Fig. 2.9B).

2.3.8. Modulation of caMC4R expression and pharmacological properties by caMRAP2

To investigate the effects of caMRAP2 on the cell surface and total expression levels of caMC4R, flow cytometry was performed. No significant difference was observed among the four groups for cell surface or total expression (Figs. 2.10A,B). Competitive ligand binding assays showed that IC_{50}s of caMC4R to ACTH (1-24) was decreased by caMRAP2 in the 1:3 and 1:5 groups, whereas no change was observed in IC_{50}s for α-

MSH among the four groups (Figs. 2.10C,D and Table 2.3).

In order to explore the effect of caMRAP2 on the cAMP signaling of caMC4R, cells were co-transfected with caMC4R and caMRAP2 in different ratios. The results showed that caMRAP2 dose-dependently decreased the basal cAMP levels (Fig. 2.11A). In addition, caMRAP2 significantly reduced signaling induced by both α-MSH and ACTH (1-24) (Figs. 2.11B,C and Table 2.4). Dose-response experiments showed that caMRAP2 only decreased the maximal response with no effect on EC_{50}s (Figs. 2.11D,E and Table 2.4).

2.4. Discussion

In this study, we cloned snakehead *mc4r* and *mrap2* genes. Sequence comparison showed that caMC4R shared more than 80% amino acid identity with other teleost MC4Rs, whereas caMRAP2 shared lower identity (37.5-77.5%) with other teleost MRAP2s, suggesting MC4R was more conserved than MRAP2 in teleosts.

Comparative gene synteny analysis showed that only a single copy of *mc4r* was identified in vertebrates with a conservative gene cluster *RNF152-CDH20-MC4R-DROSHA-CDH6*, suggesting that this receptor is highly conserved and may play similar roles in vertebrates. In tetrapod, only a single copy of *mrap2* was identified in their genomes, exhibiting a conserved gene cluster *NT5E-TBX18-CEP162-MRAP2-CYB5R4 RIPPLY2*. In teleosts, the gene number of *mrap2* is variable. In zebrafish, two copies of *mrap2* (*mrap2a* and *mrap2b*) were identified, and functional studies showed that MRAP2a decreases binding affinity for α-MSH while MRAP2b increases ligand sensitivity of MC4R (Sebag et al., 2013). In reedfish, only a single *mrap2* was identified and it shares a similar

conserved genetic locus with tetrapod *mrap2* and zebrafish *mrap2a*, suggesting that the duplication of *mrap2* might have occurred after the specific whole genome duplication event in teleost (Hughes et al., 2018). Interestingly, we found that the homolog of zebrafish *mrap2a* was lost in Perciform and Tetraodontiform fishes, including snakehead, tilapia, and puffer fish. However, the *mrap2b* paralog was retained in these teleost genomes with a conserved gene cluster *SOBPb-MRAP2b-RIPPLY2-SIM1*b, suggesting the evolutionary process of *mrap2* is complex in teleosts and the physiological role of this gene might be variable.

To investigate the evolutionary relationship of vertebrate MC4Rs and MRAP2s, phylogenetic trees were constructed. Both trees were divided into two subgroups of teleost and tetrapod subgroup, similar to previous studies (Kobayashi et al., 2008; Li et al., 2017a; Wei et al., 2013). For the MC4R tree, the Cypriniformes clade was located at the root of the subgroup, suggesting the Cypriniformes MC4R might have appeared earlier in the evolutionary history than other teleosts. Meanwhile, the snakehead MC4R was clustered into Perciformes clade, and shared a close relationship with seabass MC4R. These findings were consistent with the traditional species classification (Li et al., 2016a; Li et al., 2017a). For the MRAP2 tree, zebrafish MRAP2b shares a close relationship with MRAP2 from other teleosts, in comparison with its paralog MRAP2a, suggesting the restrained MRAP2 in snakehead and other teleosts is the homolog of zebrafish MRAP2b, consistent with gene synteny analysis.

Data from real-time quantitative PCR showed that *mc4r* was widely expressed in various tissues with high expression in brain and gonad, similar to previous studies (Kobayashi et al., 2008; Li et al., 2016a; Li et al., 2017a; Rao et al., 2019; Tao et al., 2020; Wan et al., 2012; Wei et al., 2013; Yi et al., 2018), suggesting that snakehead MC4R

might also be involved in regulating food intake (Cerdá-Reverter et al., 2003b; Kobayashi et al., 2008) and sexual maturation (Lampert et al., 2010; Van der Ploeg et al., 2002). Meanwhile, *mrap2* was also extensively distributed in several tissues, with relatively high expression in brain. This distribution pattern of *mrap2* was also found in orange-spotted grouper (Rao et al., 2019), Nile tilapia (Wang et al., 2019), and topmouth culter (Tao et al., 2020), suggesting functional identity of MRAP2 in teleosts. Additionally, *mc4r* and *mrap2* exhibited high distribution level in brain, indicating that they might interact with each other in snakehead. However, *mrap2* was highly expressed in intestine while *almost no mc4r* in intestine, indicating caMRAP2 might modulate other GPCRs function in intestine.

We measured *mc4r* and *mrap2* expression after short-term and long-term fasting and refeeding. The short-term fasting meant the period after one meal. Within 24 h after the meal, the *mc4r* expression was altered over time, which might ensure fish to maintain normal energy balance. After two-week fasting, the increased *mc4r* expression level might help fish to adapt to the poor-nutrition condition. When refeeding again, the further increased *mc4r* expression might prevent fish overeating. At the same time, *mrap2* expression was also modulated by these manipulations, indicating their potential interactions in regulating energy homeostasis. Several previous studies also investigated the expression of these genes with fasting and refeeding, obtaining conflicting results in different species (Jangprai et al., 2011; Kobayashi et al., 2008; Wan et al., 2012; Wei et al., 2013; Zhang et al., 2017). Further studies, including physiological experiments involving measuring energy balance with in vivo administration of ligands, are needed to clarify the physiological function of MC4R.

To investigate the pharmacological characteristics of caMC4R, four ligands were

used, together with hMC4R for comparison. Our results demonstrated that caMC4R was fully functional. The synthetic agonist NDP-MSH bound to caMC4R with the highest affinity with an IC_{50} of 4.50 nM, which is about 7-fold lower than hMC4R. Additionally, it stimulated caMC4R with the highest potency with an EC_{50} of 0.04 nM. α- and β-MSHs stimulated caMC4R with similar potency as hMC4R. However, ACTH (1-24) had 3-fold higher potency at caMC4R than hMC4R. Previous studies demonstrated that fish MC4Rs have decreased binding capacities (Li et al., 2016a; Li et al., 2017a; Rao et al., 2019; Tao et al., 2020; Yi et al., 2018; Zhang et al., 2019). We also found lower binding capacity in caMC4R (16.32% of that of hMC4R) (Fig. 2.7 and Table 2.1). In spotted sea bass, the cell surface and total expressions of fish MC4R were only ~2.1% to those of hMC4R (Zhang et al., 2019). We speculated that the lower binding capacity of fish MC4Rs might be caused by their lower surface expression, which needs to be further investigated. Among the three endogenous ligands used here, ACTH (1-24) showed high binding affinity, further supporting the suggestion that ACTH (1-24) might act as the ancestral ligand for MCRs.

A remarkably elevated basal cAMP activity was found in caMC4R. This phenomenon has also been reported in other fish species, such as spotted scat (Li et al., 2016a), grass carp (Li et al., 2017a), swamp eel (Yi et al., 2018), orange-spotted grouper (Rao et al., 2019), and topmouth culter (Tao et al., 2020). In contrast to hMC3R, hMC4R has some basal activity (Tao, 2007). Srinivasan and colleagues reported that part of the N-terminus functions as a tethered intramolecular ligand to maintain the constitutive activity of hMC4R (Srinivasan et al., 2004). Here, low sequence homology was found within the N-terminus in caMC4R when compared with hMC4R. We hypothesized that structural difference of N-termini may account for its high basal activity. We have analyzed the extracellular N-termini of hMC4R and fish MC4Rs with higher basal activity (Fig. S2.3).

There were eight potential residues which were conserved in fish MC4Rs but different in hMC4R. Then, site-directed mutagenesis is suggested to do to determine whether these residues are responsible for the higher basal activity in fish MC4Rs. The loss of constitutive activity in mutant hMC4Rs is one cause of obesity (Srinivasan et al., 2004; Tao, 2008). Therefore, the development of an MC4R agonist has been regarded as a therapeutic option for human obesity treatment. However, increasing food intake and decreasing energy expenditure of aquaculture species will deliver benefits for farmers. As a result, focusing on the study of caMC4R antagonists, especially inverse agonists, will promote the development of snakehead cultivation. On one hand, the inverse agonists can promote fish growth by increasing food intake and decreasing energy expenditure, which will shorten the fish breeding time to decrease the cost and put them to market sooner to get the benefits. On the other hand, the increased food intake induced by inverse agonists can reduce food residues in fish ponds, which will protect the environment.

In this study, we showed that caMRAP2 did not affect cell surface and total expression of caMC4R, similar to the observation in chicken (Zhang et al., 2017), but different from results obtained in tilapia (Wang et al., 2019) and mouse (Chan et al., 2009) (decreased cell surface expression), or zebrafish (Sebag et al., 2013) and topmouth culter (Tao et al., 2020) (increased cell surface expression). Therefore, MRAP2 has a differential effect on MC4R membrane expression in different species. Snakehead MRAP2 increased binding affinity of caMC4R to ACTH (1-24), but did not affect the IC_{50} of caMC4R to α-MSH. In topmouth culter, two isoforms of MRAP2 are also shown to increase binding affinity of MC4R to ACTH (1-24), but not to α-MSH (Tao et al., 2020). In addition to its chaperoning role, MRAP1 also enables MC2R to form the high-affinity binding pocket to ACTH (Sebag and Hinkle, 2009b). MRAP2 might also make caMC4R

to achieve a conformation with enhanced affinity to ACTH. The high constitutive activity in cAMP pathway of caMC4R was inhibited by caMRAP2, similar to our previous observations in orange-spotted grouper (Rao et al., 2019) and topmouth culter (Tao et al., 2020). In the presence of caMRAP2, significantly decreased maximal response but not EC_{50} of caMC4R in response to α-MSH or ACTH (1-24) was observed. Previous studies demonstrated that MC4R can become an ACTH receptor by increasing ligand sensitivity to ACTH in the presence of MRAP2 (Josep Agulleiro et al., 2013; Soletto et al., 2019; Zhang et al., 2017). In our experiments, ligand sensitivity to ACTH (1-24) of caMC4R was not increased by caMRAP2, despite the increased binding affinity to ACTH (1-24) by caMRAP2.

In addition to energy homeostasis, MC4R also regulates reproduction and sexual function (Tao, 2010). Compared with mammals, the evidence of MC4R in regulating teleost reproduction is relatively scarce. In swordtail fish, nonfunctional Y-linked *mc4r* copies in larger males act as dominant-negative mutants and delay puberty onset (Lampert et al., 2010). In spotted scat, MC4R stimulates *gnrh* expression in the hypothalamus, thereby modulating pituitary FSH and LH synthesis (Jiang et al., 2017). In black rockfish, α- and β-MSHs increase brain *gnih* and decrease *sgnrh* and *cgnrh* expression in vitro; they also affect expression of some ovarian genes (Zhang et al., 2020). These studies demonstrated that MC4R could play a vital role in reproductive regulation in fish. In the present study, we also observed that *mc4r* and *mrap2* were highly expressed in gonad, implying a potential role in reproduction. Therefore, future studies on MC4R regulation of reproductive function are warranted.

One shortcoming of this study is that all fasting groups were compared to the fed group at time 0, which is in fact not appropriate. In fed Atlantic salmon, the expression

level of many genes including *pomc* and *agrp* have changed over time (Valen et al., 2011). Thus, the fed group should be chosen as the control of fasting group at each time point. We should be cautious in selecting appropriate control in future studies. Additionally, we used human peptide hormones (α-, β-MSHs and ACTH) for experiments. Although snakehead POMC is not available, we analyzed the POMCs of other fishes and human (Fig. S2.4). Among these species, the α-MSH and ACTH (1-24) were 100% and 83.33% conserved, respectively, while β-MSH showed only 40.91%. Therefore, we need to interpret the data obtained for β-MSH with caution.

Table 2.1. The binding properties of caMC4R.

MC4R	B_{max} (%)	NDP-MSH	ACTH (1-24)	α-MSH	β-MSH
		IC_{50} (nM)	IC_{50} (nM)	IC_{50} (nM)	IC_{50} (nM)
hMC4R	100	27.72 ± 4.29	324.6 ± 88.97	488.2 ± 2.55	749.4 ± 93.98
caMC4R	16.32 ± 2.46[c]	4.50 ± 1.07[a]	415.1 ± 163.7	981.0 ± 45.52[b]	328.7 ± 119.6

Results were expressed as the mean ± SEM of at least three independent experiments.

[a] Significantly different from the parameter of hMC4R, $P < 0.05$.

[b] Significantly different from the parameter of hMC4R, $P < 0.01$.

[c] Significantly different from the parameter of hMC4R, $P < 0.0001$.

Table 2.2. The signaling properties of caMC4R.

MC4R		hMC4R	caMC4R
Basal (%)		100	739.2 ± 63.82[b]
NDP-MSH	EC_{50} (nM)	0.59 ± 0.18	0.04 ± 0.02
	R_{max} (%)	100	75.18 ± 27.83
ACTH (1-24)	EC_{50} (nM)	2.68 ± 0.50	0.81 ± 0.18[a]
	R_{max} (%)	100	119.0 ± 3.73[a]
α-MSH	EC_{50} (nM)	2.82 ± 0.40	2.32 ± 0.57
	R_{max} (%)	100	198.1 ± 55.95
β-MSH	EC_{50} (nM)	6.67 ± 3.41	2.49 ± 0.81
	R_{max} (%)	100	163.9 ± 89.36

Results were expressed as the mean ± SEM of at least three independent experiments.

[a] Significantly different from the parameter of hMC4R, $P < 0.05$.

[b] Significantly different from the parameter of hMC4R, $P < 0.01$.

Table 2.3. The effect of caMRAP2 on ligand binding properties of caMC4R.

caMC4R/caMRAP2	B_{max} (%)	α-MSH	ACTH (1-24)
		IC_{50} (nM)	IC_{50} (nM)
1:0	100	383.80 ± 68.82	239.90 ± 23.61
1:1	100.70 ± 6.24	461.00 ± 65.51	144.80 ± 74.73
1:3	102.80 ± 9.56	497.10 ± 147.4	49.48 ± 19.47[a]
1:5	83.62 ± 7.17	238.10 ± 60.77	24.73 ± 11.73[a]

Results were expressed as the mean ± SEM of at least three independent experiments.

[a] Significantly different from the parameter of 1:0, $P < 0.05$.

Table 2.4. The effect of caMRAP2 on signaling properties of caMC4R.

caMC4R/caMRAP2	α-MSH		ACTH (1-24)	
	EC_{50} (nM)	R_{max} (%)	EC_{50} (nM)	R_{max} (%)
1:0	0.48 ± 0.12	100	0.45 ± 0.20	100
1:5	0.61 ± 0.15	44.70 ± 7.96[c]	0.42 ± 0.13	54.81 ± 5.19[c]

Results are expressed as the mean ± SEM of at least three independent experiments.

[c] Significantly different from the parameter of 1:0, $P < 0.001$.

Table S2.1. PCR primers used for cloning and gene expression studies.

Primers	Primer sequence (5′- 3′)
mc4r-F1	GTTCCTGCTCGCTGTTAA
mc4r-R1	CACGTTGTCCATGCTTTT
mc4r-F2	CGTGTTTGACTCTATGAT
mc4r-R2	TTTTACTTGGAGATTGTA
mrap2-F1	TGTTTTCAGATAGGCTTCG
mrap2-R1	ATCACCCATCCCAGAGG
mrap2-F2	TTCTTTGTTCTCACGCTG
mrap2-R2	TCTGTGCTTTATCTGTTCC
mc4r-qF	TGCCAGTGAACAAGGACC
mc4r-qR	AGCAGCGACAACCAAGAT
mrap2-qF	TGTTCTCACGCTGCTCA
mrap2-qR	GCTTTGTCGTTTTCATCT
Tubα1-qF	AGCCTGATGGTCAAATGC
Tubα1-qR	TTCCAATGGTGTAGTGCC

Table S2.2. Listing of MC4R sequences used in this study.

Protein IDs are given to allow access to the protein sequence on Ensembl or GenBank website.

Number	*Species*	Protein ID
1	*Xiphophorus nigrensis*	ADO60278
2	*Xiphophorus maculatus*	NP_001303841
3	*Xiphophorus multilineatus*	ADO60279
4	*Haplochromis burtoni*	NP_001274332
5	*Oreochromis niloticus*	ENSONIP00000025763
6	*Channa argus*	AMM02541
7	*Larimichthys crocea*	XP_019120241
8	*Dicentrarchus labrax*	CBN82190
9	*Takifugu porphyreus*	BAB71733
10	*Takifugu rubripes*	AAO65551
11	*Takifugu radiatus*	BAB71732
12	*Tetraodon nigroviridis*	AAQ55178
13	*Clupea harengus*	XP_012679593
14	*Cyprinus carpio*	CBX89936
15	*Ctenopharyngodon idella*	AOZ60534
16	*Squaliobarbus curriculus*	ADV40875
17	*Xenocypris argentea*	ADV40878
18	*Danio rerio*	NP_775385
19	*Hypophthalmichthys molitrix*	ADV40873
20	*Hypophthalmichthys nobilis*	ADV40874
21	*Astyanax mexicanus*	ENSAMXP00000027055
22	*Sus scrofa*	ABD28176
23	*Homo sapiens*	NP_005903
24	*Canis lupus familiaris*	EDL09662
25	*Mus musculus*	EDL09662
26	*Ovis aries*	ACC77651
27	*Bos taurus*	ACR43465
28	*Ornithorhynchus anatinus*	XP_001505445
29	*Gallus gallus*	AAT73771
30	*Anolis carolinensis*	XP_003226797

Table S2.3. Listing of MRAP2 sequences used in this study.

Protein IDs are given to allow access to the protein sequence on Ensembl or GenBank website.

Number	Species	Protein ID
1	*Homo sapiens*	NP_001333471.1
2	*Mus musculus*	NP_001346884.1
3	*Ornithorhynchus anatinus*	XP_028903035.1
4	*Gallus gallus*	NP_001307836.1
5	*Anolis carolinensis*	XP_008119910.1
6	*Xenopus tropicalis*	XP_002933963.1
7	*Channa argus*	Present study
8	*Callorhinchus milii*	XP_007906624.1
9	*Danio rerio*	XP_001342923.4
10	*Danio rerio*	XP_005168578.1
11	*Epinephelus coioides*	MK425026.1
12	*Esox lucius*	XP_010888023.1
13	*Larimichthys crocea*	XP_027140224.1
14	*Oreochromis niloticus*	XP_003458293.2
15	*Oryzias latipes*	XP_004083625.1
16	*Xiphophorus couchianus*	XP_027897067.1
17	*Xiphophorus maculatus*	XP_005813802.1

A

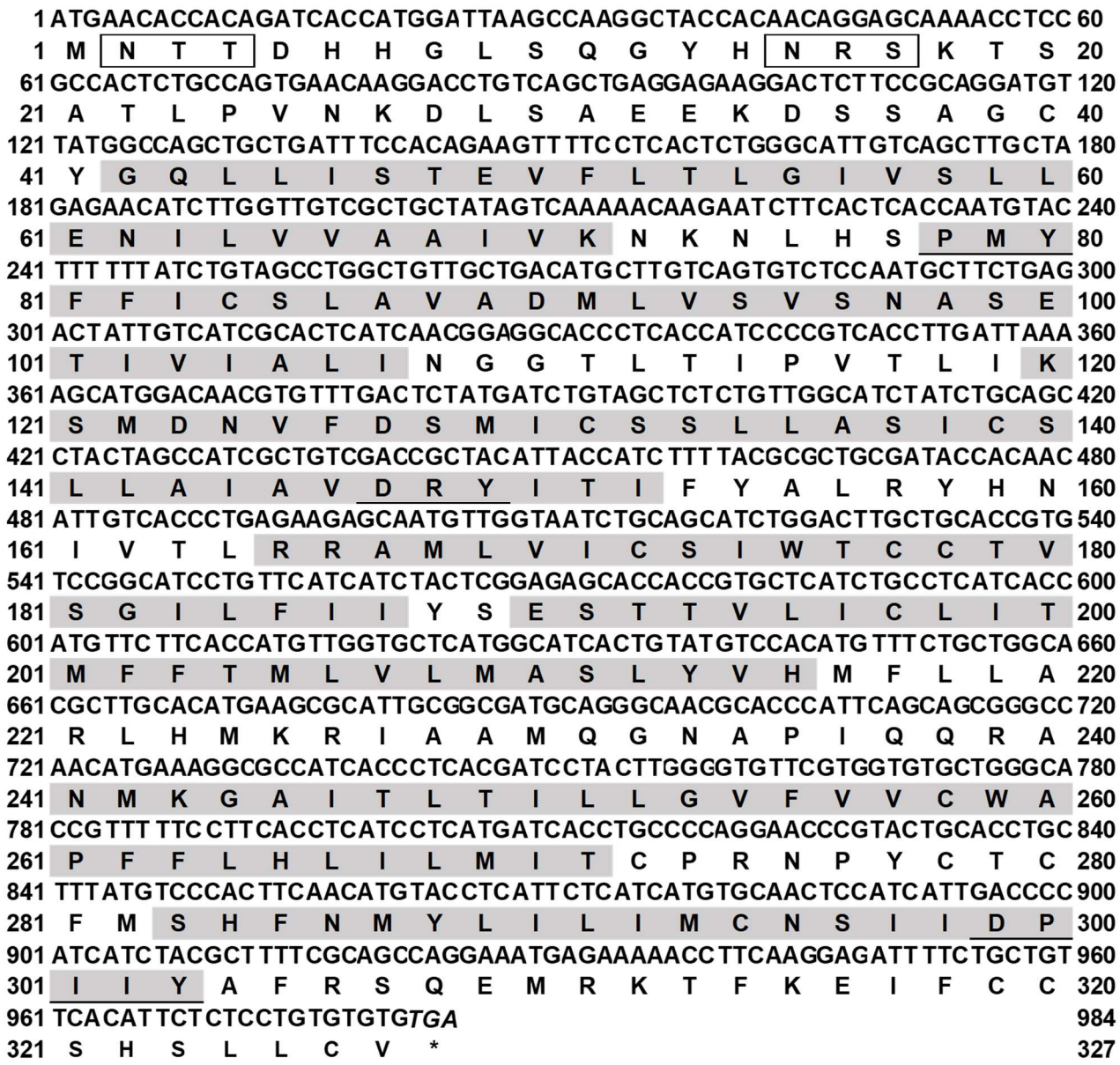
1 ATGAACACCACAGATCACCATGGATTAAGCCAAGGCTACCACAACAGGAGCAAAACCTCC 60
1 M N T T D H H G L S Q G Y H N R S K T S 20
61 GCCACTCTGCCAGTGAACAAGGACCTGTCAGCTGAGGAGAAGGACTCTTCCGCAGGATGT 120
21 A T L P V N K D L S A E E K D S S A G C 40
121 TATGGCCAGCTGCTGATTTCCACAGAAGTTTTCCTCACTCTGGGCATTGTCAGCTTGCTA 180
41 Y G Q L L I S T E V F L T L G I V S L L 60
181 GAGAACATCTTGGTTGTCGCTGCTATAGTCAAAAACAAGAATCTTCACTCACCAATGTAC 240
61 E N I L V V A A I V K N K N L H S P M Y 80
241 TTTTTTATCTGTAGCCTGGCTGTTGCTGACATGCTTGTCAGTGTCTCCAATGCTTCTGAG 300
81 F F I C S L A V A D M L V S V S N A S E 100
301 ACTATTGTCATCGCACTCATCAACGGAGGCACCCTCACCATCCCCGTCACCTTGATTAAA 360
101 T I V I A L I N G G T L T I P V T L I K 120
361 AGCATGGACAACGTGTTTGACTCTATGATCTGTAGCTCTCTGTTGGCATCTATCTGCAGC 420
121 S M D N V F D S M I C S S L L A S I C S 140
421 CTACTAGCCATCGCTGTCGACCGCTACATTACCATCTTTTACGCGCTGCGATACCACAAC 480
141 L L A I A V D R Y I T I F Y A L R Y H N 160
481 ATTGTCACCCTGAGAAGAGCAATGTTGGTAATCTGCAGCATCTGGACTTGCTGCACCGTG 540
161 I V T L R R A M L V I C S I W T C C T V 180
541 TCCGGCATCCTGTTCATCATCTACTCGGAGAGCACCACCGTGCTCATCTGCCTCATCACC 600
181 S G I L F I I Y S E S T T V L I C L I T 200
601 ATGTTCTTCACCATGTTGGTGCTCATGGCATCACTGTATGTCCACATGTTTCTGCTGGCA 660
201 M F F T M L V L M A S L Y V H M F L L A 220
661 CGCTTGCACATGAAGCGCATTGCGGCGATGCAGGGCAACGCACCCATTCAGCAGCGGGCC 720
221 R L H M K R I A A M Q G N A P I Q Q R A 240
721 AACATGAAAGGCGCCATCACCCTCACGATCCTACTTGGGGTGTTCGTGGTGTGCTGGGCA 780
241 N M K G A I T L T I L L G V F V V C W A 260
781 CCGTTTTTCCTTCACCTCATCCTCATGATCACCTGCCCCAGGAACCCGTACTGCACCTGC 840
261 P F F L H L I L M I T C P R N P Y C T C 280
841 TTTATGTCCCACTTCAACATGTACCTCATTCTCATCATGTGCAACTCCATCATTGACCCC 900
281 F M S H F N M Y L I L I M C N S I I D P 300
901 ATCATCTACGCTTTTCGCAGCCAGGAAATGAGAAAAACCTTCAAGGAGATTTTCTGCTGT 960
301 I I Y A F R S Q E M R K T F K E I F C C 320
961 TCACATTCTCTCCTGTGTGTG*TGA 984
321 S H S L L C V * 327

B

```
   1 ATGTCCGAGTTTCACAATCGGAGCCAAACCAGCGCACGTCGCAGTGACTACGTGTGGCAG  60
   1  M  S  E  F  H  N  R  S  Q  T  S  A  R  R  S  D  Y  V  W  Q   20
  61 TATGAATATTATGACGAAGAGCCGGTGTCTTTCGAGGGACTCAAAGCGCACAGATACTCA 120
  21  Y  E  Y  Y  D  E  E  P  V  S  F  E  G  L  K  A  H  R  Y  S   40
 121 ATTGTAATCGGCTTTTGGGTCGGACTCGCCGTGTTTGTCATATTCATGTTCTTTGTTCTC 180
  41  I  V  I  G  F  W  V  G  L  A  V  F  V  I  F  M  F  F  V  L   60
 181 ACGCTGCTCACAAAGACAGGAGCACCACATCAAGAAAACCCAGACTCTGCTGATAAGCGC 240
  61  T  L  L  T  K  T  G  A  P  H  Q  E  N  P  D  S  A  D  K  R   80
 241 CATCGACCAGATAGCTGTCTGGTTGACATTGATGGCCTTCAAGATGAAAACGACAAAGCT 300
  81  H  R  P  D  S  C  L  V  D  I  D  G  L  Q  D  E  N  D  K  A  100
 301 TTCTCTCGACCATTGCTAGCGGGGTCCCACTCATATTTACATTTTATGTCAACAAGGAG 360
 101  F  S  R  P  L  L  A  G  S  H  S  Y  L  H  F  Y  V  N  K  E  120
 361 GATCAGGGTCAGGGGAAGCAAAAAACTGAAGATATGAATGGTGGAAAGCACCCAGGGGCG 420
 121  D  Q  G  Q  G  K  Q  K  T  E  D  M  N  G  G  K  H  P  G  A  140
 421 TGGGCCCATCCTGGAGCCTGCAGTGGGGCAAGGGGTATTGGCTCCTCTGGGATGGGTGAT 480
 141  W  A  H  P  G  A  C  S  G  A  R  G  I  G  S  S  G  M  G  D  160
 481 ATGGAAGAGGAGGCTGAGGAAACTGGGGGAAATCAACCTCTTAAAGGTCTATTGGAAGAC 540
 161  M  E  E  E  A  E  E  T  G  G  N  Q  P  L  K  G  L  L  E  D  180
 541 AGTACAGACAGAGAGTCTGCATTTCTGTCCCACTTCAACATCCCTAATTTTGTGAACTTG 600
 181  S  T  D  R  E  S  A  F  L  S  H  F  N  I  P  N  F  V  N  L  200
 601 GAGCACAGTTCAATATTTGGAGAGGAGGATCTGTACGAGCCGTCCGTCATGCTGGAGCCC 660
 201  E  H  S  S  I  F  G  E  E  D  L  Y  E  P  S  V  M  L  E  P  220
 661 CCGTCTCACTCTCAGCACTGTGACCTCCACTAA                             693
 221  P  S  H  S  Q  H  C  D  L  H  *                             230
```

Fig. 2.1. Nucleotide and deduced protein sequences of snakehead MC4R (A) and MRAP2 (B).

Positions of nucleotide and amino acid sequences were indicated on both sides. Open boxes denoted the consensus sequence for N-linked glycosylation sites. Amino acids in shaded boxes indicated putative transmembrane domains. Underlines showed PMY, DRY, and DPxxY motifs in MC4R. Asterisk (*) indicated stop codon.

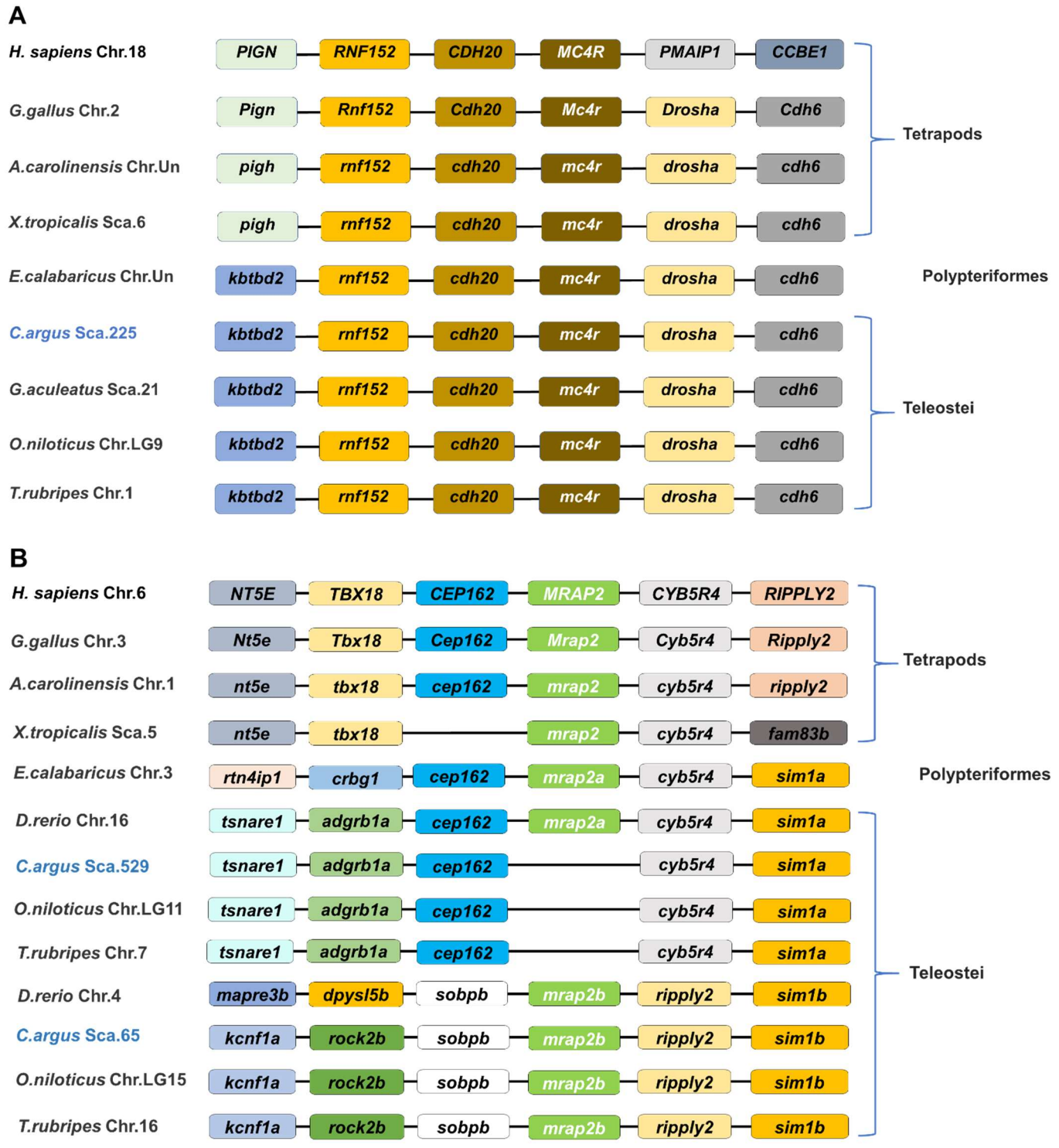

Fig. 2.2. Comparative gene synteny of *MC4R* (A) and *MRAP2* (B) among representative vertebrate genomes.

The colored boxes represent genes and solid lines stand for intergenic regions. The genes showing conserved synteny were indicated with same color. Taxon names of selected species were shown on the left side of the figure.

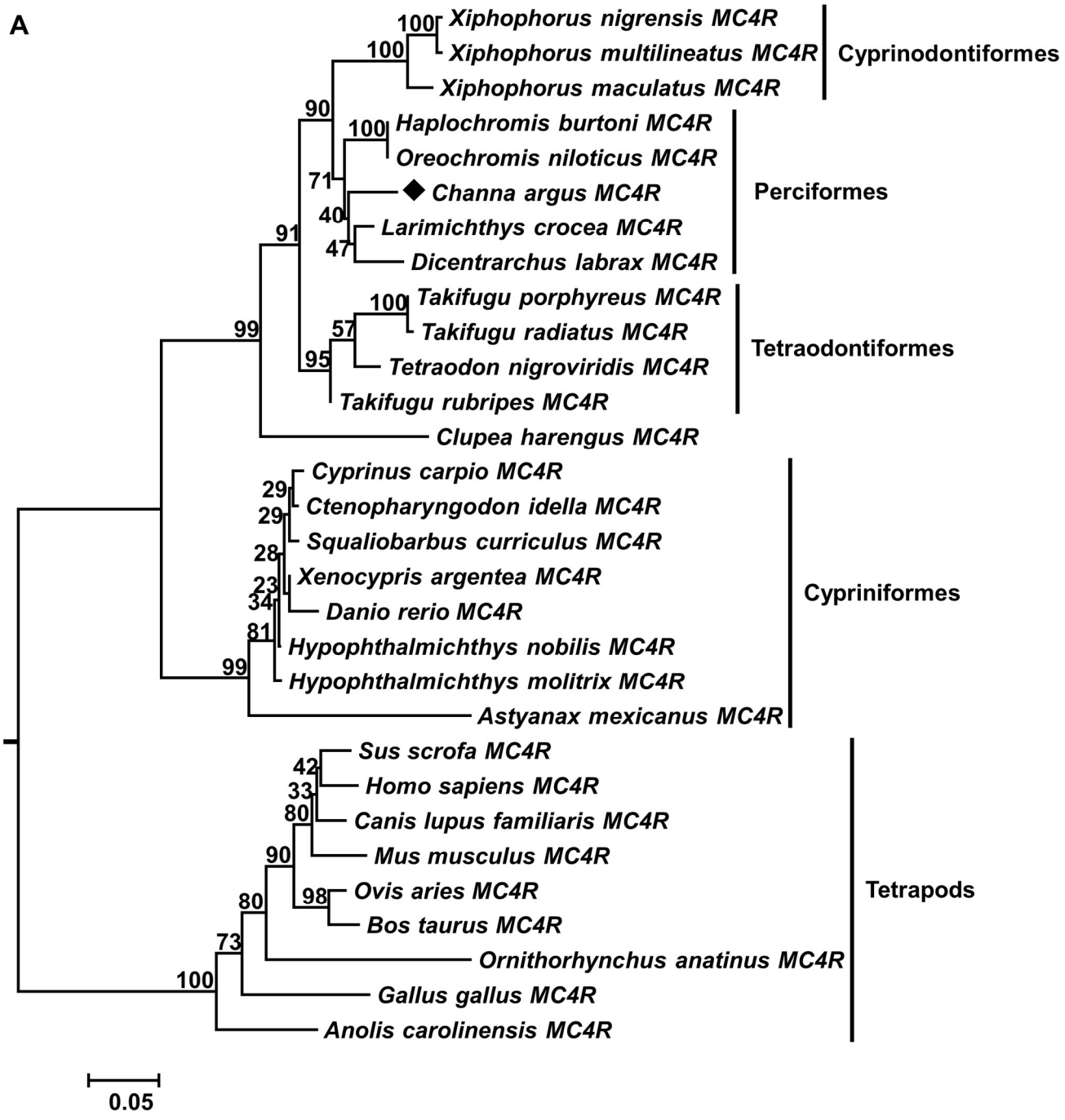
A
Xiphophorus nigrensis MC4R
Xiphophorus multilineatus MC4R
Xiphophorus maculatus MC4R
Cyprinodontiformes
Haplochromis burtoni MC4R
Oreochromis niloticus MC4R
Channa argus MC4R
Larimichthys crocea MC4R
Dicentrarchus labrax MC4R
Perciformes
Takifugu porphyreus MC4R
Takifugu radiatus MC4R
Tetraodon nigroviridis MC4R
Takifugu rubripes MC4R
Tetraodontiformes
Clupea harengus MC4R
Cyprinus carpio MC4R
Ctenopharyngodon idella MC4R
Squaliobarbus curriculus MC4R
Xenocypris argentea MC4R
Danio rerio MC4R
Hypophthalmichthys nobilis MC4R
Hypophthalmichthys molitrix MC4R
Astyanax mexicanus MC4R
Cypriniformes
Sus scrofa MC4R
Homo sapiens MC4R
Canis lupus familiaris MC4R
Mus musculus MC4R
Ovis aries MC4R
Bos taurus MC4R
Ornithorhynchus anatinus MC4R
Gallus gallus MC4R
Anolis carolinensis MC4R
Tetrapods
0.05

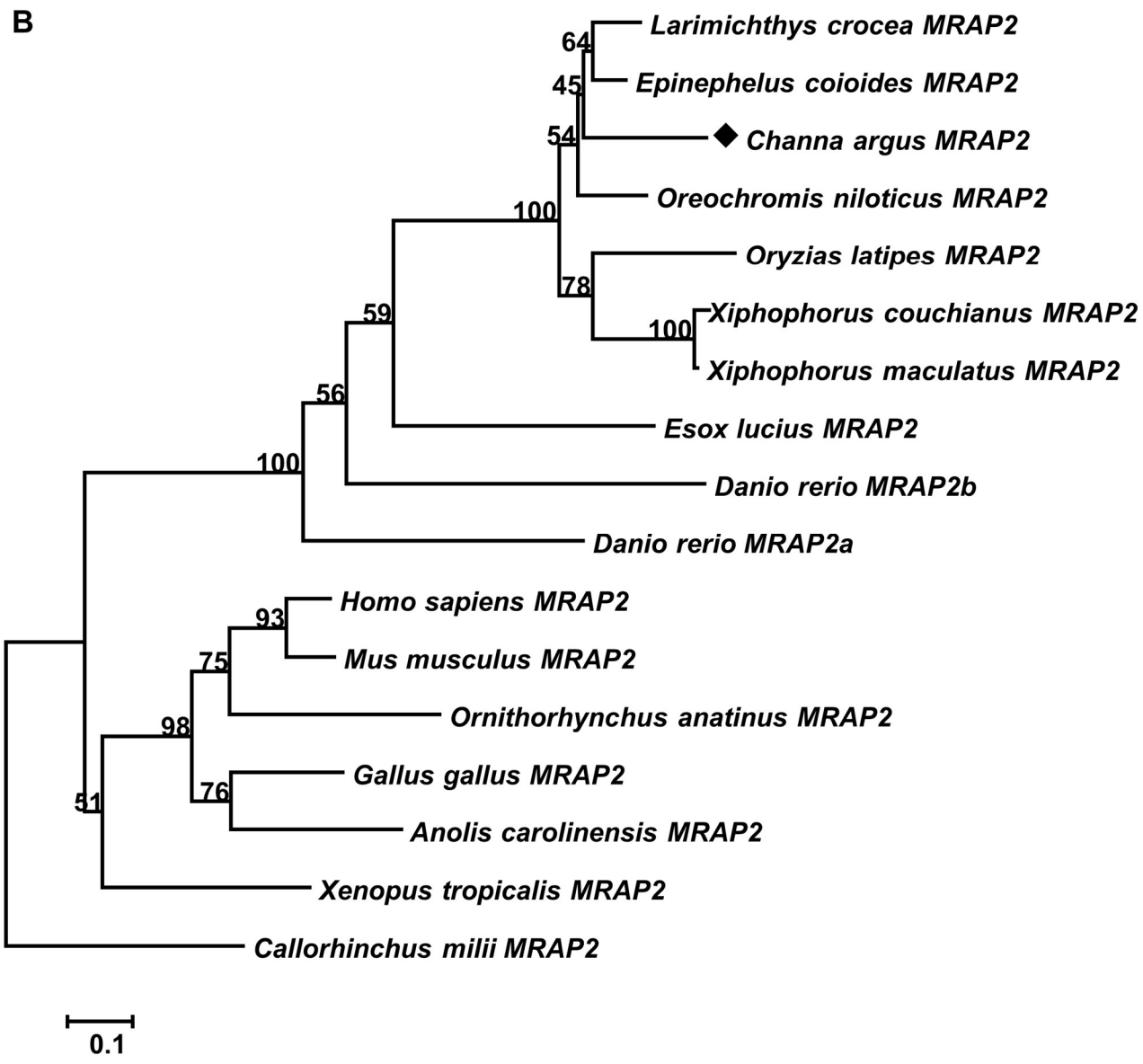

Fig. 2.3. Phylogenetic trees of vertebrate MC4R (A) and MRAP2 (B).

Both trees were constructed with MEGA 6.0 software based on protein datasets. The values at the nodes represented boot-strap percentages from 1000 replicates. The caMC4R and caMRAP2 were marked with a black diamond. The IDs of protein sequences used in present study were shown in Table S2.2 and Table S2.3.

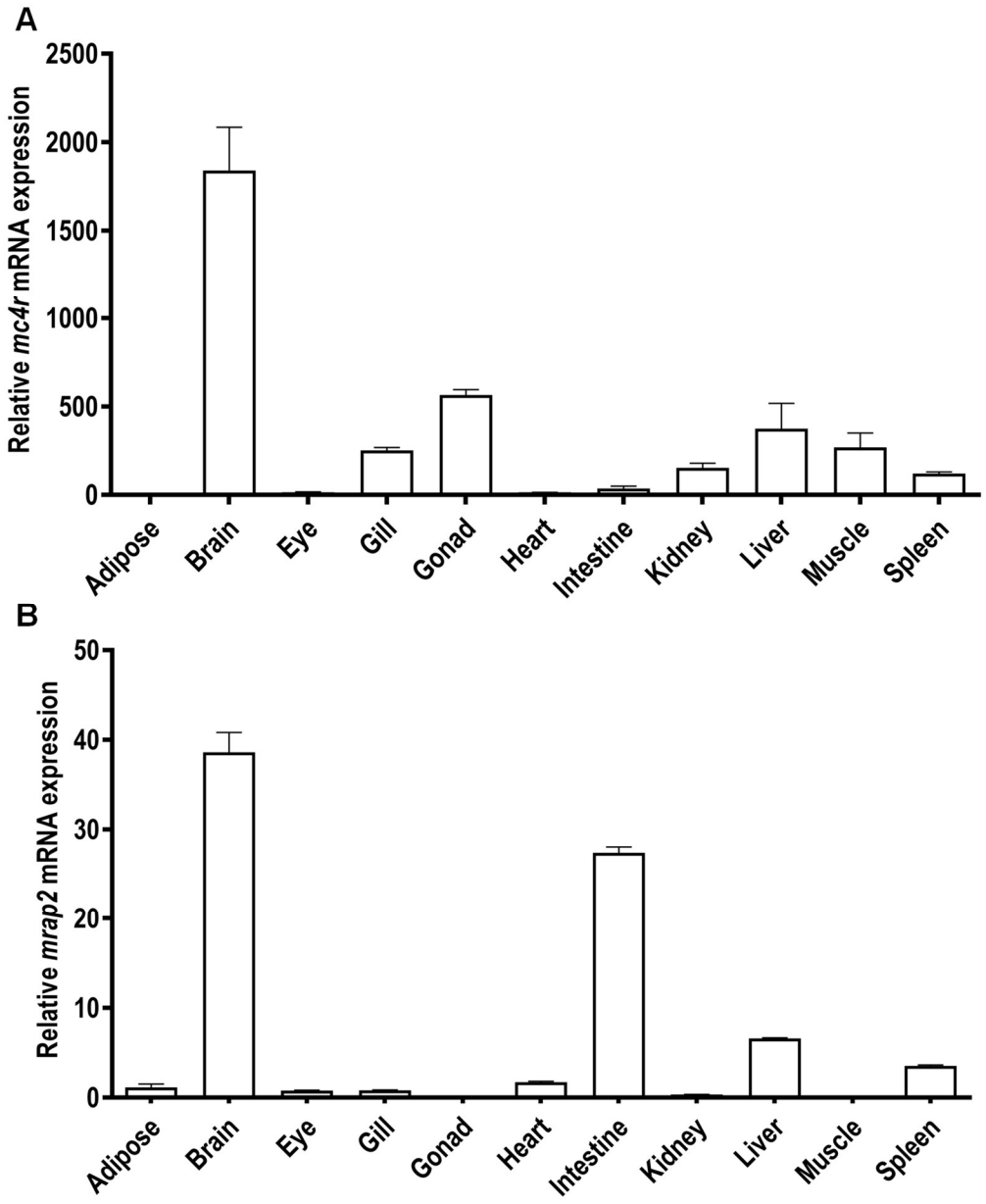

Fig. 2.4. Tissue distribution patterns of snakehead *mc4r* (A) and *mrap2* (B).

Eleven tissues were studied in the present study. Results were expressed as relative expression levels and standardized by tubα1-b gene. Error bars represented standard error of the mean (SEM) (n = 6).

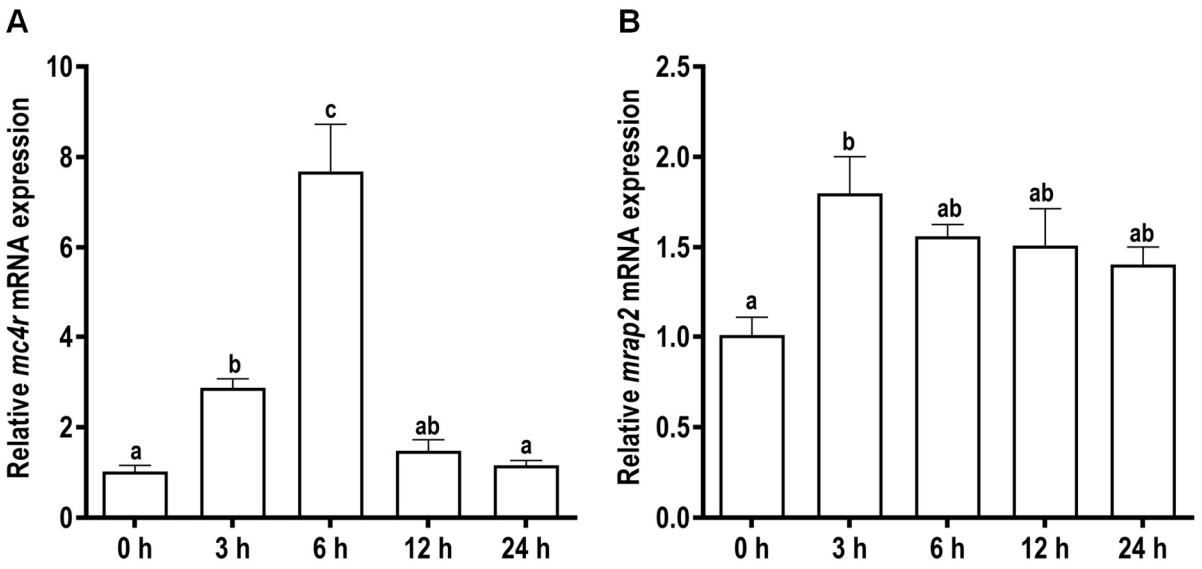

Fig. 2.5. Effects of short-term (24 h) fasting on the expressions of cerebral *mc4r* (A) and *mrap2* (B) in snakehead.

Data were represented as mean ± SEM (n = 6). Significant differences ($P < 0.05$) between groups were detected using a one-way ANOVA. Groups that differ significantly were indicated by different letters above bars.

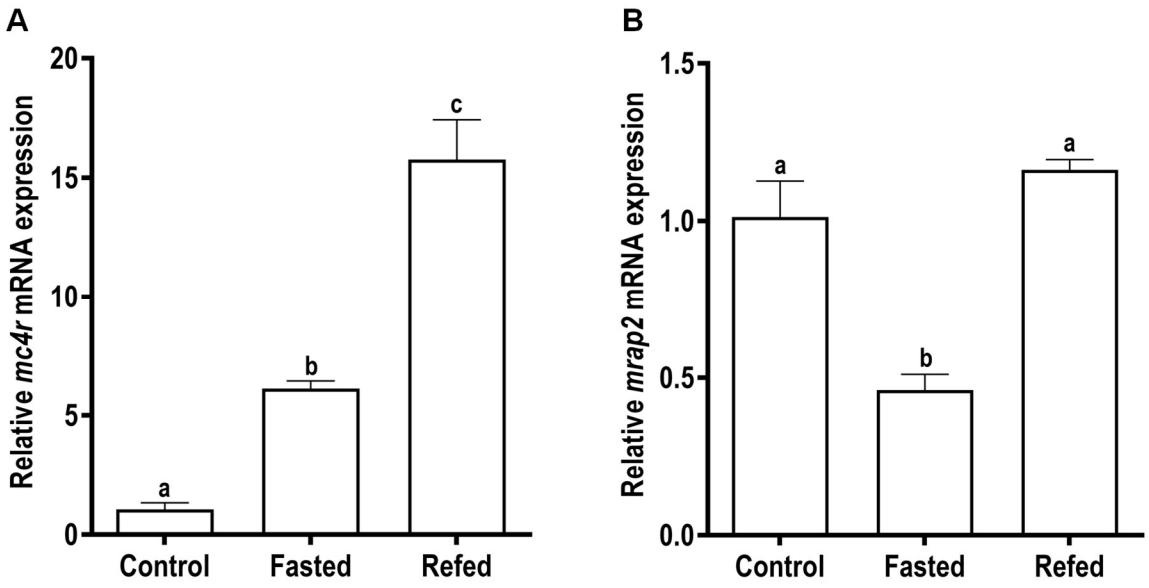

Fig. 2.6. Effects of long-term (2 weeks) fasting and refeeding on expressions of brain *mc4r* (A) and *mrap2* (B) in snakehead.

Data were presented as mean ± SEM (n = 6). Significant difference ($P < 0.05$) between groups was determined using one-way ANOVA. Groups that differ significantly were indicated by different letters above bars.

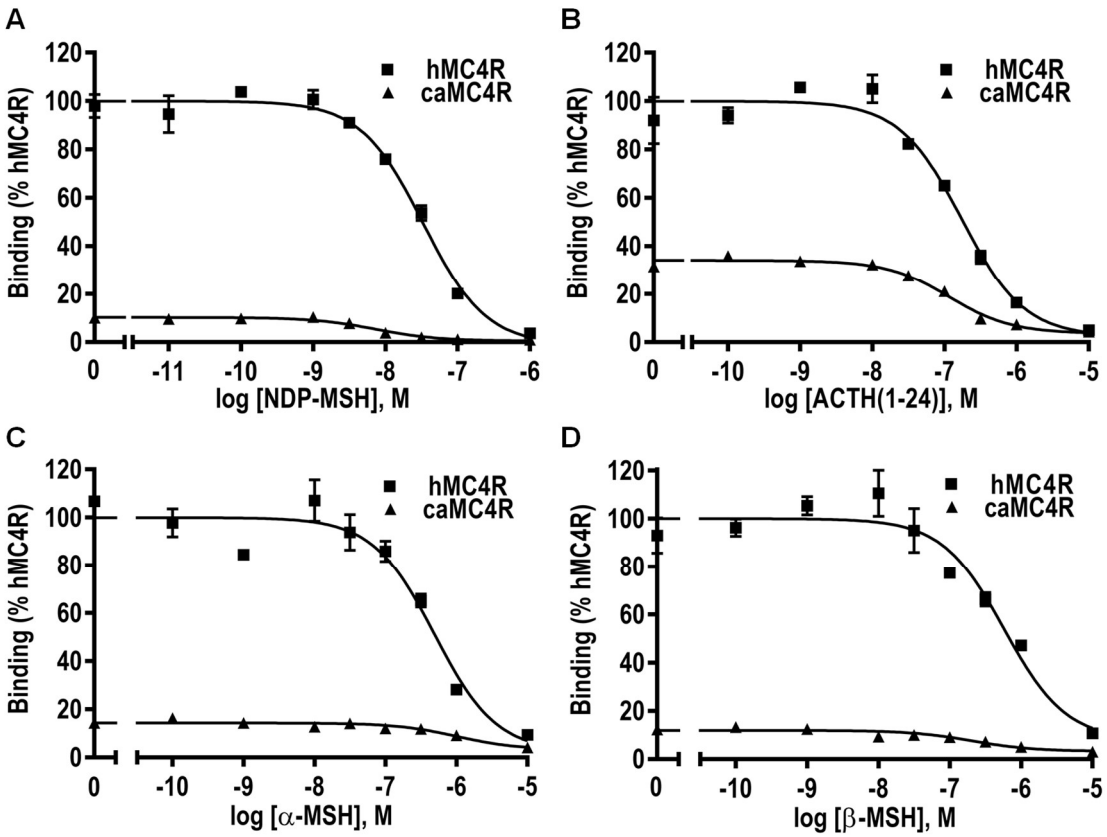

Fig. 2.7. Ligand binding properties of caMC4R.

HEK293T cells were transiently transfected with MC4R plasmids, and the binding properties were measured 48 h later by displacing the binding of ^{125}I-NDP-MSH using different concentrations of unlabeled NDP-MSH (A), ACTH (1-24) (B), α-MSH (C), or β-MSH (D) as described in Materials and Methods. Data were expressed as % of hMC4R binding ± range in the absence of competitor from duplicate measurements within one experiment. All experiments were performed at least three times independently.

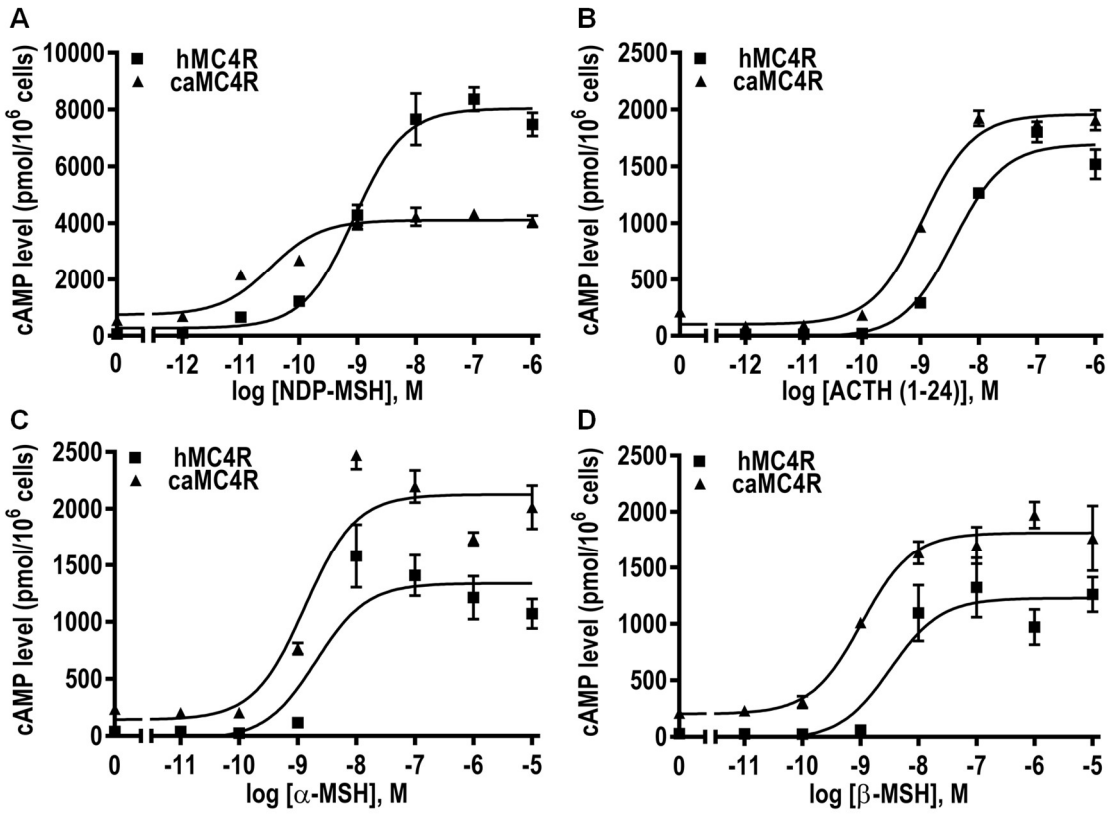

Fig. 2.8. Signaling properties of caMC4R.

HEK293T cells were transiently transfected with MC4R plasmids, and the intracellular cAMP levels were measured 48 h later via radioimmunoassay. Different concentrations of NDP-MSH (A), ACTH (1-24) (B), α-MSH (C), or β-MSH (D) were used to stimulate HEK293T cell. Data were expressed as mean ± SEM from triplicate measurements within one experiment. The curves were representative of at least three independent experiments.

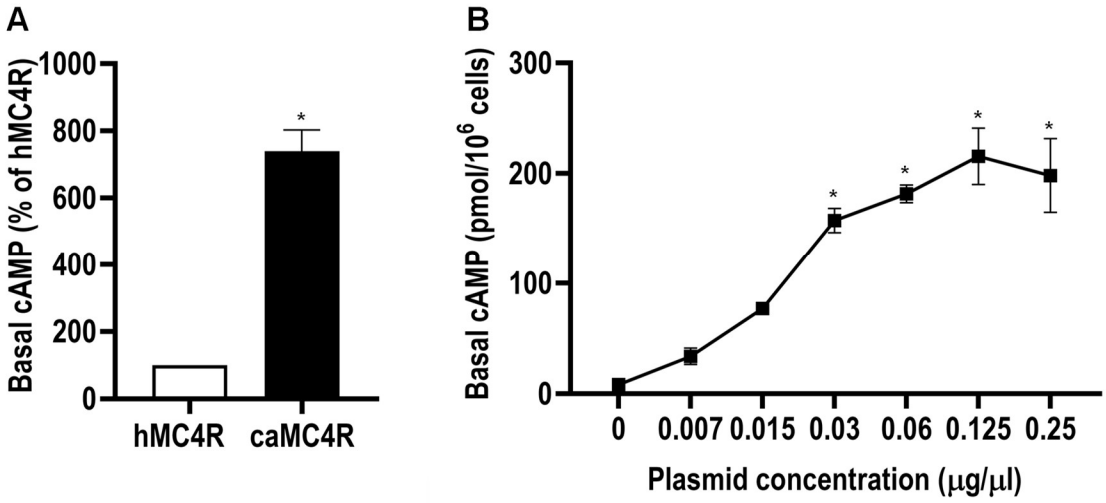

Fig. 2.9. Constitutive activities of caMC4R in cAMP signaling pathway.

HEK293T cells were transiently transfected with 0.25 μg/μL hMC4R or caMC4R to compare their basal cAMP activity (A) or transfected with increasing concentrations of caMC4R (B). Data were expressed as mean ± SEM (n ≥ 3). Asterisk (*) showed significant difference ($P < 0.05$) of basal cAMP level compared with respective control group (Student's t-test in A and one-way ANOVA followed by Tukey-test in B).

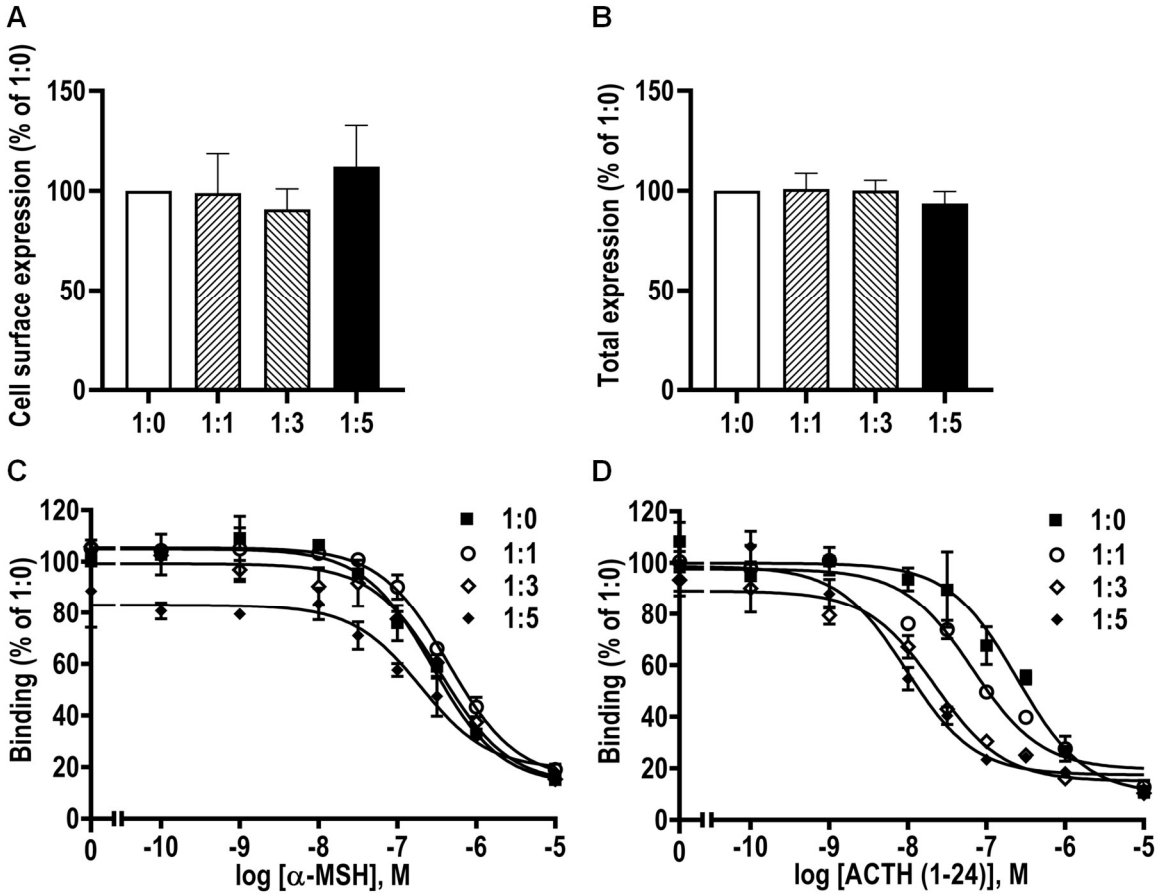

Fig. 2.10. Modulation of caMC4R expression and binding properties by caMRAP2. HEK293T cells were co-transfected with caMC4R/caMRAP2 in four different ratios (1:0, 1:1, 1:3, and 1:5). Cell surface (A) and total (B) expression levels of caMC4R were measured by flow cytometry. Ligand binding experiments (C,D) were performed as in Fig. 2.7. The results, calculated as percentage of 1:0 group, were expressed as the mean ± SEM of at least three independent experiments.

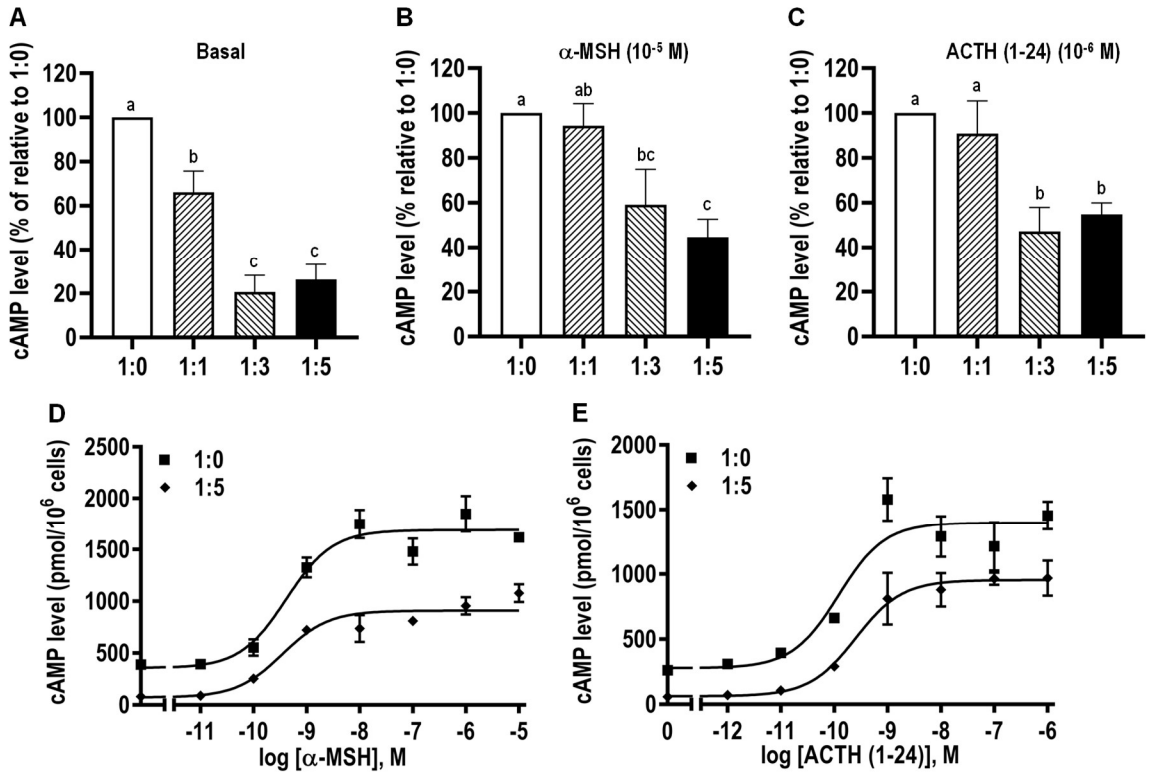

Fig. 2.11. Effects of caMRAP2 on signaling properties of caMC4R.

HEK293T cells were co-transfected with caMC4R/caMRAP2 in four different ratios (1:0, 1:1, 1:3, and 1:5), and cAMP levels under basal (A) or stimulated with 10^{-5} M α-MSH or 10^{-6} M ACTH (1-24) (B,C) were measured. The results were calculated as a percentage of 1:0 group. Results were expressed as mean ± SEM (n ≥ 3). Different letters indicate significant difference (one-way ANOVA followed by Tukey-test). (D,E) The curves represented at least three independent experiments in which different concentrations of α-MSH or ACTH (1-24) were used to stimulate cells co-transfected with caMC4R and caMRAP2 at the ratios of 1:0 and 1:5.

A

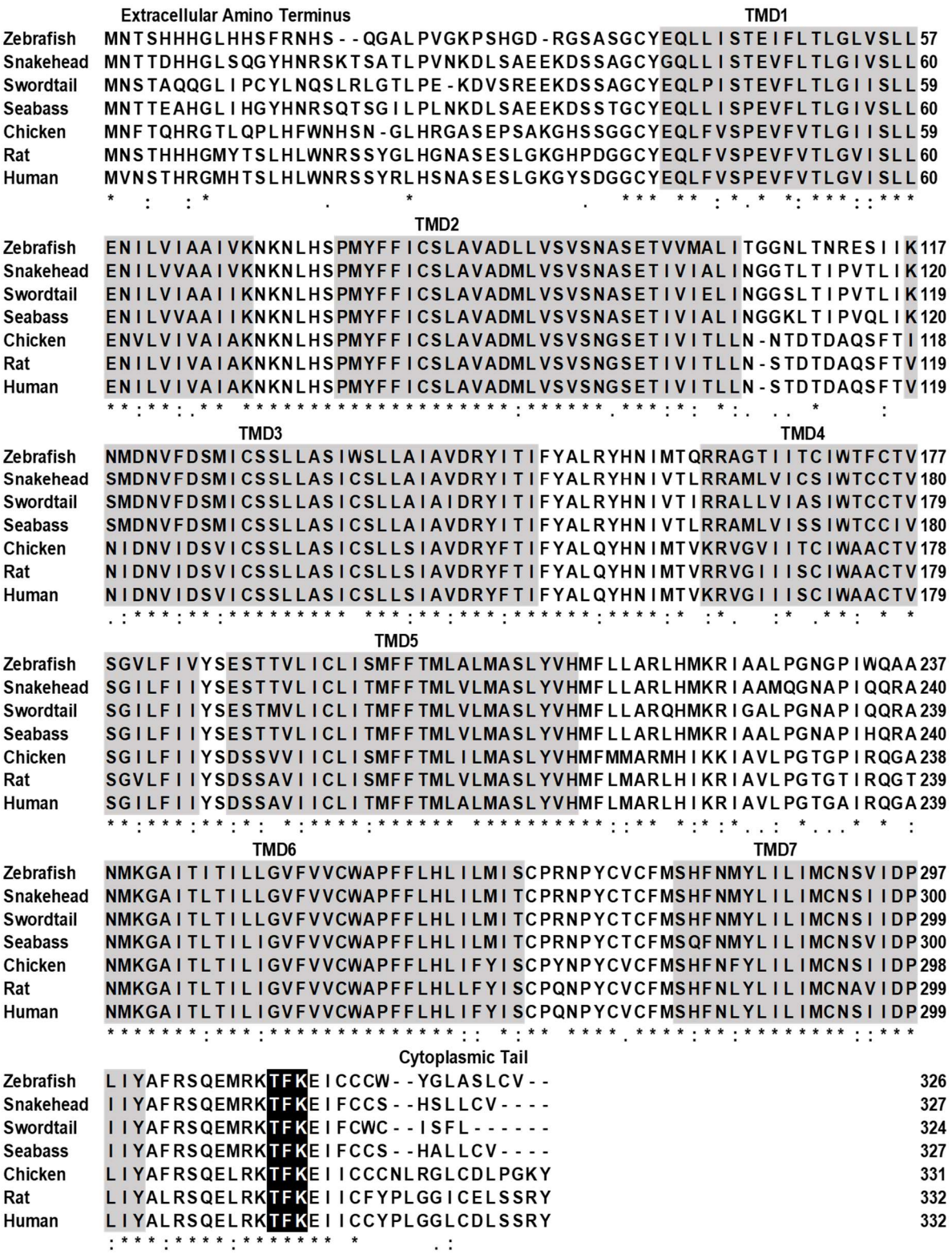
Extracellular Amino Terminus
TMD1
TMD2
TMD3
TMD4
TMD5
TMD6
TMD7
Cytoplasmic Tail
Zebrafish MNTSHHHGLHHSFRNHS--QGALPVGKPSHGD-RGSASGCYEQLLISTEIFLTLGLVSLL 57
Snakehead MNTTDHHGLSQGYHNRSKTSATLPVNKDLSAEEKDSSAGCYGQLLISTEVFLTLGIVSLL 60
Swordtail MNSTAQQGLIPCYLNQSLRLGTLPE-KDVSREEKDSSAGCYEQLPISTEVFLTLGIISLL 59
Seabass MNTTEAHGLIHGYHNRSQTSGILPLNKDLSAEEKDSSTGCYEQLLISPEVFLTLGIVSLL 60
Chicken MNFTQHRGTLQPLHFWNHSN-GLHRGASEPSAKGHSSGGCYEQLFVSPEVFVTLGIISLL 59
Rat MNSTHHHGMYTSLHLWNRSSYGLHGNASESLGKGHPDGGCYEQLFVSPEVFVTLGVISLL 60
Human MVNSTHRGMHTSLHLWNRSSYRLHSNASESLGKGYSDGGCYEQLFVSPEVFVTLGVISLL 60
Zebrafish ENILVIAAIVKNKNLHSPMYFFICSLAVADLLVSVSNASETVVMALITGGNLTNRESIIK 117
Snakehead ENILVVAAIVKNKNLHSPMYFFICSLAVADMLVSVSNASETIVIALINGGTLTIPVTLIK 120
Swordtail ENILVIAAIIKNKNLHSPMYFFICSLAVADMLVSVSNASETIVIELINGGSLTIPVTLIK 119
Seabass ENILVVAAIIKNKNLHSPMYFFICSLAVADMLVSVSNASETIVIALINGGKLTIPVQLIK 120
Chicken ENVLVIVAIAKNKNLHSPMYFFICSLAVADMLVSVSNGSETIVITLLN-NTDTDAQSFTI 118
Rat ENILVIVAIAKNKNLHSPMYFFICSLAVADMLVSVSNGSETIVITLLN-STDTDAQSFTV 119
Human ENILVIVAIAKNKNLHSPMYFFICSLAVADMLVSVSNGSETIVITLLN-STDTDAQSFTV 119
Zebrafish NMDNVFDSMICSSLLASIWSLLAIAVDRYITIFYALRYHNIMTQRRAGTIITCIWTFCTV 177
Snakehead SMDNVFDSMICSSLLASICSLLAIAVDRYITIFYALRYHNIVTLRRAMLVICSIWTCCTV 180
Swordtail SMDNVFDSMICSSLLASICSLLAIAIDRYITIFYALRYHNIVTIRRALLVIASIWTCCTV 179
Seabass SMDNVFDSMICSSLLASICSLLAIAVDRYITIFYALRYHNIVTLRRAMLVISSIWTCCIV 180
Chicken NIDNVIDSVICSSLLASICSLLSIAVDRYFTIFYALQYHNIMTVKRVGVIITCIWAACTV 178
Rat NIDNVIDSVICSSLLASICSLLSIAVDRYFTIFYALQYHNIMTVRRVGIIISCIWAACTV 179
Human NIDNVIDSVICSSLLASICSLLSIAVDRYFTIFYALQYHNIMTVKRVGIIISCIWAACTV 179
Zebrafish SGVLFIVYSESTTVLICLISMFFTMLALMASLYVHMFLLARLHMKRIAALPGNGPIWQAA 237
Snakehead SGILFIIYSESTTVLICLITMFFTMLVLMASLYVHMFLLARLHMKRIAAMQGNAPIQQRA 240
Swordtail SGILFIIYSESTMVLICLITMFFTMLVLMASLYVHMFLLARQHMKRIGALPGNAPIQQRA 239
Seabass SGILFIIYSESTTVLICLITMFFTMLVLMASLYVHMFLLARLHMKRIAALPGNAPIHQRA 240
Chicken SGILFIIYSDSSVVIICLISMFFTMLILMASLYVHMFMMARMHIKKIAVLPGTGPIRQGA 238
Rat SGVLFIIYSDSSAVIICLISMFFTMLVLMASLYVHMFLMARLHIKRIAVLPGTGTIRQGT 239
Human SGILFIIYSDSSAVIICLITMFFTMLALMASLYVHMFLMARLHIKRIAVLPGTGAIRQGA 239
Zebrafish NMKGAITITILLGVFVVCWAPFFLHLILMISCPRNPYCVCFMSHFNMYLILIMCNSVIDP 297
Snakehead NMKGAITLTILLGVFVVCWAPFFLHLILMITCPRNPYCTCFMSHFNMYLILIMCNSIIDP 300
Swordtail NMKGAITLTILLGVFVVCWAPFFLHLILMITCPRNPYCTCFMSHFNMYLILIMCNSIIDP 299
Seabass NMKGAITLTILIGVFVVCWAPFFLHLILMITCPRNPYCTCFMSQFNMYLILIMCNSVIDP 300
Chicken NMKGAITLTILIGVFVVCWAPFFLHLIFYISCPYNPYCVCFMSHFNFYLILIMCNSIIDP 298
Rat NMKGAITLTILIGVFVVCWAPFFLHLLFYISCPQNPYCVCFMSHFNLYLILIMCNAVIDP 299
Human NMKGAITLTILIGVFVVCWAPFFLHLIFYISCPQNPYCVCFMSHFNLYLILIMCNSIIDP 299
Zebrafish LIYAFRSQEMRKTFKEICCCW--YGLASLCV-- 326
Snakehead IIYAFRSQEMRKTFKEIFCCS--HSLLCV---- 327
Swordtail IIYAFRSQEMRKTFKEIFCWC--ISFL------ 324
Seabass IIYAFRSQEMRKTFKEIFCCS--HALLCV---- 327
Chicken LIYAFRSQELRKTFKEIICCCNLRGLCDLPGKY 331
Rat LIYALRSQELRKTFKEIICFYPLGGICELSSRY 332
Human LIYALRSQELRKTFKEIICCYPLGGLCDLSSRY 332

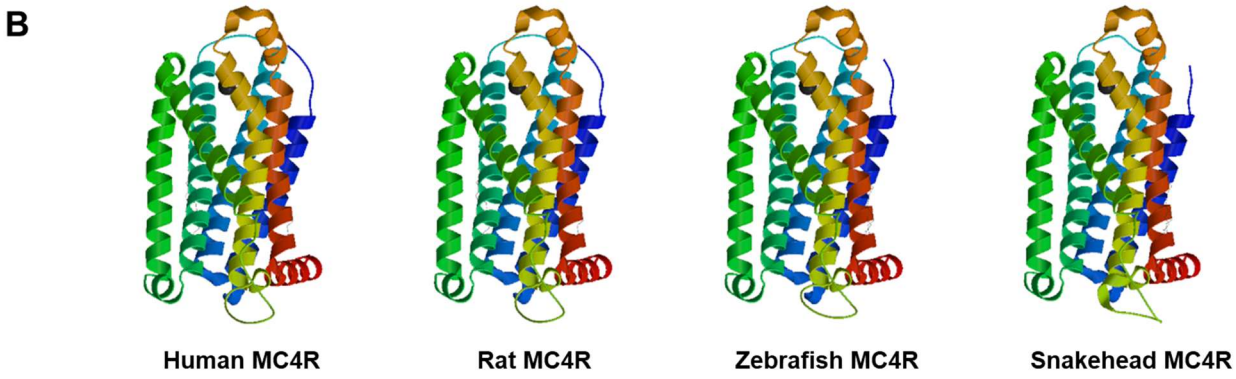

Fig. S2.1. Comparison of amino acid sequences between caMC4R and MC4Rs from other species (A) and the putative three-dimensional structure of snakehead MC4R and those of relative model species (B).

Labeled as follows: transmembrane domains were shown in shaded boxes and named as TMD 1-7, amino and carboxyl termini were represented as extracellular amino terminus and cytoplasmic tail, respectively. Predicted phosphorylation sites were shown by dark shadow. Asterisk (*) indicated the same amino acids. Cellular was shown by a green frame box, followed with an extracellular N-terminus and intracellular C-terminus, respectively. Seven transmembrane domains were shown in the figure. Amino acid was represented by a circular round.

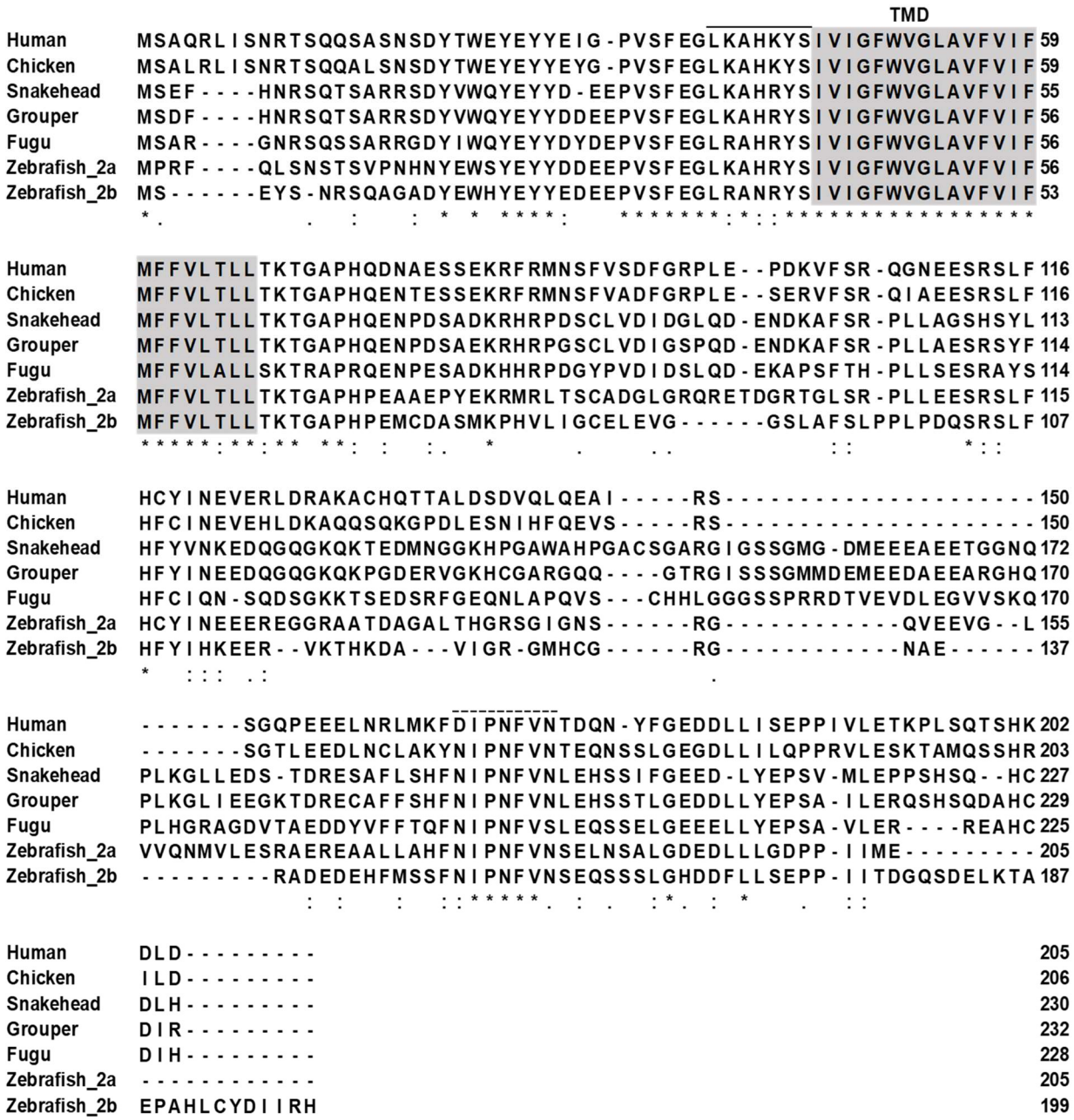

Fig. S2.2. Multiple alignment of snakehead MRAP2 with that of other species.

The transmembrane domain (TMD) was boxed. The above solid line showed the conserved motif (LKAHRYS) required for the formation of antiparallel homodimer. The above dashed line denoted the conserved motif (NIPNFVN) in C-terminus. Asterisk (*) indicated the same amino acids.

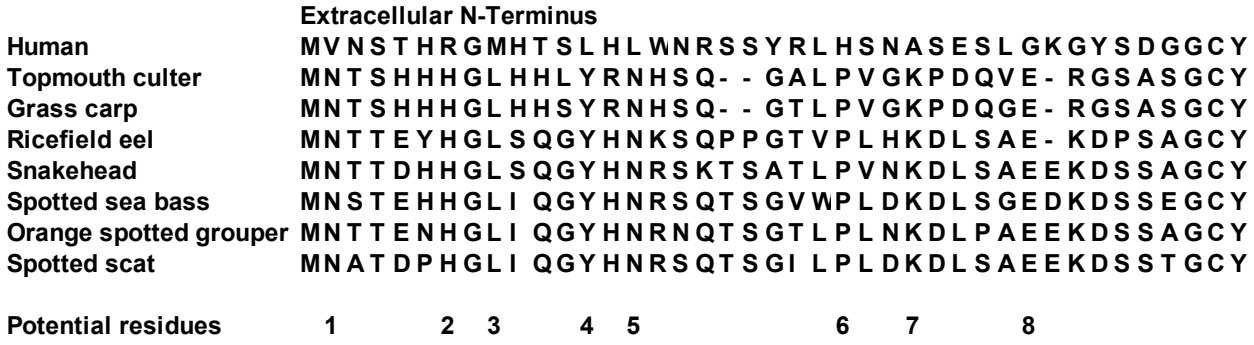

Fig. S2.3. Multiple alignment of extracellular N-termini of hMC4R and fish MC4Rs with higher basal activity.

The potential residues represented the amino acids which were conserved in fish MC4Rs, but different in hMC4R.

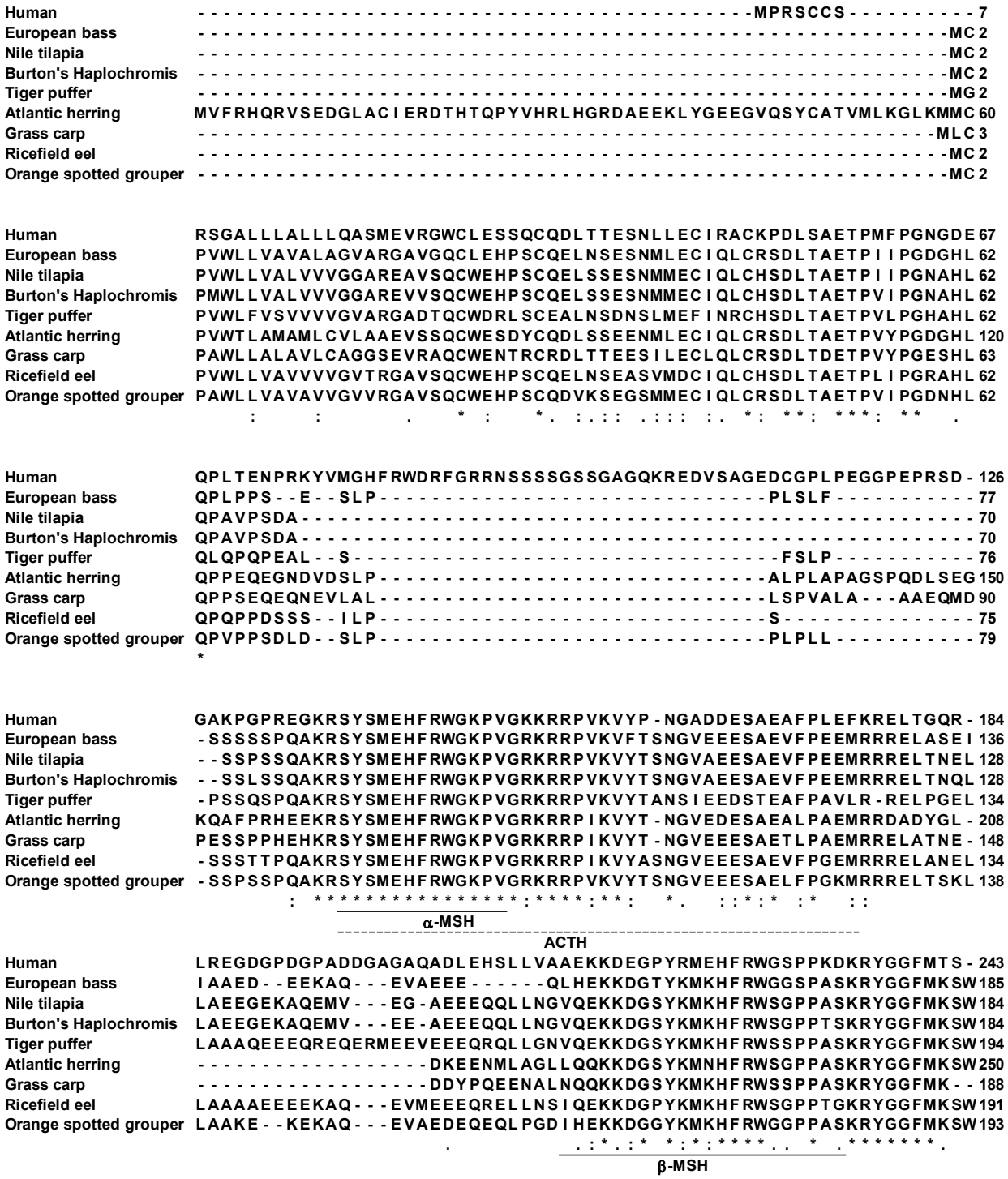
Human
European bass
Nile tilapia
Burton's Haplochromis
Tiger puffer
Atlantic herring
Grass carp
Ricefield eel
Orange spotted grouper
α-MSH
ACTH
β-MSH

Fig. S2.4. Comparison of amino acid sequences of POMC between fish and human. Labeled as follows: the solid line represented α-MSH and β-MSH, and dashed line indicated the ACTH. Asterisk (*) indicated the same amino acids.

Chapter 3: Regulation of melanocortin-5 receptor pharmacology by two isoforms of MRAP2 in ricefield eel (*Monopterus albus*)

3.1. Introduction

Melanocortin receptors (MCRs), consisting of five members (MC1R to MC5R), belong to Family A (rhodopsin-like) G protein-coupled receptors (GPCRs) (Cone, 2006; Tao, 2017). The MCRs are unique since they have both natural agonists, including α-melanocyte stimulating hormone (MSH), β-MSH, γ-MSH and ACTH, and antagonists, including agouti-signaling protein and agouti-related peptide (AGRP) (Ringholm et al., 2002). The agonists are the products of proopiomelanocortin (POMC) through tissue-specific post-translational processing, whereas the antagonists are generated from separate precursors (Ringholm et al., 2002). After activation, MC1R mediates effects of MSH on pigmentation, MC2R regulates the adrenal steroidogenesis, whereas MC3R and MC4R play crucial nonredundant roles in energy homeostasis (Cone, 2006; Tao, 2017).

In mammals, MC5R is expressed in the central nervous system, exocrine gland, immune cells and a multitude of other peripheral tissues (Chhajlani, 1996; Griffon et al., 1994; Xu et al., 2020). *Mc5r* knockout mice exhibit severe dysfunction in exocrine secretion, resulting in reduced hair lipid content, defect in water repulsion, and impaired thermoregulatory function (Chen et al., 1997; Morgan and Cone, 2006; Morgan et al., 2004). This suggests that MC5R is centrally involved in sebogenesis and can serve as a marker of sebocyte differentiation (Zhang et al., 2006). MC5R is also involved in murine adipocyte differentiation and stimulates lipolysis and suppresses re-esterification upon α-MSH stimulation (Boston and Cone, 1996; Rodrigues et al., 2013). An et al. demonstrated that MC5R plays an important role in fatty acid oxidation in skeletal muscles (An et al.,

2007). In addition, MC5R is also associated with inflammatory response in adipocytes and eyes (Jun et al., 2010; Taylor et al., 2006) (reviewed in (Xu et al., 2020)).

A few studies have characterized fish MC5Rs. The piscine MC5Rs display similar tissue distribution as in mammals, in both central and peripheral tissues (Cerdá-Reverter et al., 2003a; Klovins et al., 2004; Liao et al., 2019; Ringholm et al., 2002; Sánchez et al., 2009a). In sea bass, MTII stimulates hepatic lipolysis through MC5R *in vitro*, suggesting that MC5R is involved in the control of hepatic lipid metabolism (Sánchez et al., 2009a). In blunt snout bream, MC5R expression levels of skin, eye and brain are affected significantly by catching stress, indicating that MC5R might play a role in stress response (Liao et al., 2019). In addition, color change of flounder may be controlled by heterodimerization of MC1R and MC5R (Kobayashi et al., 2016).

Melanocortin-2 receptor accessory protein 2 (MRAP2), together with MRAP1, are single-transmembrane proteins and involved in regulating expression, binding, and signaling of MCRs (Asai et al., 2013; Cerdá-Reverter et al., 2013; Chan et al., 2009; Sebag et al., 2013). MRAP1 primarily chaperones MC2R to the plasma membrane and is also involved in both ACTH binding and ACTH-induced cAMP generation (Roy et al., 2007; Webb and Clark, 2010). *MRAP1* mutations are responsible for about 20% of familial glucocorticoid deficiency (Metherell et al., 2005). MRAP2 was reported to be involved in the regulation of energy homeostasis (Rouault et al., 2017b). In European cohorts with severe early-onset obesity, three *MRAP2* mutations have been identified (Asai et al., 2013). In mammals, the number of *MC5R* and *MRAP2* gene is constant. However, it varies in fishes. There are two forms of *mc5r* (*mc5ra* and *mc5rb*) in zebrafish and *mc5ra* is identified as the evolutionarily homologous paralog to the mammalian *MC5R* (Zhu et al., 2019a). Similarly, there are also two copies of *mrap2* (*mrap2a* and *mrap2b*) in

zebrafish and topmouth culter and functional studies showed that two MRAP2s in these fishes perform different roles in regulating MCRs (Sebag et al., 2013; Tao et al., 2020; Zhu et al., 2019a).

So far, a few studies have investigated the modulation of MC5R pharmacology by MRAP2, in human, mouse, chicken, zebrafish, gar, whale shark and elephant shark (Barney et al., 2019; Chan et al., 2009; Dores et al., 2020; Hoglin et al., 2020; Thomas et al., 2018; Wolverton et al., 2019; Zhu et al., 2019a). To further reveal the interaction between MC5R and MRAP2, herein we explored MC5R pharmacology and its regulation by MRAP2 in ricefield eel.

Ricefield eel, *Monopterus albus* (family Synbranchidae; order Synbranchiformes), is an air-breathing protogynous sex-reversing fish (Liu, 1944; Tao et al., 1993; Yi et al., 2018). This fish is distributed in the tropical and subtropical areas with significant economic and research value, for example, as a model for vertebrate sexual development (Cheng et al., 2003). The eel *mc5r* and two transcript variants of *mrap2* gene have been published online. In this study, we explored the pharmacological characteristics of maMC5R and the influences of maMRAP2s on maMC5R.

3.2. Materials and Methods

3.2.1. Ligands and plasmids

The ligands used included [Nle^4, D-Phe^7]-α-MSH (NDP-MSH) purchased from Peptides International (Louisville, KY, USA), human α-MSH from Pi Proteomics (Huntsville, AL, USA), and ACTH (1-24) from Phoenix Pharmaceuticals (Burlingame, CA, USA). We

analyzed ricefield eel *pomc* gene and discovered that the homology of eel α-MSH and ACTH (1-24) with human counterparts were 100% and 88%, respectively (Fig. S3.1). [^{125}I]-NDP-MSH and [^{125}I]-cAMP were iodinated using chloramine T method as described previously (Mo et al., 2012; Steiner et al., 1969). The N-terminal c-myc-tagged wild-type hMC5R was subcloned into pcDNA3.1 vector as previously described (Tao and Segaloff, 2003). Ricefield eel MC5R, MRAP2X1, and MRAP2X2 orthologs, were synthesized from sequences available in NCBI genome browser: *mc5r* (XM_020606732.1), *mrap2x1* (XM_020589331.1), *mrap2x2* (XM_020589337.1) (Li et al., 2017b). N-terminal c-myc-tagged maMC5R, N-terminal FLAG-tagged maMRAP2X1, and N-terminal FLAG-tagged maMRAP2X2 were subcloned into pcDNA3.1 vector by GenScript (Piscataway, NJ, USA) to generate the plasmids used for transfection.

3.2.2. Homology, phylogenetic, and chromosome synteny analyses

Multiple alignments of amino acid sequences of MC5Rs, POMCs, and MRAP2s from different species were performed using Clustal Omega. The putative transmembrane domains (TMDs) of maMC5R were predicted based on the crystal structure of rhodopsin (Palczewski et al., 2000). A phylogenetic tree based on the amino acid sequences was generated by MEGA 7.0 with the neighbor-joining (NJ) method which was set with 1000 bootstrap replications (Kumar et al., 2016; Saitou and Nei, 1987). Chromosome synteny analysis was performed between several fish and mammalian species with Ensembl (https://useast.ensembl.org/index.html) and NCBI genome browser (https://www.ncbi.nlm.nih.gov).

3.2.3. Cell culture and transfection

Human embryonic kidney (HEK) 293T cells (ATCC, Manassas, VA, USA) were used for pharmacological analysis. Cells were cultured in a 5% CO_2-humidified atmosphere at 37°C. The Dulbecco's Modified Eagle's medium (DMEM) (Invitrogen, Carlsbad, CA, USA) contained 10% newborn calf serum, 10 mM HEPES, 0.25 μg/mL of amphotericin B, 50 μg/mL of gentamicin, 100 μg/mL of streptomycin and 100 IU/mL of penicillin. Cells were seeded into 6-well or 24-well plates (Corning, NY, USA) pre-coated with 0.1% gelatin. Cells were transfected with MC5R with or without MRAP2 plasmids at approximately 60 ~ 70% confluence by calcium phosphate precipitation method (Chen and Okayama, 1987). The empty vector pcDNA3.1 was used to normalize the total DNA in each well.

3.2.4. Flow cytometry assay

The effects of maMRAP2X1 or maMRAP2X2 displayed on the cell surface and total expression levels of maMC5R were studied using flow cytometry as described previously (Zhang et al., 2019). Cells were plated into 6-well plates and transfected with maMC5R and maMRAP2X1 or maMRAP2X2 plasmids in four ratios (1:0, 1:1, 1:3, and 1:5). The C6 Accuri Cytometer (Accuri Cytometers, Ann Arbor, MI, USA) was used to analyze fluorescence of cells. The fluorescence signals of group 1:0 (maMC5R fluorescence - pcDNA3.1 fluorescence) was set as 100%. The expression levels of maMC5R from other groups were calculated as the percentage of 1:0 group (Wang et al., 2008).

3.2.5. Ligand binding assays

Competitive binding assay was used to study the binding properties of maMC5R as described previously (Tao and Segaloff, 2003; Zhang et al., 2019). Cells were transfected with MC5R plasmids and three ligands were used (NDP-MSH (from 10^{-11} to 10^{-6} M), α-

MSH and ACTH (1-24) (both from 10^{-10} to 10^{-5} M)). To study the influence of maMRAP2X1 or maMRAP2X2 on the binding property of maMC5R, cells were co-transfected with maMC5R and maMRAP2X1 or maMRAP2X2 in two ratios (1:0 and 1:5). Different concentrations of α-MSH and ACTH (1-24) (from 10^{-10} to 10^{-5} M) were used.

3.2.6. cAMP assays

The intracellular cAMP level was detected via radioimmunoassay (RIA) as described previously (Steiner et al., 1969; Tao et al., 2010). The final concentration of ligands used for signaling assays were NDP-MSH (from 10^{-12} to 10^{-6} M), α-MSH and ACTH (1-24) (both from 10^{-11} to 10^{-5} M). To investigate the potential influences of maMRAP2X1 and maMRAP2X2 on maMC5R signaling, cells were co-transfected with maMC5R and maMRAP2X1 or maMRAP2X2 plasmids in two ratios (1:0 and 1:5). Two ligands, α-MSH and ACTH (1-24) (from 10^{-11} to 10^{-5} M) were used.

3.2.7. Statistical analysis

All data were shown as mean ± SEM. Prism 8.3 software (GraphPad, San Diego, CA, USA) was used to calculate parameters including maximal binding (B_{max}), IC_{50}, maximal response (R_{max}), EC_{50}, and analyze statistical differences. The significance of differences in ligand binding and signaling between maMC5R and hMC5R was determined by Student's t-test. The parameters of maMC5R regulated by maMRAP2s in flow cytometry, ligand binding, and cAMP were analyzed using one-way analysis of variance (ANOVA) for significance of differences.

3.3. Results

3.3.1. Amino acid sequence analysis of maMC5R, maMRAP2X1 and maMRAP2X2

The ricefield eel MC5R had seven putative hydrophobic TMDs with an extracellular N-terminus, three extracellular loops (ECLs), three intracellular loops (ICLs), and an intracellular C-terminus (Fig. 3.1A and Fig. S3.2). The PMY, DRY, and DPxxY motifs in TMDs, and the most conserved residue in each TMD for Family A GPCRs were observed in maMC5R (Fig. 3.1A and Fig. S3.2). Multiple sequence alignment analysis showed that maMC5R shared high identities with other piscine and chicken MC5Rs, and low sequence identities with mouse, horse, and human (Fig. S3.2 and Table 3.1). Phylogenetic tree between maMC5R and other MC5Rs revealed that maMC5R was localized in a clade of European sea bass and Japanese flounder (Fig. 3.1B).

Two isoforms of MRAP2 were present in ricefield eel: maMRAP2X1 and maMRAP2X2. These two maMRAP2s were encoded by a single *mrap2* through alternative splicing with maMRAP2X1 possessing 4 exons and maMRAP2X2 3 exons. The eel MRAP2X1 had similar features to other MRAP2s that contained a single TMD, and a long C-terminal tail (Fig. 3.2A and Fig. S3.3). In addition, a putative motif (LKAHKYS) lying just prior to TMD, crucial for antiparallel-homodimer formation (Sebag and Hinkle, 2009b), was present in maMRAP2X1 (Fig. 3.2A and Fig. S3.3). However, eel MRAP2X2 lost these important regions (Fig. 3.2B and Fig. S3.3). Multiple sequence alignment analysis showed that maMRAP2X1 and maMRAP2 shared extremely high identity. Compared with MRAP2s from other species, both maMRAP2X1 and maMRAP2X2 shared high identity with Nile tilapia MRAP2, and lower identities with MRAP2s from other species (Fig. S3.3 and Table 3.2). The two isoforms of maMRAP2s were clustered with

teleost MRAP2, and evolutionarily closer to orange-spotted grouper MRAP2 (Fig. 3.2C).

3.3.2. Chromosome synteny analyses of *mc5r*, *mrap2x1* and *mrap2x2*

Comparative gene synteny analysis was performed between ricefield eel, spotted gar, zebrafish, human, mouse, and rat (Figs. 3.3A,B). Our results showed that adjacent genes of eel *mc5r* including *fam210a*, *ldlrad4a*, *cep192*, *seh1l*, *mc2r*, were identical with those of spotted gar, zebrafish, human, mouse and rat *MC5Rs* (Fig. 3.3A). However, only three adjacent genes of eel *mrap2* (*ripply2*, *grik2* and *sobpb*) were identical with those of representative fishes (spotted gar and zebrafish) (Fig. 3.3B). If compared with mammals (human, mouse, and rat), eel *mrap2* shared only one conserved adjacent gene, *ripply2*.

3.3.3. Ligand binding properties of maMC5R

In competitive binding assay, different concentrations of three unlabeled agonists (NDP-MSH, α-MSH and ACTH (1-24)) were used to compete with a fixed amount of ^{125}I-NDP-MSH. The B_{max} of maMC5R was 46.78 ± 2.96% of that of the hMC5R (Fig. 3.4 and Table 3.3). Similar as the binding affinity order of hMC5R, maMC45R bound to super-potent agonist NDP-MSH with the highest affinity, followed by α-MSH and ACTH (1-24) (Table 3). MaMC5R displayed significantly higher binding affinities to α-MSH and ACTH (1-24) than hMC5R (Fig. 3.4 and Table 3.3).

3.3.4. cAMP signaling properties of maMC5R

Eel MC5R showed increased cAMP generation dose-dependently with all three ligands (NDP-MSH, α-MSH and ACTH (1-24)) (Fig. 3.5). There was no significant

difference of basal signaling between maMC5R and hMC5R (Fig. 3.5 and Table 3.4). Both maMC5R and hMC5R showed similar EC_{50} and R_{max} to NDP-MSH stimulation, whereas maMC5R had significantly lower EC_{50}s and R_{max}s to α-MSH and ACTH (1-24) stimulation than hMC5R (Fig. 3.5 and Table 3.4).

3.3.5. Modulation of maMC5R expression and pharmacology by maMRAP2s

Flow cytometry assay showed that neither maMRAP2X1 nor maMRAP2X2 displayed significant modulatory effect on cell surface and total expression levels of maMC5R (Figs. 3.6A-D). Competitive ligand binding assay showed that both maMRAP2X1 and maMRAP2X2 significantly increased the B_{max} of maMC5R in the 1:5 group (Figs. 3.7A,B and Table 3.5). The binding affinity to ACTH (1-24) of maMC5R was significantly reduced when co-expressed with maMRAP2X2 (Fig. 3.7B and Table 3.5). The cAMP assay showed that maMRAP2X1 or maMRAP2X2 did not affect EC_{50}s, but they decreased R_{max} significantly (Figs. 3.7C,D and Table 3.6). The basal cAMP level of maMC5R was not influenced by either maMRAP2X1 or maMRAP2X2 (Figs. 3.7C,D and Table 3.6).

3.4. Discussion

In the present study, ricefield eel MC5R and MRAP2X1 showed similar structural characteristics as MC5Rs and MRAP2s of other species, respectively. Notably, maMRAP2X2 did not possess the regions that are conserved in other species. Sequence alignment showed that maMC5R shared more than 80% amino acid identity with other teleost MC5Rs, whereas maMRAP2s shared lower identity with other teleost MRAP2s, suggesting MC5R was more conserved than MRAP2 in teleosts. Synteny analysis further demonstrated that genes located upstream of eel *mc5r* were highly conserved compared

with those in spotted gar, zebrafish, human, mouse and rat. Only a single copy *mrap2* existed in ricefield eel (*mrap2b*) and it showed two conserved adjacent genes with zebrafish *mrap2b* (*ripply2*, *sobpb*). Additionally, adjacent genes of MRAP2 were more conserved in mammalian species than in teleosts. Thus, *mc5r* and *mrap2* in fishes might undergo complex evolutional processes.

Eel MC5R was functional since it could bind to three agonists and increase intracellular cAMP generation, in line with previous results of other fish MC5Rs (Cerdá-Reverter et al., 2003a; Haitina et al., 2004; Hoglin et al., 2020; Klovins et al., 2004; Kobayashi et al., 2016; Liao et al., 2019; Reinick et al., 2012; Ringholm et al., 2002; Sánchez et al., 2009a). Among the three agonists used here, NDP-MSH acted as the most potent agonist in maMC5R, consistent with findings in sea bass (Sánchez et al., 2009a) and blunt snout bream (Liao et al., 2019). In response to α-MSH and ACTH (1-24), maMC5R displayed higher potency but lower efficacy than hMC5R, which might be caused by higher binding affinity and lower binding capacity in maMC5R.

The constitutive activity of GPCRs is an important pharmacological parameter, with clinical implications (Seifert and Wenzel-Seifert, 2002; Tao, 2008). In human, the MC3R has little or no constitutive activity, whereas the MC4R has significant constitutive activity that can be easily detected (Tao, 2007; Tao et al., 2010). Interestingly, several fish MC3Rs and MC4Rs show significantly higher constitutive activities in cAMP pathway when compared with corresponding human MC3R and MC4R, respectively (Li et al., 2016a; Li et al., 2017a; Rao et al., 2019; Renquist et al., 2013; Tao et al., 2020; Yang et al., 2019; Yang et al., 2020; Yi et al., 2018; Zhang et al., 2019). The constitutive activity of fish MC4R is physiological relevant. The reduced basal activity caused by *mc4r* mutation helps cavefish to adapt to nutrient-poor conditions (Aspiras et al., 2015). In zebrafish,

decreased constitutive activity of MC4R by MRAP2 maximizes the larval growth (Sebag et al., 2013). Here, we showed that eel MC5R did not have any constitutive activity, similar to human MC5R, suggesting that not all fish melanocortin receptors are constitutively active.

The pharmacology of maMC5R could be regulated by two isoforms of maMRAP2s. Both maMRAP2X1 and maMRAP2X2 significantly increased binding capacity and decreased efficacy of maMC5R, with no effect on expression level. In human, MRAP2 decreases hMC5R trafficking and responsiveness of MC5R to NDP-MSH (Chan et al., 2009). In mouse, MRAP2 dose-dependently inhibits the efficacy of MC5R but does not influence MC5R trafficking (Zhu et al., 2019a). In zebrafish, two MRAP2s behave differently with MRAP2a reducing cell surface expression and maximal activity of both MC5Ra and MC5Rb, whereas MRAP2b inhibiting MC5Ra activity but increasing MC5Rb activity without affecting cell surface expression of MC5Rs (Zhu et al., 2019a). In gar, MRAP2 increases trafficking of MC5R to the plasma membrane but has no effect on ligand sensitivity for MC5R (Wolverton et al., 2019). These data suggest that the effect of MRAP2 on MC5R might be species specific.

Alternative splicing of human MRAP1 leads to two proteins, MRAP1α and MRAP1β (Hinkle and Sebag, 2009). In ricefield eel, two isoforms of MRAP2s were produced by alternative splicing of *mrap2*. Having similar structural properties with MRAP2 in other species, maMRAP2X1 could modulate maMC5R with increased binding capacity but decreased maximal response. Surprisingly, maMRAP2X2 was functional and could also regulate maMC5R similarly, although maMRAP2X2 did not have conserved TMD and the LKAHKYS motif, which was an exciting finding. Sebag and Hinkle showed that both TMD and the LKAHKYS motif of MRAP1 are required for MC2R to reach cell membrane and

produce ACTH-induced cAMP generation (Sebag and Hinkle, 2009b), but not required for the inhibitory action on MC5R (Sebag and Hinkle, 2009a). Our data with maMRAP2X2 were consistent with the observation between MRAP1 and MC5R by Sebag and Hinkle (Sebag and Hinkle, 2009a). In zebrafish, two MRAP2s affect MC5R pharmacology by disrupting the dimerization of MC5R homodimers and heterodimers (Zhu et al., 2019a). Given the special structure of maMRAP2X2, there might be a distinct mechanism for MRAP2 to affect MC5R function. We hypothesized that maMRAP2X2 might interact with intracellular loops or C-terminus of maMC5R in cytosol, which will further impact maMC5R pharmacology. This remains to be investigated.

In summary, our studies on ricefield eel MC5R and two MRAP2 isoforms and their interaction contributes to a better understanding of fish MC5Rs. These results will lay the foundation for future physiological studies on ricefield eel MC5R. In the livestock industry, the marbled meat provides not only good taste but also high nutritional value. It also applies to the aquaculture. Considering that MC5R can stimulate lipolysis in adipocytes and increase fatty acid oxidation in skeletal muscles, we hypothesized that MC5R might be involved in intermuscular fat metabolism. Then thus MC5R might be helpful to produce the tasty fish.

Table 3.1. The identity of the MC5R amino acid sequence from different species.

	Ricefield eel	Blunt snout bream	Common carp	Fugu	Zebrafish MC5Ra	Zebrafish MC5Rb	Chicken	Mouse	Horse	Human
Ricefield eel	100	91	91	86	91	83	81	78	74	78
Blunt snout bream		100	97	83	98	78	80	74	77	76
Common carp			100	83	98	81	77	73	77	76
Fugu				100	86	79	76	76	75	77
Zebrafish MC5Ra					100	81	80	73	77	76
Zebrafish MC5Rb						100	72	72	71	70
Chicken							100	79	81	78
Mouse								100	83	82
Horse									100	87
Human										100

Table 3.2. The identity of the MRAP2 amino acid sequence from different species.

	Ricefield eel MRAP2X1	Ricefield eel MRAP2X2	Zebrafish MRAP2a	Zebrafish MRAP2b	Japanese medaka	Rainbow trout	Nile tilapia	Chicken	Mouse	Human
Ricefield eel MRAP2X1	100	99	52	47	66	49	81	45	47	49
Ricefield eel MRAP2X2		100	41	34	54	38	73	33	37	37
Zebrafish MRAP2a			100	53	52	55	51	48	51	50
Zebrafish MRAP2b				100	45	45	47	45	49	46
Japanese medaka					100	48	70	46	46	48
Rainbow trout						100	51	42	45	47
Nile tilapia							100	45	45	47
Chicken								100	72	74
Mouse									100	88
Human										100

Table 3.3. Ligand binding properties of maMC5R.

MC5R	B_{max} (%)	NDP-MSH	α-MSH	ACTH
		IC_{50} (nM)	IC_{50} (nM)	IC_{50} (nM)
hMC5R	100	5.60 ± 0.71	975.50 ± 58.48	4646.00 ± 809.80
maMC5R	46.78 ± 2.96[d]	4.14 ± 0.80	591.70 ± 55.80[b]	675.50 ± 87.66[a]

Results were expressed as the mean ± SEM of at least three independent experiments.

[a] Significantly different from the parameter of hMC5R, $P < 0.05$.

[b] Significantly different from the parameter of hMC5R, $P < 0.01$.

[d] Significantly different from the parameter of hMC5R, $P < 0.0001$.

Table 3.4. Signaling properties of maMC5R.

MC5R	Basal (%)	NDP-MSH		α-MSH		ACTH	
		EC_{50} (nM)	R_{max} (%)	EC_{50} (nM)	R_{max} (%)	EC_{50} (nM)	R_{max} (%)
hMC5R	100	3.41 ± 1.44	100	56.53 ± 10.70	100	35.01 ± 7.68	100
maMC5R	86.02 ± 8.92	0.18 ± 0.01	138.80 ± 15.87	2.13 ± 1.28[a]	48.65 ± 4.98[b]	1.60 ± 0.52[a]	56.16 ± 6.56[b]

Results were expressed as the mean ± SEM of at least three independent experiments.

[a] Significantly different from the parameter of hMC5R, $P < 0.05$.

[b] Significantly different from the parameter of hMC5R, $P < 0.01$.

Table 3.5. The effect of maMRAP2X1 and maMRAP2X2 on ligand binding properties of maMC5R.

maMC5R/maMRAP2X1 or maMRAP2X2	B_{max} (%)	α-MSH	ACTH
		IC_{50} (nM)	IC_{50} (nM)
maMC5R (1:0)	100	591.30 ± 40.62	440.90 ± 100.30
maMC5R/maMRAP2X1 (1:5)	125.10 ± 6.68[a]	2591.00 ± 609.80	191.10 ± 41.93
maMC5R/maMRAP2X2 (1:5)	147.80 ± 7.82[d]	2833.00 ± 802.00	1668.00 ± 19.33[d]

Results were expressed as the mean ± SEM of at least three independent experiments.

[a] Significantly different from the parameter of 1:0, $P < 0.05$.

[d] Significantly different from the parameter of 1:0, $P < 0.0001$.

Table 3.6. The effect of maMRAP2X1 and maMRAP2X2 on signaling properties of maMC5R.

maMC5R/maMRAP2X1 or maMRAP2X2	Basal (%)	α-MSH		ACTH	
		EC_{50} (nM)	R_{max} (%)	EC_{50} (nM)	R_{max} (%)
maMC5R (1:0)	100	4.00 ± 0.85	100	2.87 ± 0.80	100
maMC5R/maMRAP2X1 (1:5)	99.09 ± 6.09	2.92 ± 0.51	62.00 ± 9.00[a]	1.22 ± 0.54	51.67 ± 10.44[a]
maMC5R/maMRAP2X2 (1:5)	104.30 ± 5.98	1.52 ± 0.48	66.16 ± 11.78[a]	1.05 ± 0.32	62.43 ± 11.38[a]

Results were expressed as the mean ± SEM of at least three independent experiments.

[a] Significantly different from the parameter of 1:0, $P < 0.05$.

A

```
   1 ATG AAC ATG TCT GAT GAG TCC TCT TAC CAT GAG GAG GTG CTA CTG AGT AAC TCC ACC TGG  60
   1 M   N   M   S   D   E   S   S   Y   H   E   E   V   L   L   S   N   S   T   W   20
  61 GGT TAC TTC TAC AGT TAC CAA AAC TAC ACC GTG TCC CCT CCT TTG CTA CCA GAC ATG ACA 120
  21 G   Y   F   Y   S   Y   Q   N   Y   T   V   S   P   P   L   L   P   D   M   T   40
 121 AGC ACC TCC AAA CCG GCA GCA TGT GAG CAG GTC CAC ATC GCT GTA GAG GTC TTT CTG ATC 180
  41 S   T   S   K   P   A   A   C   E   Q   V   H   I   A   V   E   V   F   L   I   60
 181 CTG GGT ATC ATA TCC CTG CTG GAG AAC ATC CTG GTC ATC ACA GCC ATC ATC AAA AAC AAG 240
  61 L   G   I   I   S   L   L   E   N   I   L   V   I   T   A   I   I   K   N   K   80
 241 AAC CTC CAC TCA CCC ATG TAC TTC TTC GTC TGC AGT CTG GCA GTC GCA GAC ATG TTG GTG 300
  81 N   L   H   S   P   M   Y   F   F   V   C   S   L   A   V   A   D   M   L   V  100
 301 AGT GTG TCC AAC GCC TGG GAG ACC ATC ATT ATT TAC CTT CTG AAC AAC AGA CAG CTA GTG 360
 101 S   V   S   N   A   W   E   T   I   I   I   Y   L   L   N   N   R   Q   L   V  120
 361 GTG GAG GAC CAC TTC ATC CGG CAA ATG GAC AAC GTG TTT GAC TCC ATG ATC TGC ATC TCT 420
 121 V   E   D   H   F   I   R   Q   M   D   N   V   F   D   S   M   I   C   I   S  140
 421 GTC GTT GCA TCA ATG TGC AGC CTA CTG GCC ATT GCT GTG GAC AGG TAC GTC ACT ATC TTC 480
 141 V   V   A   S   M   C   S   L   L   A   I   A   V   D   R   Y   V   T   I   F  160
 481 TAT GCA CTG AGG TAC CAC AAC ATT ATG ACA GTG AGG AGA GCT GGC TGC ATT ATC GCA GGA 540
 161 Y   A   L   R   Y   H   N   I   M   T   V   R   R   A   G   C   I   I   A   G  180
 541 ATC TGG ACC TTC TGC ACA GGC TGC GGT ATT GTC TTC ATC ATC TAC TCA GAC ACC ACC CCC 600
 181 I   W   T   F   C   T   G   C   G   I   V   F   I   I   Y   S   D   T   T   P  200
 601 GTG ATC ATC TGT CTG GTC TCC ATG TTC TTC GCC ATG CTA CTC ATC ATG GCT TCC CTC TAC 660
 201 V   I   I   C   L   V   S   M   F   F   A   M   L   L   I   M   A   S   L   Y  220
 661 AGC CAC ATG TTC ATG CTG GCC CGT TCG CAT GTC AAG CGC ATT GCC GCC CTG CCT GGC TAC 720
 221 S   H   M   F   M   L   A   R   S   H   V   K   R   I   A   A   L   P   G   Y  240
 721 AAC TCC ATC CAC CAG CGG GCC AGC ATG AAG GGG GCC ATC ACA CTG ACC ATC CTG CTG GGG 780
 241 N   S   I   H   Q   R   A   S   M   K   G   A   I   T   L   T   I   L   L   G  260
 781 ATC TTC ATT GTC TGC TGG GCT CCA TTC TTC CTG CAC CTG ATC CTG ATG ATC TCC TGT CCA 840
 261 I   F   I   V   C   W   A   P   F   F   L   H   L   I   L   M   I   S   C   P  280
 841 CGG AAC CTC TAC TGC GTA TGC TTC ATG TCC CAC TTC AAC ATG TAC CTC ATC CTC ATC ATG 900
 281 R   N   L   Y   C   V   C   F   M   S   H   F   N   M   Y   L   I   L   I   M  300
 901 TGC AAC TCT GTG ATT GAC CCG CTC ATC TAT GCC TTC AGG AGT CAG GAG ATG AGG AAG ACT 960
 301 C   N   S   V   I   D   P   L   I   Y   A   F   R   S   Q   E   M   R   K   T  320
 961 TTT AAG GAG ATC ATT TGT TGC TAC AGC CTG AGA AAC ATC TGC ACC AAC ATC TGC ACT CTG 1020
 321 F   K   E   I   I   C   C   Y   S   L   R   N   I   C   T   N   I   C   T   L  340
1021 ACT GGT CCT GTA CAG AAC TGC TGT CCC TCC AAC TAA                                1056
 341 T   G   P   V   Q   N   C   C   P   S   N   *                                  351
```

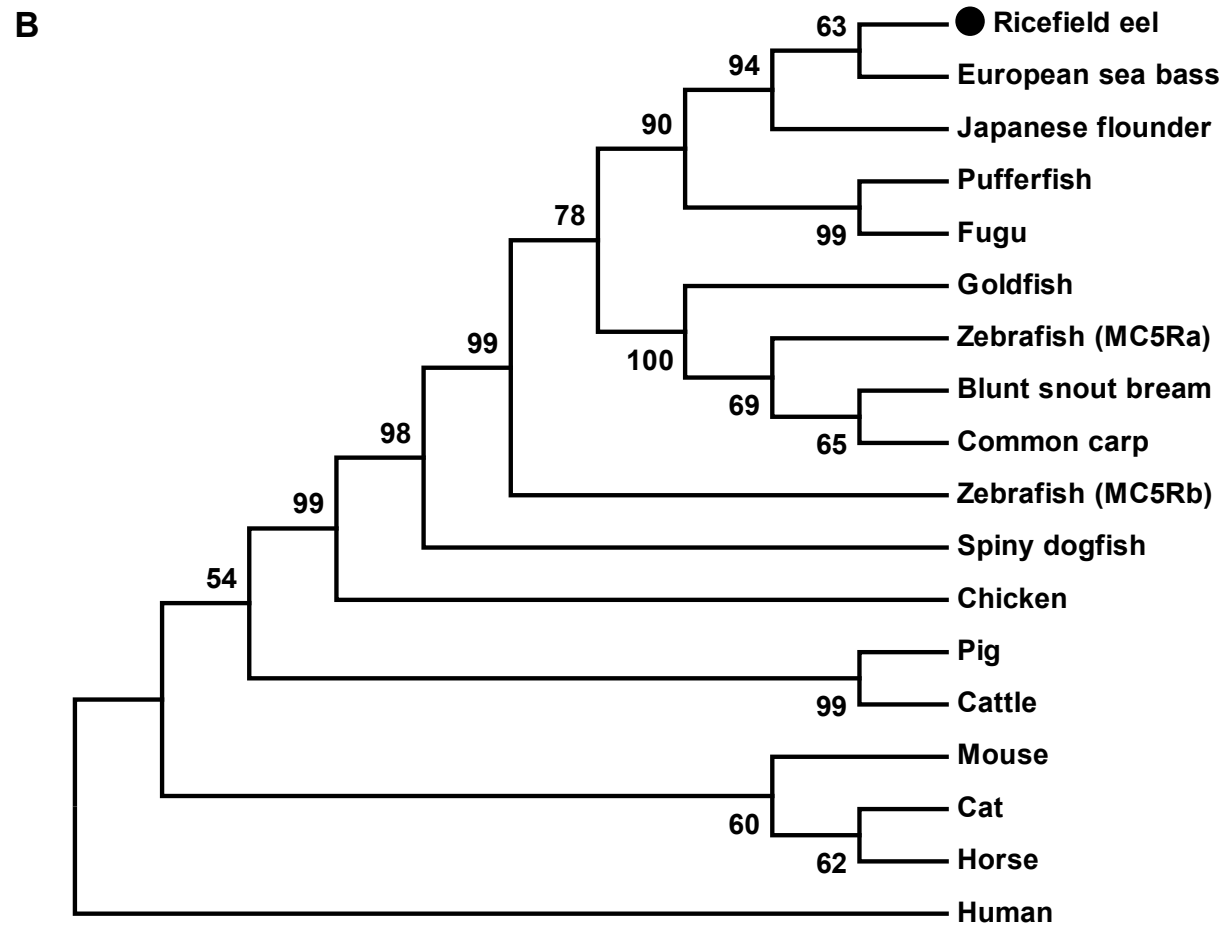

Fig. 3.1. Nucleotide and amino acid sequence of maMC5R (A) and phylogenetic tree of MC5Rs (B).

Positions of nucleotide and amino acid sequences were labeled on both sides. The seven TMDs were shaded in grey. The conserved motifs (PMY, DRY, and DPLIY) were highlighted with solid line. Open boxes presented N-linked glycosylation sites. Asterisk (*) denoted stop codon. The tree was constructed by the neighbor-joining (NJ) method with MEGA 7.0. Numbers at nodes indicated the bootstrap percentages from 1,000 replicates. Black circle showed maMC5R. MC5Rs: Ricefield eel: QCI09904.2; Blunt snout bream: AHN92036.1; Common carp: CAH04351.1; Fugu: NP_001027937.1; Zebrafish MC5Ra: NP_775386.1; Zebrafish MC5Rb: NP_775387.1; Goldfish: CAE11349.1; Pufferfish:

AAQ55179.1; Japanese flounder: XP_019946633.1; European sea bass: CAZ69796.1; Spiny dogfish: AAS67890.1; Chicken: AHC02482.1; Cat: XP_019669930.1; Pig: XP_020953265.1; Cattle: NP_001015542.1; Mouse: NP_038624.3; Horse: XP_023503243.1; Human: NP_005904.1.

A

```
1   ATG TCC GAC TTC CAC AAC CGG AGC CAA ACC AGC GCA CGT CGC AGT GAC TAC GTG TGG CAG  60
1   M   S   D   F   H   N   R   S   Q   T   S   A   R   R   S   D   Y   V   W   Q   20
61  TAT GAG TAT TAT GAC GAC GAG GAG CCC GTG TCT TTT GAG GGA CTC AAA GCG CAC AGA TAC 120
21  Y   E   Y   Y   D   D   E   E   P   V   S   F   E   G   L   K   A   H   R   Y   40
121 TCC ATC GTC ATT GGC TTC TGG GTC GGA CTT GCT GTG TTT GTC ATA TTC ATG TTC TTT GTT 180
41  S   I   V   I   G   F   W   V   G   L   A   V   F   V   I   F   M   F   F   V   60
181 CTC ACA CTG CTC ACA AAG ACA GGA GCG CCA CAT CAA GAA AAC CCA GAT TCT GCT GAA AAG 240
61  L   T   L   L   T   K   T   G   A   P   H   Q   E   N   P   D   S   A   E   K   80
241 CAT CAT CGA CCA GGA ACT TGT CTG GCA GAC ATT GAA GGC CCC CAG GAC GAA AAT GAC AAA 300
81  H   H   R   P   G   T   C   L   A   D   I   E   G   P   Q   D   E   N   D   K   100
301 GCC TTC TTC CGT CCT TTG CTC GGG GAG TCT CGC TCA TAC TTT CAT TTC TAC ATC AAT GAG 360
101 A   F   F   R   P   L   L   G   E   S   R   S   Y   F   H   F   Y   I   N   E   120
361 GAG GAC CAG GGT CAG GGG AAG GAA AAA ACT GAA AAT AAG AAG GTT GGA AAG CAC ACA AGG 420
121 E   D   Q   G   Q   G   K   E   K   T   E   N   K   K   V   G   K   H   T   R   140
421 GCA GGA GTC CAG CAG GGG ACC TGC AAC CAA CCC AGA GGT ATC AGC TCC TTG GGT GTG GAT 480
141 A   G   V   Q   Q   G   T   C   N   Q   P   R   G   I   S   S   L   G   V   D   160
481 GAT ATG GAA GAG GAT GTC GAG GAA GCT GGA GGA CAC CAG CCT TTC AAA GGA TTA ACA GAT 540
161 D   M   E   E   D   V   E   E   A   G   G   H   Q   P   F   K   G   L   T   D   180
541 GAG AGC AAG ACG GGC CGA GAT TGT GCC TTT CTG TCT CAC TTC AAC ATC CCT AAC TTT GTG 600
181 E   S   K   T   G   R   D   C   A   F   L   S   H   F   N   I   P   N   F   V   200
601 AAC TTG GAG CAC AGT TCA ACA TTT GGA GAG GAT GAT CTG CTG TAT GAG CCA GCT GTC ATA 660
201 N   L   E   H   S   S   T   F   G   E   D   D   L   L   Y   E   P   A   V   I   220
661 CTG GAG CAG CAG TCC CGC TCT CAG GAT GCT CAC TGT GAC ATC CAC TAA                 708
221 L   E   Q   Q   S   R   S   Q   D   A   H   C   D   I   H   *                 235
```

B

```
1   ATG AGT ATT ATG ACG ACG AGG AGC CCG TGT CTT TTG AGG GAC TCA AAG CGC ACA GAT ACA  60
1   M   S   I   M   T   T   R   S   P   C   L   L   R   D   S   K   R   T   D   T   20
61  GGA GCG CCA CAT CAA GAA AAC CCA GAT TCT GCT GAA AAG CAT CAT CGA CCA GGA ACT TGT 120
21  G   A   P   H   Q   E   N   P   D   S   A   E   K   H   H   R   P   G   T   C   40
121 CTG GCA GAC ATT GAA GGC CCC CAG GAC GAA AAT GAC AAA GCC TTC TTC CGT CCT TTG CTC 180
41  L   A   D   I   E   G   P   Q   D   E   N   D   K   A   F   F   R   P   L   L   60
181 GGG GAG TCT CGC TCA TAC TTT CAT TTC TAC ATC AAT GAG GAG GAC CAG GGT CAG GGG AAG 240
61  G   E   S   R   S   Y   F   H   F   Y   I   N   E   E   D   Q   G   Q   G   K   80
241 GAA AAA ACT GAA AAT AAG AAG GTT GGA AAG CAC ACA AGG GCA GGA GTC CAG CAG GGG ACC 300
81  E   K   T   E   N   K   K   V   G   K   H   T   R   A   G   V   Q   Q   G   T   100
301 TGC AAC CAA CCC AGA GGT ATC AGC TCC TTG GGT GTG GAT GAT ATG GAA GAG GAT GTC GAG 360
101 C   N   Q   P   R   G   I   S   S   L   G   V   D   D   M   E   E   D   V   E   120
361 GAA GCT GGA GGA CAC CAG CCT TTC AAA GGA TTA ACA GAT GAG AGC AAG ACG GGC CGA GAT 420
121 E   A   G   G   H   Q   P   F   K   G   L   T   D   E   S   K   T   G   R   D   140
421 TGT GCC TTT CTG TCT CAC TTC AAC ATC CCT AAC TTT GTG AAC TTG GAG CAC AGT TCA ACA 480
141 C   A   F   L   S   H   F   N   I   P   N   F   V   N   L   E   H   S   S   T   160
481 TTT GGA GAG GAT GAT CTG CTG TAT GAG CCA GCT GTC ATA CTG GAG CAG CAG TCC CGC TCT 540
161 F   G   E   D   D   L   L   Y   E   P   A   V   I   L   E   Q   Q   S   R   S   180
541 CAG GAT GCT CAC TGT GAC ATC CAC TAA                                           567
181 Q   D   A   H   C   D   I   H   *                                           188
```

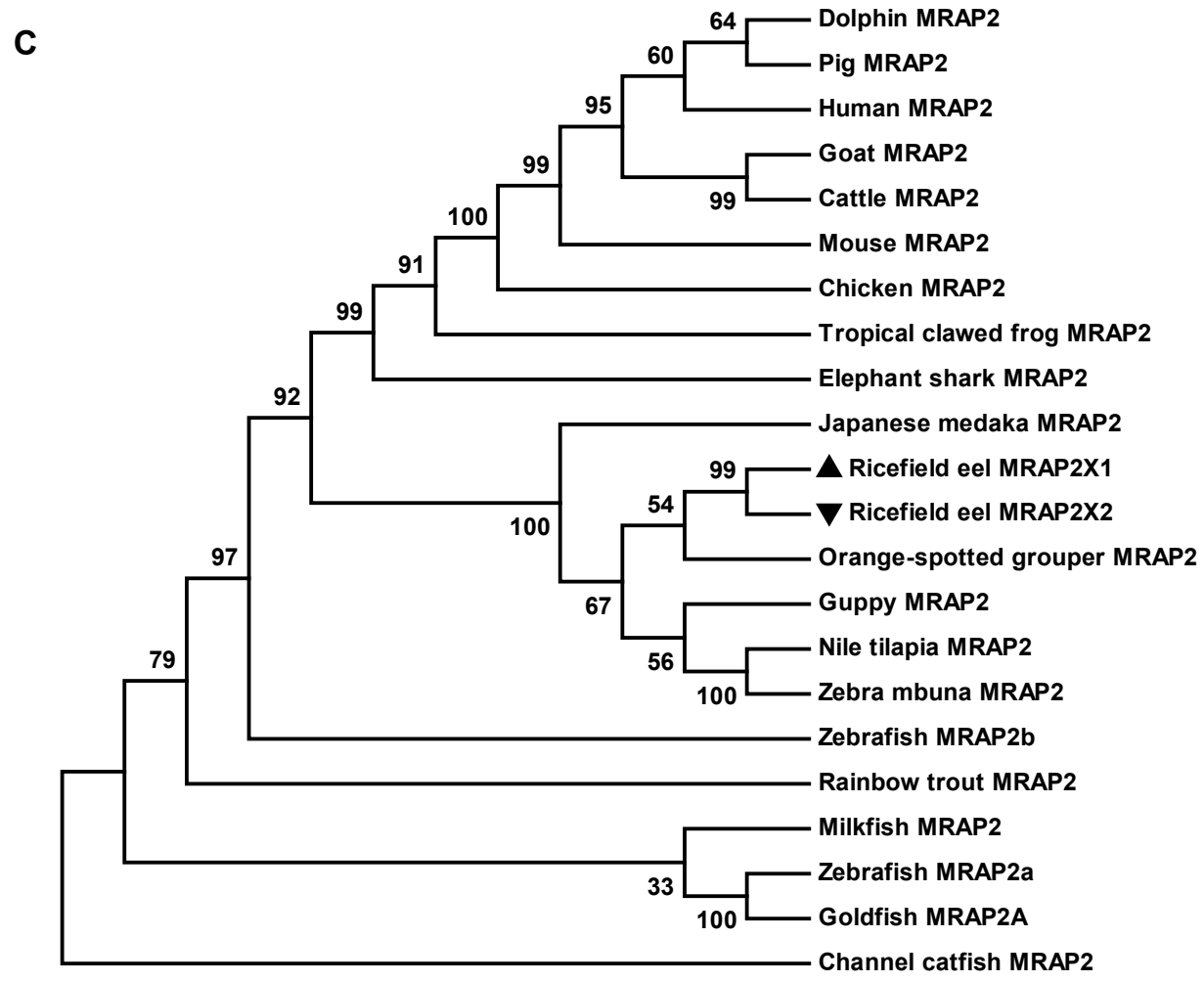

Fig. 3.2. Nucleotide and amino acid sequences of maMRAP2X1 (A) and maMRAP2X2 (B) and phylogenetic tree of MRAP2s (C).

Positions of nucleotide and amino acid sequences were labeled on both sides. The TMD was shaded in grey. Open boxes indicated *N*-linked glycosylation site. Underline showed initiation and stop codons. Asterisk (*) denoted stop codon. The tree was constructed by the NJ method with MEGA 7.0. Numbers at nodes indicated the bootstrap percentages from 1,000 replicates. Black triangles showed maMRAP2X1 and maMRAP2X2. MRAP2s: Ricefield eel MRAP2X1: XP_020444987.1; Ricefield eel MRAP2X2: XP_020444993.1; Zebrafish MRAP2a: F8W4H9.1; Zebrafish MRAP2b: F8W4H9.1; Channel catfish:

XP_017313206.1; Orange-spotted grouper: QED39647.1; Japanese medaka: XP_023809099.1; Rainbow trout: NP_001233282.1; Nile tilapia: XP_003458293.2; Elephant shark, XP_007906624.1; Goldfish: XP_026139519.1; Guppy: XP_008395815.1; Milkfish: XP_030637912.1; Tropical clawed frog: XP_002933963.1; Chicken: ALO81626.1; Mouse: NP_001346884.1; Zebra mbuna: XP_004568825.1; Goat: XP_017908670.1; Dolphin: XP_033723423.1; Cattle: NP_001092863.1; Pig: XP_013848111.1; Human: NP_001333473.1.

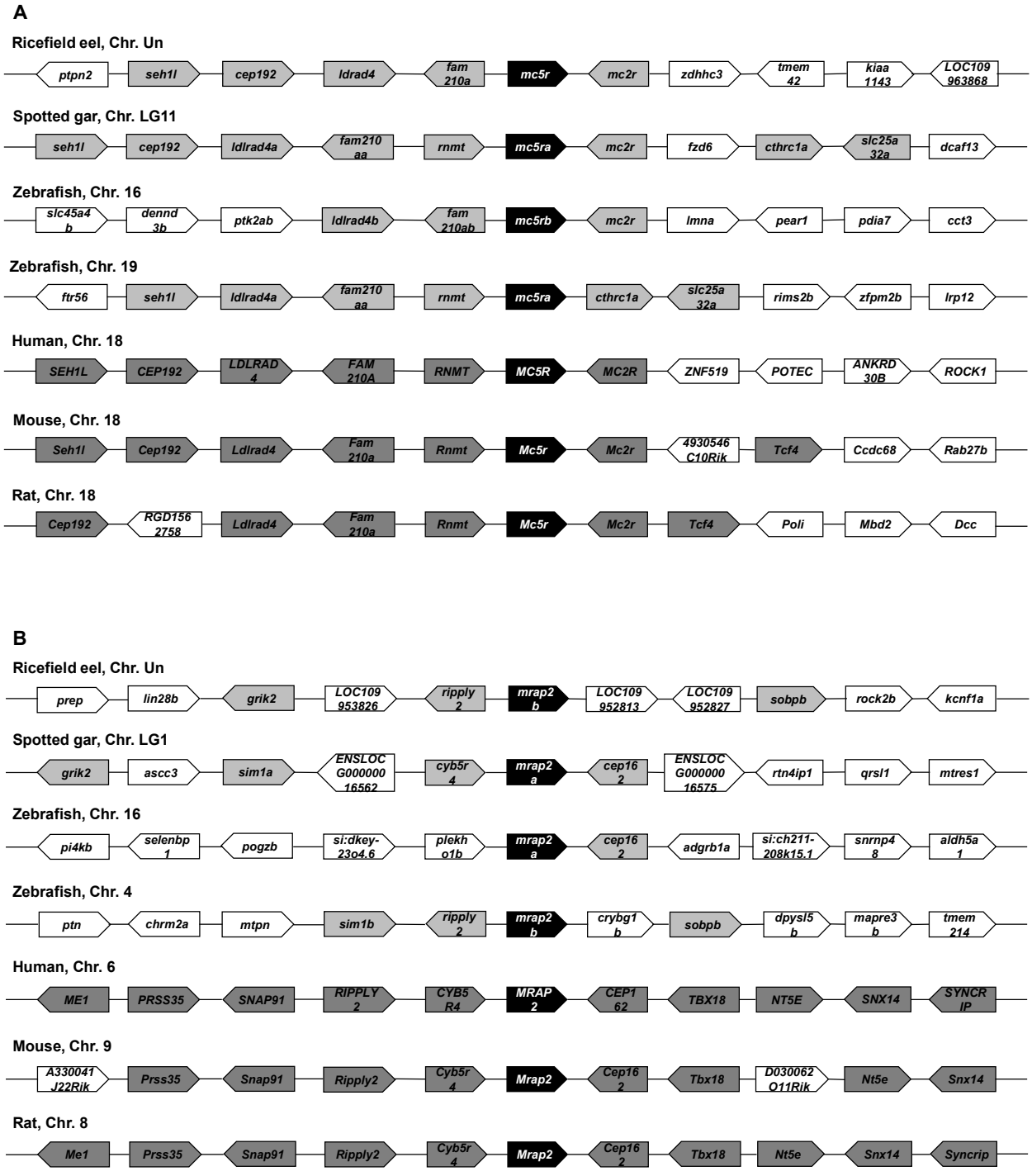

Fig. 3.3. Comparative gene synteny of *MC5R* (A) and *MRAP2* (B) genes among different species.

The syntenic genes were indicated as boxes with the directions and linked by lines. *MC5R*

and *MRAP2* genes were shown in black boxes. The genes showing conserved synteny in mammals were shown in dark grey boxes and those conserved in fishes were indicated in light grey boxes.

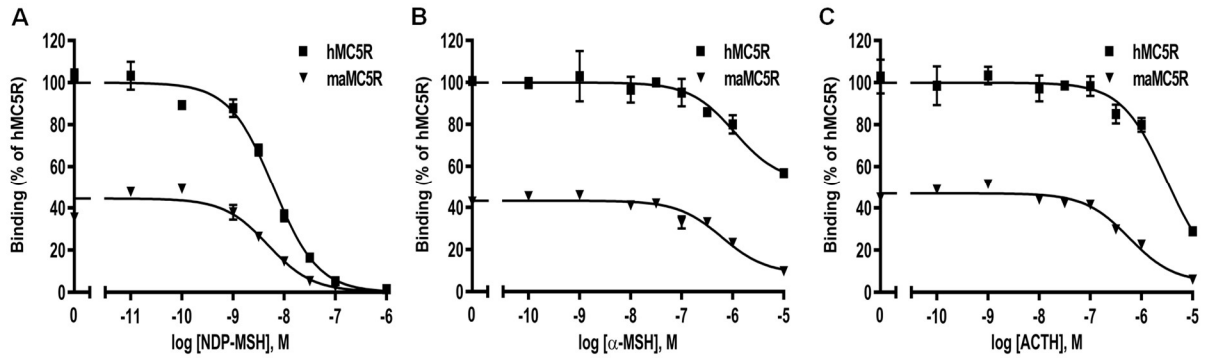

Fig. 3.4. Ligand binding properties of maMC5R in HEK293T cells.

The cells were transiently transfected with hMC5R and maMC5R plasmids, and the binding properties were measured 48 h later via competitive bidding assay. Different concentrations of unlabeled NDP-MSH (A), α-MSH (B), ACTH (1-24) (C) were used to displace the binding of ^{125}I-NDP-MSH. Results were expressed as % of hMC5R binding ± range (in the absence of competitor) from duplicate measurements within one experiment. All experiments were performed at least three times independently.

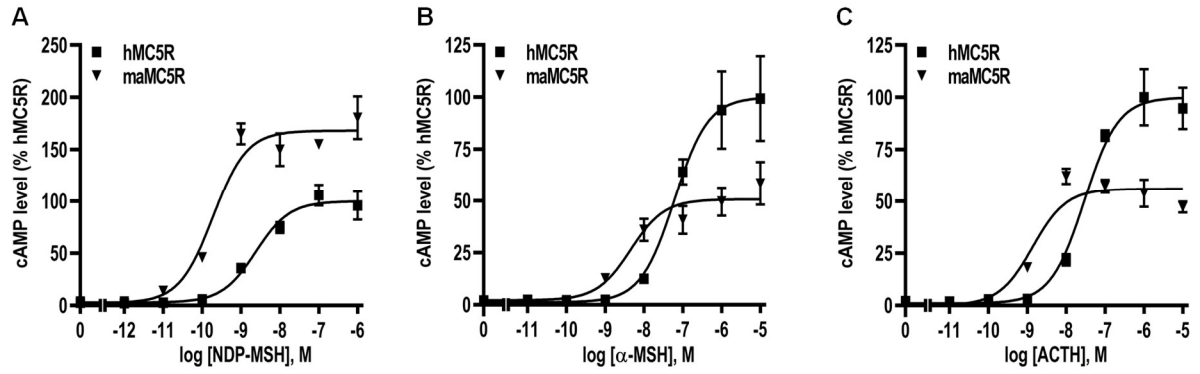

Fig. 3.5. Signaling properties of maMC5R in HEK293T cells.

The cells were transiently transfected with hMC5R or maMC5R plasmids, and the cAMP generation were measured 48 h later via radioimmunoassay (RIA). Different concentrations of NDP-MSH (A), α-MSH (B), or ACTH (1-24) (C) were used. Data were expressed as % of hMC5R mean ± SEM (in the presence of highest-concentration ligand) from triplicate measurements within one experiment. All experiments were performed at least three times independently.

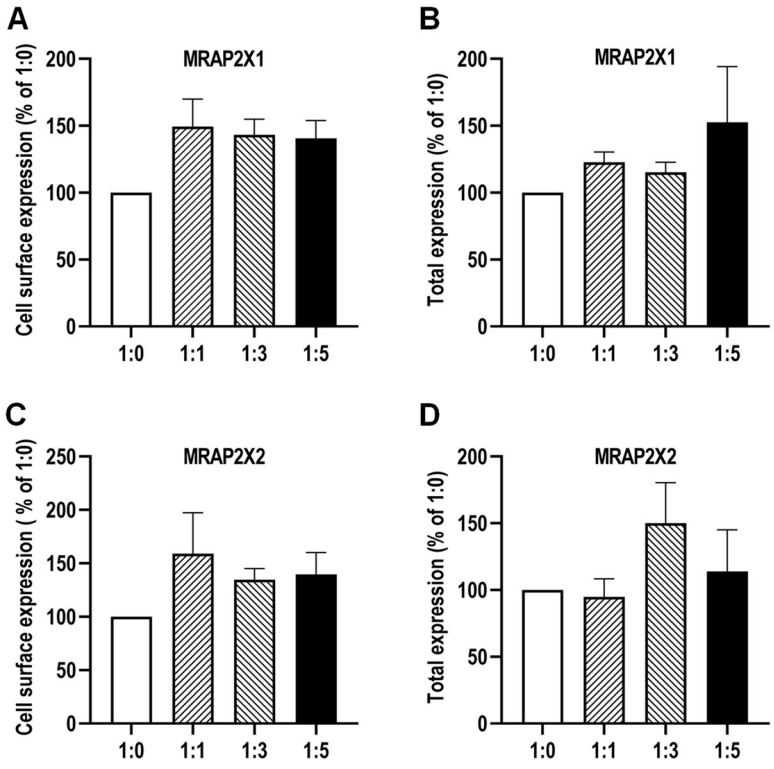

Fig. 3.6. Regulation of maMC5R expression by maMRAP2X1 (A, B) or maMRAP2X2 (C, D).

HEK293T cells were co-transfected with four ratios of maMC5R/maMRAP2X1 or maMC5R/maMRAP2X2 (1:0, 1:1, 1:3, and 1:5). After 48 h, flow cytometry was performed to measure cell surface and total expression of maMC5R. The results were calculated as % of 1:0 group. Each data point was expressed as mean ± SEM of at least three independent experiments.

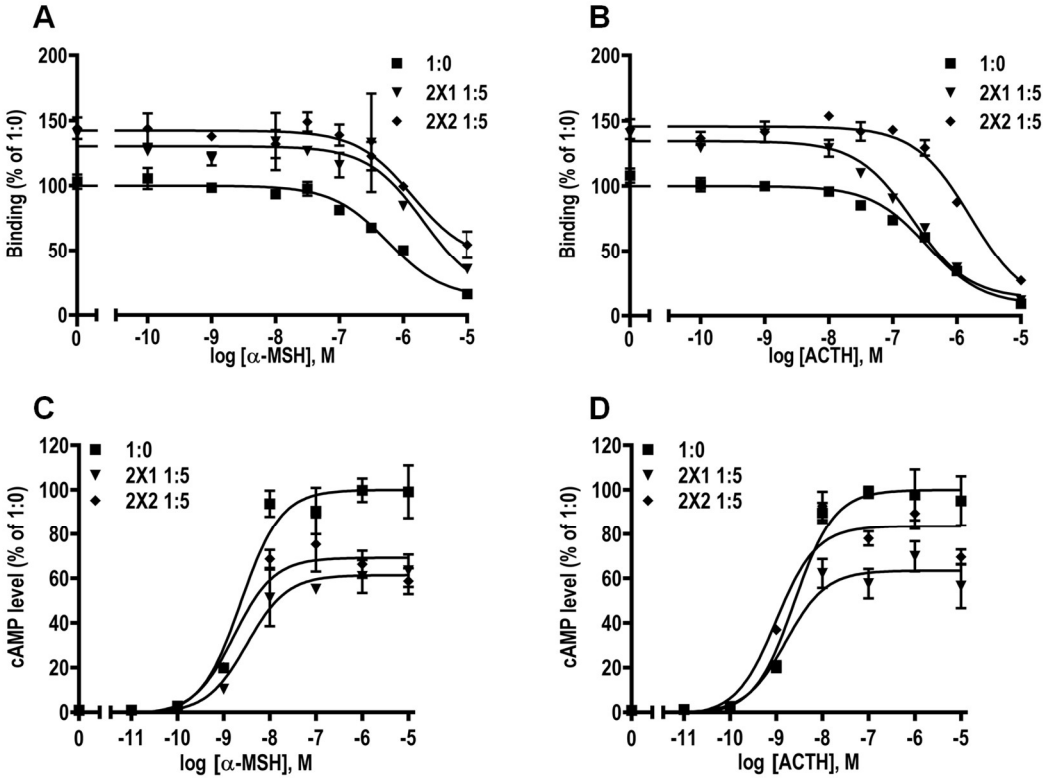

Fig. 3.7. Modulation of maMC5R pharmacology by maMRAP2X1 or maMRAP2X2. HEK293T cells were co-transfected with two ratios of maMC5R/maMRAP2X1 or maMC5R/maMRAP2X2 (1:0 and 1:5). Results were calculated as described in detail in Fig. 3.4 and Fig. 3.5.

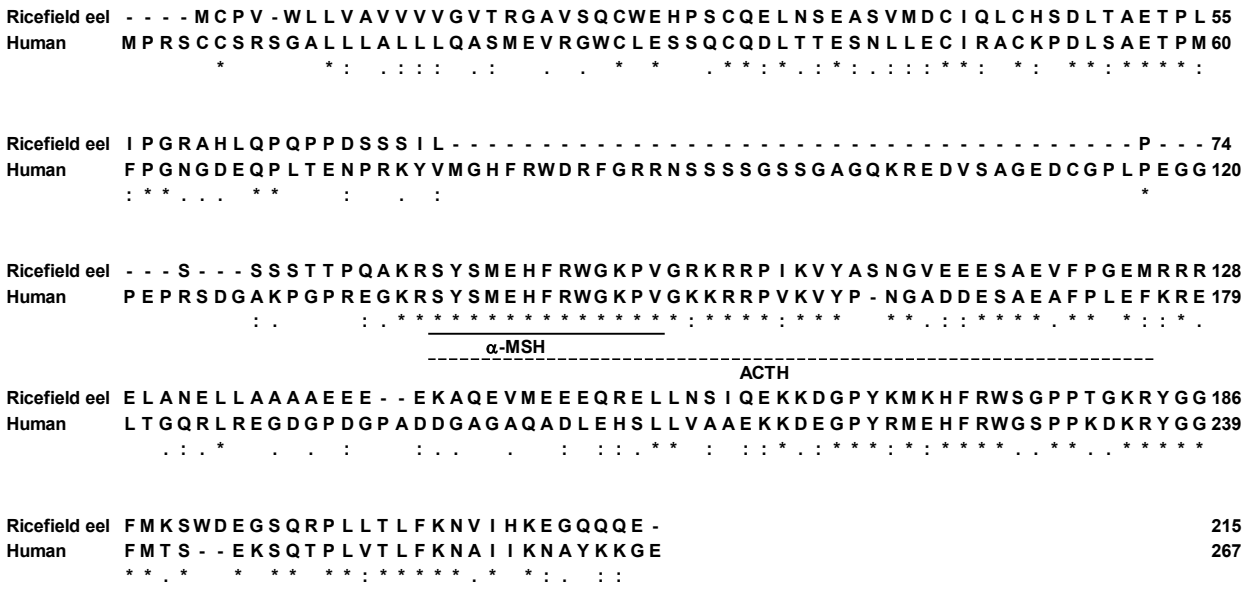

Fig. S3.1. Comparison of amino acid sequences of POMC between ricefield eel and human.

Labeled as follows: the solid line represented α-MSH, and dashed line indicated the ACTH. Asterisk (*) indicated the same amino acids.

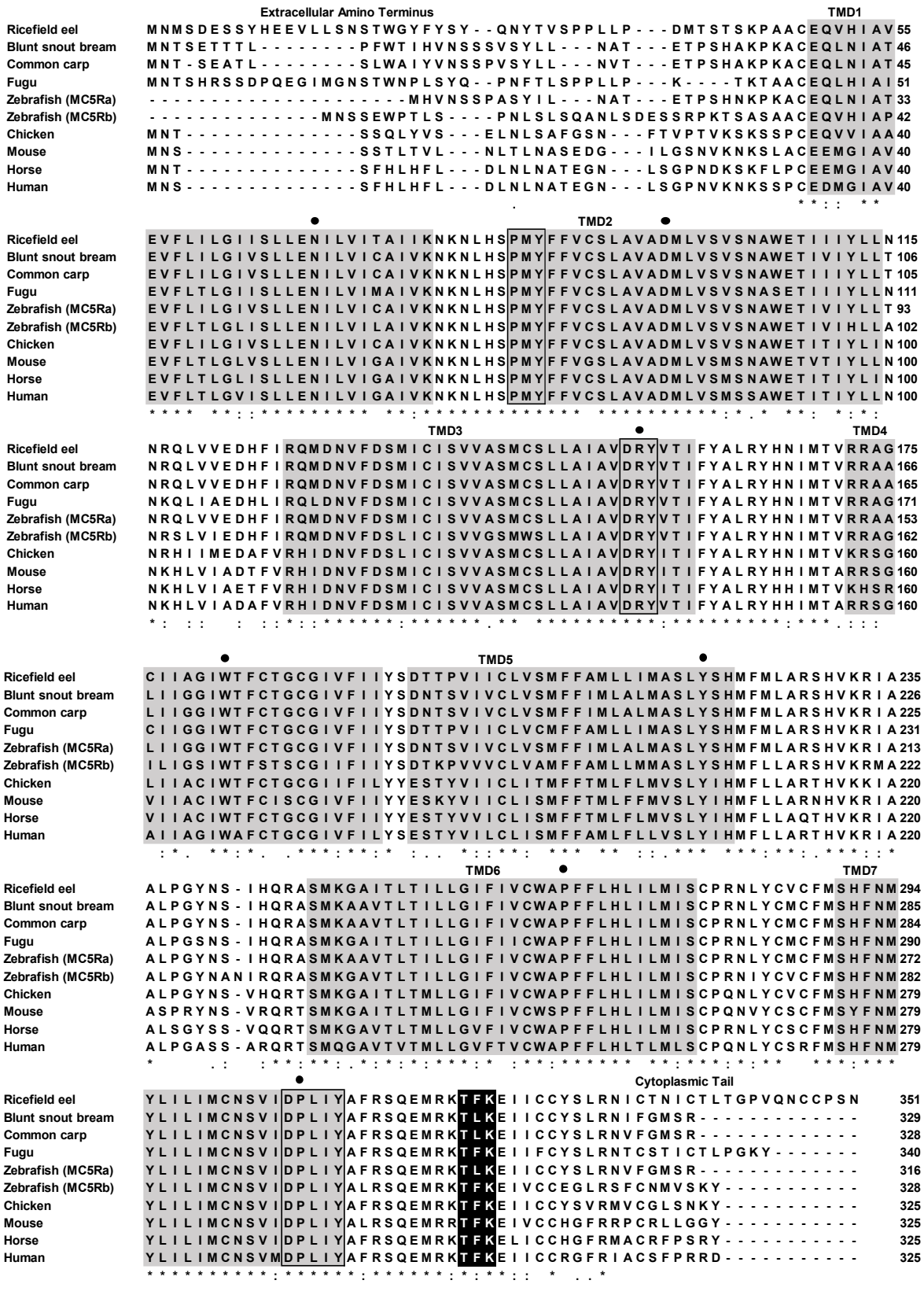
Extracellular Amino Terminus
TMD1
TMD2
TMD3
TMD4
TMD5
TMD6
TMD7
Cytoplasmic Tail
Ricefield eel
Blunt snout bream
Common carp
Fugu
Zebrafish (MC5Ra)
Zebrafish (MC5Rb)
Chicken
Mouse
Horse
Human

Fig. S3.2. Comparison of amino acid sequences between maMC5R and MC5Rs from other species.

Labeled as follows: transmembrane domains (TMDs) were shown in shaded boxes and named as TMD 1-7, amino and carboxyl termini were represented as extracellular amino terminus and cytoplasmic tail, respectively. Predicted phosphorylation sites were shown by dark shadow. The most conserved residues in each TMD were shown by black dots. PMY, DRY, DPxxY motifs were shown in open boxes. Asterisk (*) indicated the same amino acids. The IDs of MC5Rs were the same as that in Fig. 3.1.

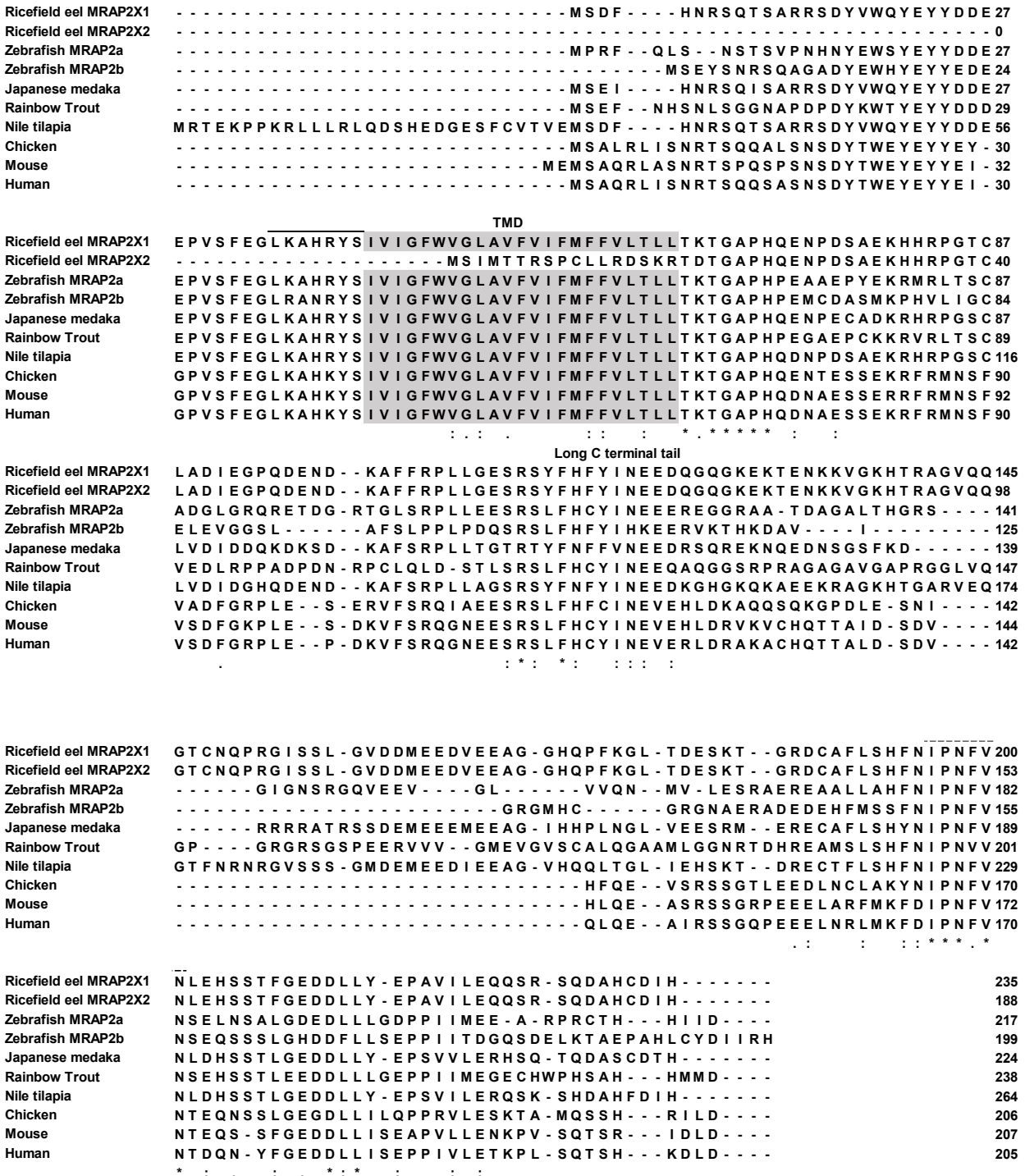

Fig. S3.3. Comparison of amino acid sequences between maMRAP2s and MRAP2s from other species.

Labeled as follows: transmembrane domain was shown in shaded box and named as

TMD. The above solid line showed the conserved motif (LKAHKYS) required for the formation of antiparallel homodimer. The above dashed line denoted the conserved motif (IPNFVN) in C-terminus. Asterisk (*) indicated the same amino acids. The IDs of MRAP2s were the same as that in Fig. 3.2.

Conclusion

In conclusion, firstly, we functionally investigated MC4R and its regulation by MRAP2 in snakehead fish. Four agonists, including NDP-MSH, ACTH, α-MSH, and β-MSH, were used in the pharmacological studies. Our results showed that the maximal binding value of caMC4R was significantly lower than that of hMC4R. All ligands could increase the intracellular cAMP level in a dose-dependent manner. In addition, caMC4R had significantly higher basal activity than hMC4R. Moreover, caMRAP2 dose-dependently decreased the basal cAMP levels. Our studies on snakehead MC4R and MRAP2 and their interaction contributes to a better understanding of fish MC4Rs. However, our data, combined with literature, suggested that functional implications of MRAP2 on MC4R are divergent in different species. Whether MC4R could be modulated to improve growth and reproduction of snakehead remains to be investigated.

Secondly, we studied the pharmacological characteristics of MC5R and its modulation by two spliced variants of MRAP2 in ricefield eel. Three agonists, NDP-MSH, α-MSH, and ACTH, could bind to maMC5R and induce intracellular cAMP production dose-dependently. Two maMRAP2s had no effect on cell surface and total expression of maMC5R, whereas they significantly increased maximal binding. Only maMRAP2X2 significantly decreased the binding affinity of ACTH. Both maMRAP2X1 and maMRAP2X2 significantly reduced R_{max} but did not affect EC_{50} in response to α-MSH or ACTH. The availability of maMC5R pharmacological characteristics and modulation by maMRAP2s will facilitate the investigation of its function in regulating diverse physiological processes in ricefield eel.

References

Abascal, F., Zardoya, R., Posada, D., 2005. ProtTest: selection of best-fit models of protein evolution. Bioinformatics 21, 2104-2105.

Agosti, F., López Soto, E.J., Cabral, A., Castrogiovanni, D., Schioth, H.B., Perelló, M., Raingo, J., 2014. Melanocortin 4 receptor activation inhibits presynaptic N-type calcium channels in amygdaloid complex neurons. Eur J Neurosci 40, 2755-2765.

An, J.J., Rhee, Y., Kim, S.H., Kim, D.M., Han, D.H., Hwang, J.H., Jin, Y.J., Cha, B.S., Baik, J.H., Lee, W.T., 2007. Peripheral effect of α-melanocyte-stimulating hormone on fatty acid oxidation in skeletal muscle. J Biol Chem 282, 2862-2870.

Anderson, E.J.P., Ghamari-Langroudi, M., Cakir, I., Litt, M.J., Chen, V., Reggiardo, R.E., Millhauser, G.L., Cone, R.D., 2019. Late onset obesity in mice with targeted deletion of potassium inward rectifier Kir7.1 from cells expressing the melanocortin-4 receptor. J Neuroendocrinol 31, e12670.

Asai, M., Ramachandrappa, S., Joachim, M., Shen, Y., Zhang, R., Nuthalapati, N., Ramanathan, V., Strochlic, D.E., Ferket, P., Linhart, K., Ho, C., Novoselova, T.V., Garg, S., Ridderstrale, M., Marcus, C., Hirschhorn, J.N., Keogh, J.M., O'Rahilly, S., Chan, L.F., Clark, A.J., Farooqi, I.S., Majzoub, J.A., 2013. Loss of function of the melanocortin 2 receptor accessory protein 2 is associated with mammalian obesity. Science 341, 275-278.

Aspiras, A.C., Rohner, N., Martineau, B., Borowsky, R.L., Tabin, C.J., 2015. Melanocortin 4 receptor mutations contribute to the adaptation of cavefish to nutrient-poor conditions. Proc Natl Acad Sci USA 112, 9668-9673.

Balthasar, N., Dalgaard, L.T., Lee, C.E., Yu, J., Funahashi, H., Williams, T., Ferreira, M., Tang, V., McGovern, R.A., Kenny, C.D., Christiansen, L.M., Edelstein, E., Choi, B., Boss, O., Aschkenasi, C., Zhang, C.Y., Mountjoy, K., Kishi, T., Elmquist, J.K.,

Lowell, B.B., 2005. Divergence of melanocortin pathways in the control of food intake and energy expenditure. Cell 123, 493-505.

Barney, E., Dores, M.R., McAvoy, D., Davis, P., Racareanu, R.C., Iki, A., Hyodo, S., Dores, R.M., 2019. Elephant shark melanocortin receptors: novel interactions with MRAP1 and implication for the HPI axis. Gen Comp Endocrinol 272, 42-51.

Berg, A.L., Rafnsson, A.T., Johannsson, M., Dallongeville, J., Arnadottir, M., 2006. The effects of adrenocorticotrophic hormone and an equivalent dose of cortisol on the serum concentrations of lipids, lipoproteins, and apolipoproteins. Metabolism 55, 1083-1087.

Berruien, N.N.A., Smith, C.L., 2020. Emerging roles of melanocortin receptor accessory proteins (MRAP and MRAP2) in physiology and pathophysiology. Gene 757, 144949.

Bertagna, X., 1994. Proopiomelanocortin-derived peptides. Endocrinol Metab Clin North Am 23, 467-485.

Bockaert, J., Pin, J.P., 1999. Molecular tinkering of G protein-coupled receptors: an evolutionary success. EMBO J 18, 1723-1729.

Boston, B.A., Cone, R.D., 1996. Characterization of melanocortin receptor subtype expression in murine adipose tissues and in the 3T3-L1 cell line. Endocrinology 137, 2043-2050.

Branson, R., Potoczna, N., Kral, J.G., Lentes, K.U., Hoehe, M.R., Horber, F.F., 2003. Binge eating as a major phenotype of melanocortin 4 receptor gene mutations. N Engl J Med 348, 1096-1103.

Bruschetta, G., Kim, J.D., Diano, S., Chan, L.F., 2018. Overexpression of melanocortin 2 receptor accessory protein 2 (MRAP2) in adult paraventricular MC4R neurons regulates energy intake and expenditure. Mol Metab 18, 79-87.

Büch, T.R., Heling, D., Damm, E., Gudermann, T., Breit, A., 2009. Pertussis toxin-

sensitive signaling of melanocortin-4 receptors in hypothalamic GT1-7 cells defines agouti-related protein as a biased agonist. J Biol Chem 284, 26411-26420.

Buggy, J.J., 1998. Binding of α-melanocyte-stimulating hormone to its G-protein- coupled receptor on B-lymphocytes activates the Jak/STAT pathway. Biochem J 331, 211-216.

Caruso, C., Durand, D., Schioth, H.B., Rey, R., Seilicovich, A., Lasaga, M., 2007. Activation of melanocortin 4 receptors reduces the inflammatory response and prevents apoptosis induced by lipopolysaccharide and interferon-γ in astrocytes. Endocrinology 148, 4918-4926.

Cerdá-Reverter, J.M., Agulleiro, M.J., Cortés, R., Sánchez, E., Guillot, R., Leal, E., Fernández-Durán, B., Puchol, S., Eley, M., 2013. Involvement of melanocortin receptor accessory proteins (MRAPs) in the function of melanocortin receptors. Gen Comp Endocrinol 188, 133-136.

Cerdá-Reverter, J.M., Ling, M.K., Schiöth, H.B., Peter, R.E., 2003a. Molecular cloning, characterization and brain mapping of the melanocortin 5 receptor in the goldfish. J Neurochem 87, 1354-1367.

Cerdá-Reverter, J.M., Ringholm, A., Schioth, H.B., Peter, R.E., 2003b. Molecular cloning, pharmacological characterization, and brain mapping of the melanocortin 4 receptor in the goldfish: involvement in the control of food intake. Endocrinology 144, 2336-2349.

Cerdá-Reverter, J.M., Schioth, H.B., Peter, R.E., 2003c. The central melanocortin system regulates food intake in goldfish. Regul Pept 115, 101-113.

Chagnon, Y.C., Chen, W.J., Pérusse, L., Chagnon, M., Nadeau, A., Wilkison, W.O., Bouchard, C., 1997. Linkage and association studies between the melanocortin receptors 4 and 5 genes and obesity-related phenotypes in the Quebec Family Study. Mol Med 3, 663-673.

Chai, B., Li, J.Y., Zhang, W., Newman, E., Ammori, J., Mulholland, M.W., 2006. Melanocortin-4 receptor-mediated inhibition of apoptosis in immortalized hypothalamic neurons via mitogen-activated protein kinase. Peptides 27, 2846-2857.

Chai, B., Li, J.Y., Zhang, W., Wang, H., Mulholland, M.W., 2009. Melanocortin-4 receptor activation inhibits c-Jun N-terminal kinase activity and promotes insulin signaling. Peptides 30, 1098-1104.

Chaly, A.L., Srisai, D., Gardner, E.E., Sebag, J.A., 2016. The melanocortin receptor accessory protein 2 promotes food intake through inhibition of the prokineticin receptor-1. eLife 5, e12397.

Chambers, J.C., Elliott, P., Zabaneh, D., Zhang, W., Li, Y., Froguel, P., Balding, D., Scott, J., Kooner, J.S., 2008. Common genetic variation near MC4R is associated with waist circumference and insulin resistance. Nat Genet 40, 716-718.

Chan, L.F., Webb, T.R., Chung, T.T., Meimaridou, E., Cooray, S.N., Guasti, L., Chapple, J.P., Egertova, M., Elphick, M.R., Cheetham, M.E., Metherell, L.A., Clark, A.J., 2009. MRAP and MRAP2 are bidirectional regulators of the melanocortin receptor family. Proc Natl Acad Sci USA 106, 6146-6151.

Chen, C., Okayama, H., 1987. High-efficiency transformation of mammalian cells by plasmid DNA. Mol Cell Biol 7, 2745-2752.

Chen, M., Shrestha, Y.B., Podyma, B., Cui, Z., Naglieri, B., Sun, H., Ho, T., Wilson, E.A., Li, Y.Q., Gavrilova, O., Weinstein, L.S., 2017. $G_s\alpha$ deficiency in the dorsomedial hypothalamus underlies obesity associated with $G_s\alpha$ mutations. J Clin Invest 127, 500-510.

Chen, W., 2000. The melanocortin-5 receptor, in: Cone, R.D. (Ed.) The melanocortin receptors. Springer, pp. 449-472.

Chen, W., Kelly, M.A., Opitz-Araya, X., Thomas, R.E., Low, M.J., Cone, R.D., 1997.

Exocrine gland dysfunction in MC5-R-deficient mice: evidence for coordinated regulation of exocrine gland function by melanocortin peptides. Cell 91, 789-798.

Cheng, H., Guo, Y., Yu, Q., Zhou, R., 2003. The rice field eel as a model system for vertebrate sexual development. Cytogenetic and Genome Research 101, 274-277.

Chhajlani, V., 1996. Distribution of cDNA for melanocortin receptor subtypes in human tissues. Biochemistry and Molecular Biology International 38, 73-80.

Chhajlani, V., Muceniece, R., Wikberg, J.E., 1993. Molecular cloning of a novel human melanocortin receptor. Biochem Biophys Res Commun 195, 866-873.

Chowdhary, B.P., Gustavsson, I., Wikberg, J.E.S., Chhajlani, V., 1995. Localization of the human melanocortin-5 receptor gene (MC5R) to chromosome band 18p11. 2 by fluorescence in situ hybridization. Cytogenetics and cell genetics 68, 79-81.

Clément, K., Biebermann, H., Farooqi, I.S., Van der Ploeg, L., Wolters, B., Poitou, C., Puder, L., Fiedorek, F., Gottesdiener, K., Kleinau, G., 2018. MC4R agonism promotes durable weight loss in patients with leptin receptor deficiency. Nat Med 24, 551-555.

Cole, S.A., Butte, N.F., Voruganti, V.S., Cai, G., Haack, K., Kent Jr, J.W., Blangero, J., Comuzzie, A.G., McPherson, J.D., Gibbs, R.A., 2010. Evidence that multiple genetic variants of MC4R play a functional role in the regulation of energy expenditure and appetite in Hispanic children. Am J Clin Nutr 91, 191-199.

Cone, R.D., 2005. Anatomy and regulation of the central melanocortin system. Nat Neurosci 8, 571-578.

Cone, R.D., 2006. Studies on the physiological functions of the melanocortin system. Endocr Rev 27, 736-749.

Cortés, R., Agulleiro, M.J., Navarro, S., Guillot, R., Sánchez, E., Cerdá-Reverter, J.M., 2014. Melanocortin receptor accessory protein 2 (MRAP2) interplays with the zebrafish melanocortin 1 receptor (MC1R) but has no effect on its pharmacological

profile. Gen Comp Endocrinol 201, 30-36.

Damm, E., Buech, T.R., Gudermann, T., Breit, A., 2012. Melanocortin-induced PKA activation inhibits AMPK activity via ERK-1/2 and LKB-1 in hypothalamic GT1-7 cells. Mol Endocrinol 26, 643-654.

Daniels, D., Patten, C.S., Roth, J.D., Yee, D.K., Fluharty, S.J., 2003. Melanocortin receptor signaling through mitogen-activated protein kinase in vitro and in rat hypothalamus. Brain Res 986, 1-11.

Dores, R.M., Oberer, N., Hoglin, B., Thomas, A., Faught, E., Vijayan, M.M., 2020. Evaluating interactions between the melanocortin-5 receptor, MRAP1, and ACTH(1-24): A phylogenetic study. Gen Comp Endocrinol 294, 113476.

Dubern, B., Bisbis, S., Talbaoui, H., Le Beyec, J., Tounian, P., Lacorte, J.M., Clément, K., 2007. Homozygous null mutation of the melanocortin-4 receptor and severe early-onset obesity. J Pediatr 150, 613-617. e611.

Eisinger, M., Li, W.H., Anthonavage, M., Pappas, A., Zhang, L., Rossetti, D., Huang, Q.L., Seiberg, M., 2011. A melanocortin receptor 1 and 5 antagonist inhibits sebaceous gland differentiation and the production of sebum-specific lipids. J Dermatol Sci 63, 23-32.

Entwistle, M.L., Hann, L.E., Sullivan, D.A., Tatro, J.B., 1990. Characterization of functional melanotropin receptors in lacrimal glands of the rat. Peptides 11, 477-483.

Fan, W., Boston, B.A., Kesterson, R.A., Hruby, V.J., Cone, R.D., 1997. Role of melanocortinergic neurons in feeding and the agouti obesity syndrome. Nature 385, 165-168.

Farooqi, I.S., Keogh, J.M., Yeo, G.S.H., Lank, E.J., Cheetham, T., O'Rahilly, S., 2003. Clinical spectrum of obesity and mutations in the melanocortin 4 receptor gene. N Engl J Med 348, 1085-1095.

Farooqi, I.S., Yeo, G.S.H., Keogh, J.M., Aminian, S., Jebb, S.A., Butler, G., Cheetham, T.,

O'Rahilly, S., 2000. Dominant and recessive inheritance of morbid obesity associated with melanocortin 4 receptor deficiency. J Clin Invest. 106, 271-279.

Fong, T.M., Mao, C., MacNeil, T., Kalyani, R., Smith, T., Weinberg, D., Tota, M.R., Van der Ploeg, L.H., 1997. ART (protein product of agouti-related transcript) as an antagonist of MC-3 and MC-4 receptors. Biochem Biophys Res Commun 237, 629-631.

Gantz, I., Fong, T.M., 2003. The melanocortin system. Am J Physiol 284, E468-E474.

Gantz, I., Miwa, H., Konda, Y., Shimoto, Y., Tashiro, T., Watson, S.J., DelValle, J., Yamada, T., 1993. Molecular cloning, expression, and gene localization of a fourth melanocortin receptor. J Biol Chem 268, 15174-15179.

Gardiner, K., Slavov, D., Bechtel, L., Davisson, M., 2002. Annotation of human chromosome 21 for relevance to down syndrome: gene structure and expression analysis. Genomics 79, 833-843.

Ghamari-Langroudi, M., Digby, G.J., Sebag, J.A., Millhauser, G.L., Palomino, R., Matthews, R., Gillyard, T., Panaro, B.L., Tough, I.R., Cox, H.M., 2015. G-protein-independent coupling of MC4R to Kir7. 1 in hypothalamic neurons. Nature 520, 94-98.

Gillyard, T., Fowler, K., Williams, S.Y., Cone, R.D., 2019. Obesity-associated mutant melanocortin-4 receptors with normal $G\alpha_s$ coupling frequently exhibit other discoverable pharmacological and biochemical defects. J Neuroendocrinol 31, e12795.

Giraudo, S.Q., Billington, C.J., Levine, A.S., 1998. Feeding effects of hypothalamic injection of melanocortin 4 receptor ligands. Brain Res 809, 302-306.

Gorrigan, R.J., Guasti, L., King, P., Clark, A.J., Chan, L.F., 2011. Localisation of the melanocortin-2-receptor and its accessory proteins in the developing and adult adrenal gland. J Mol Endocrinol 46, 227-232.

Greenfield, J.R., Miller, J.W., Keogh, J.M., Henning, E., Satterwhite, J.H., Cameron, G.S., Astruc, B., Mayer, J.P., Brage, S., See, T.C., 2009. Modulation of blood pressure by central melanocortinergic pathways. N Engl J Med 360, 44-52.

Griffon, N., Mignon, V., Facchinetti, P., Diaz, J., Schwartz, J.C., Sokoloff, P., 1994. Molecular cloning and characterization of the rat fifth melanocortin receptor. Biochem Biophys Res Commun 200, 1007-1014.

Habara, M., Mori, N., Okada, Y., Kawasumi, K., Nakao, N., Tanaka, Y., Arai, T., Yamamoto, I., 2018. Molecular characterization of feline melanocortin 4 receptor and melanocortin 2 receptor accessory protein 2. Gen Comp Endocrinol 261, 31-39.

Haitina, T., Klovins, J., Andersson, J., Fredriksson, R., Lagerstrom, M.C., Larhammar, D., Larson, E.T., Schioth, H.B., 2004. Cloning, tissue distribution, pharmacology and three-dimensional modelling of melanocortin receptors 4 and 5 in rainbow trout suggest close evolutionary relationship of these subtypes. Biochem J 380, 475-486.

Haskell-Luevano, C., Monck, E.K., 2001. Agouti-related protein functions as an inverse agonist at a constitutively active brain melanocortin-4 receptor. Regul Pept 99, 1-7.

Hatta, N., Dixon, C., Ray, A.J., Phillips, S.R., Cunliffe, W.J., Dale, M., Todd, C., Meggit, S., Birch-Machin, M.A., Rees, J.L., 2001. Expression, candidate gene, and population studies of the melanocortin 5 receptor. J Invest Dermatol 116, 564-570.

Hauser, A.S., Attwood, M.M., Rask-Andersen, M., Schioth, H.B., Gloriam, D.E., 2017. Trends in GPCR drug discovery: new agents, targets and indications. Nat Rev Drug Discov 16, 829-842.

Hill, C.A., Fox, A.N., Pitts, R.J., Kent, L.B., Tan, P.L., Chrystal, M.A., Cravchik, A., Collins, F.H., Robertson, H.M., Zwiebel, L.J., 2002. G protein-coupled receptors in *Anopheles gambiae*. Science 298, 176-178.

Hinkle, P.M., Sebag, J.A., 2009. Structure and function of the melanocortin2 receptor accessory protein (MRAP). Mol Cell Endocrinol 300, 25-31.

Hoglin, B.E., Miner, M., Dores, R.M., 2020. Pharmacological properties of whale shark (*Rhincodon typus*) melanocortin-2 receptor and melancortin-5 receptor: Interaction with MRAP1 and MRAP2. Gen Comp Endocrinol 293, 113463.

Hughes, L.C., Ortí, G., Huang, Y., Sun, Y., Baldwin, C.C., Thompson, A.W., Arcila, D., Betancur-R, R., Li, C., Becker, L., 2018. Comprehensive phylogeny of ray-finned fishes (Actinopterygii) based on transcriptomic and genomic data. Proc Natl Acad Sci USA 115, 6249-6254.

Huszar, D., Lynch, C.A., Fairchild-Huntress, V., Dunmore, J.H., Fang, Q., Berkemeier, L.R., Gu, W., Kesterson, R.A., Boston, B.A., Cone, R.D., Smith, F.J., Campfield, L.A., Burn, P., Lee, F., 1997. Targeted disruption of the melanocortin-4 receptor results in obesity in mice. Cell 88, 131-141.

Iepsen, E.W., Zhang, J., Hollensted, M., Madsbad, S., Hansen, T., Holst, J.J., Jørgensen, N.R., Holm, J.C., Torekov, S.S., 2020. Adults with pathogenic MC4R mutations have increased final height and thereby increased bone mass. J Bone Miner Metab 38, 117-125.

Inoue, A., Raimondi, F., Kadji, F.M.N., Singh, G., Kishi, T., Uwamizu, A., Ono, Y., Shinjo, Y., Ishida, S., Arang, N., 2019. Illuminating G-protein-coupling selectivity of GPCRs. Cell 177, 1933-1947. e1925.

Irani, B.G., Xiang, Z., Moore, M.C., Mandel, R.J., Haskell-Luevano, C., 2005. Voluntary exercise delays monogenetic obesity and overcomes reproductive dysfunction of the melanocortin-4 receptor knockout mouse. Biochem Biophys Res Commun 326, 638-644.

Jangprai, A., Boonanuntanasarn, S., Yoshizaki, G., 2011. Characterization of melanocortin 4 receptor in Snakeskin Gourami and its expression in relation to

daily feed intake and short-term fasting. Gen Comp Endocrinol 173, 27-37.

Jiang, D.N., Li, J.T., Tao, Y.X., Chen, H.P., Deng, S.P., Zhu, C.H., Li, G.L., 2017. Effects of melanocortin-4 receptor agonists and antagonists on expression of genes related to reproduction in spotted scat, *Scatophagus argus*. J Comp Physiol B 187, 603-612.

Josefsson, L.G., Rask, L., 1997. Cloning of a putative G-protein-coupled receptor from *Arabidopsis thaliana*. Eur J Biochem 249, 415-420.

Josep Agulleiro, M., Cortes, R., Fernandez-Duran, B., Navarro, S., Guillot, R., Meimaridou, E., Clark, A.J.L., Cerda-Reverter, J.M., 2013. Melanocortin 4 receptor becomes an ACTH receptor by coexpression of melanocortin receptor accessory protein 2. Mol Endocrinol 27, 1934-1945.

Jun, D.J., Na, K.Y., Kim, W., Kwak, D., Kwon, E.J., Yoon, J.H., Yea, K., Lee, H., Kim, J., Suh, P.G., 2010. Melanocortins induce interleukin 6 gene expression and secretion through melanocortin receptors 2 and 5 in 3T3-L1 adipocytes. J Mol Endocrinol 44, 225.

Kay, E.I., Botha, R., Montgomery, J.M., Mountjoy, K.G., 2013a. hMRAPa increases αMSH-induced hMC1R and hMC3R functional coupling and hMC4R constitutive activity. J Mol Endocrinol 50, 203-215.

Kay, E.I., Botha, R., Montgomery, J.M., Mountjoy, K.G., 2013b. hMRAPa specifically alters hMC4R molecular mass and N-linked complex glycosylation in HEK293 cells. J Mol Endocrinol 50, 217-227.

Kay, E.I., Botha, R., Montgomery, J.M., Mountjoy, K.G., 2015. hMRAPα, but not hMRAP2, enhances hMC4R constitutive activity in HEK293 cells and this is not dependent on hMRAPα induced changes in hMC4R complex N-linked glycosylation. PloS One 10, e0140320.

Klovins, J., Haitina, T., Fridmanis, D., Kilianova, Z., Kapa, I., Fredriksson, R., Gallo-Payet,

N., Schioth, H.B., 2004. The melanocortin system in Fugu: determination of POMC/AGRP/MCR gene repertoire and synteny, as well as pharmacology and anatomical distribution of the MCRs. Mol Biol Evol 21, 563-579.

Kobayashi, Y., Hamamoto, A., Takahashi, A., Saito, Y., 2016. Dimerization of melanocortin receptor 1 (MC1R) and MC5R creates a ligand-dependent signal modulation: Potential participation in physiological color change in the flounder. Gen Comp Endocrinol 230, 103-109.

Kobayashi, Y., Tsuchiya, K., Yamanome, T., Schiöth, H.B., Kawauchi, H., Takahashi, A., 2008. Food deprivation increases the expression of melanocortin-4 receptor in the liver of barfin flounder, *Verasper moseri*. Gen Comp Endocrinol 155, 280-287.

Krakoff, J., Ma, L., Kobes, S., Knowler, W.C., Hanson, R.L., Bogardus, C., Baier, L.J., 2008. Lower metabolic rate in individuals heterozygous for either a frameshift or a functional missense MC4R variant. Diabetes 57, 3267-3272.

Kumar, S., Stecher, G., Tamura, K., 2016. MEGA7: molecular evolutionary genetics analysis version 7.0 for bigger datasets. Mol Biol Evol 33, 1870-1874.

Lampert, K.P., Schmidt, C., Fischer, P., Volff, J.N., Hoffmann, C., Muck, J., Lohse, M.J., Ryan, M.J., Schartl, M., 2010. Determination of onset of sexual maturation and mating behavior by melanocortin receptor 4 polymorphisms. Curr Biol 20, 1729-1734.

Li, J.T., Yang, Z., Chen, H.P., Zhu, C.H., Deng, S.P., Li, G.L., Tao, Y.X., 2016a. Molecular cloning, tissue distribution, and pharmacological characterization of melanocortin-4 receptor in spotted scat, *Scatophagus argus*. Gen Comp Endocrinol 230, 143 - 152.

Li, L., Yang, Z., Zhang, Y.P., He, S., Liang, X.F., Tao, Y.X., 2017a. Molecular cloning, tissue distribution, and pharmacological characterization of melanocortin-4 receptor in grass carp (*Ctenopharyngodon idella*). Domest Anim Endocrinol 59, 140-151.

Li, Y.Q., Shrestha, Y., Pandey, M., Chen, M., Kablan, A., Gavrilova, O., Offermanns, S., Weinstein, L.S., 2016b. $G_{q/11}\alpha$ and $G_s\alpha$ mediate distinct physiological responses to central melanocortins. J Clin Investig 126, 40-49.

Li, Z.G., Chen, F., Huang, C.H., Zheng, W.X., Yu, C.L., Cheng, H.H., Zhou, R.J., 2017b. Genome-wide mapping and characterization of microsatellites in the swamp eel genome. Sci Rep 7, 1-9.

Liao, S.C., Dong, J.J., Xu, W.N., Xi, B.W., Tao, Y.X., Liu, B., Xie, J., 2019. Molecular cloning, tissue distribution, and pharmacological characterization of blunt snout bream (*Megalobrama amblycephala*) melanocortin-5 receptor. Fish Physiol Biochem 45, 311-321.

Liu, C.K., 1944. Rudimentary hermaphroditism in the symbranchoid eel, *Monopterus javanensis*. Sinensia 15, 1-8.

Livak, K.J., Schmittgen, T.D., 2001. Analysis of relative gene expression data using real-time quantitative PCR and the $2^{-\Delta\Delta C_T}$ method. Methods 25, 402-408.

Logan, D.W., Bryson-Richardson, R.J., Pagan, K.E., Taylor, M.S., Currie, P.D., Jackson, I.J., 2003. The structure and evolution of the melanocortin and MCH receptors in fish and mammals. Genomics 81, 184-191.

Loos, R.J., Lindgren, C.M., Li, S., Wheeler, E., Zhao, J.H., Prokopenko, I., Inouye, M., Freathy, R.M., Attwood, A.P., Beckmann, J.S., Berndt, S.I., Jacobs, K.B., Chanock, S.J., Hayes, R.B., Bergmann, S., Bennett, A.J., Bingham, S.A., Bochud, M., Brown, M., Cauchi, S., Connell, J.M., Cooper, C., Smith, G.D., Day, I., Dina, C., De, S., Dermitzakis, E.T., Doney, A.S., Elliott, K.S., Elliott, P., Evans, D.M., Sadaf Farooqi, I., Froguel, P., Ghori, J., Groves, C.J., Gwilliam, R., Hadley, D., Hall, A.S., Hattersley, A.T., Hebebrand, J., Heid, I.M., Lamina, C., Gieger, C., Illig, T., Meitinger, T., Wichmann, H.E., Herrera, B., Hinney, A., Hunt, S.E., Jarvelin, M.R., Johnson, T., Jolley, J.D., Karpe, F., Keniry, A., Khaw, K.T., Luben, R.N., Mangino, M.,

Marchini, J., McArdle, W.L., McGinnis, R., Meyre, D., Munroe, P.B., Morris, A.D., Ness, A.R., Neville, M.J., Nica, A.C., Ong, K.K., O'Rahilly, S., Owen, K.R., Palmer, C.N., Papadakis, K., Potter, S., Pouta, A., Qi, L., Randall, J.C., Rayner, N.W., Ring, S.M., Sandhu, M.S., Scherag, A., Sims, M.A., Song, K., Soranzo, N., Speliotes, E.K., Syddall, H.E., Teichmann, S.A., Timpson, N.J., Tobias, J.H., Uda, M., Vogel, C.I., Wallace, C., Waterworth, D.M., Weedon, M.N., Willer, C.J., Wraight, Yuan, X., Zeggini, E., Hirschhorn, J.N., Strachan, D.P., Ouwehand, W.H., Caulfield, M.J., Samani, N.J., Frayling, T.M., Vollenweider, P., Waeber, G., Mooser, V., Deloukas, P., McCarthy, M.I., Wareham, N.J., Barroso, I., Jacobs, K.B., Chanock, S.J., Hayes, R.B., Lamina, C., Gieger, C., Illig, T., Meitinger, T., Wichmann, H.E., Kraft, P., Hankinson, S.E., Hunter, D.J., Hu, F.B., Lyon, H.N., Voight, B.F., Ridderstrale, M., Groop, L., Scheet, P., Sanna, S., Abecasis, G.R., Albai, G., Nagaraja, R., Schlessinger, D., Jackson, A.U., Tuomilehto, J., Collins, F.S., Boehnke, M., Mohlke, K.L., 2008. Common variants near MC4R are associated with fat mass, weight and risk of obesity. Nat Genet 40, 768-775.

Lotta, L.A., Mokrosiński, J., de Oliveira, E.M., Li, C., Sharp, S.J., Luan, J., Brouwers, B., Ayinampudi, V., Bowker, N., Kerrison, N., 2019. Human gain-of-function MC4R variants show signaling bias and protect against obesity. Cell 177, 597-607. e599.

Lu, D., Willard, D., Patel, I.R., Kadwell, S., Overton, L., Kost, T., Luther, M., Chen, W., Woychik, R.P., Wilkison, W.O., Cone, R.D., 1994. Agouti protein is an antagonist of the melanocyte-stimulating-hormone receptor. Nature 371, 799-802.

Mandrika, I., Petrovska, R., Wikberg, J., 2005. Melanocortin receptors form constitutive homo- and heterodimers. Biochem Biophys Res Commun 326, 349-354.

Martinelli, C.E., Keogh, J.M., Greenfield, J.R., Henning, E., van der Klaauw, A.A., Blackwood, A., O'Rahilly, S., Roelfsema, F., Camacho-Hübner, C., Pijl, H., 2011. Obesity due to melanocortin 4 receptor (MC4R) deficiency is associated with

increased linear growth and final height, fasting hyperinsulinemia, and incompletely suppressed growth hormone secretion. J Clin Endocrinol Metab 96, E181-E188.

Metherell, L.A., Chapple, J.P., Cooray, S., David, A., Becker, C., Ruschendorf, F., Naville, D., Begeot, M., Khoo, B., Nurnberg, P., Huebner, A., Cheetham, M.E., Clark, A.J.L., 2005. Mutations in *MRAP*, encoding a new interacting partner of the ACTH receptor, cause familial glucocorticoid deficiency type 2. Nat Genet 37, 166-170.

Metzger, P., Carlson, B., Sun, H., Cui, Z., Gavrilova, O., Chen, M., Weinstein, L., 2019. OR12-3 mice with MC4R site mutation (F51L) develop severe obesity independent of G_s-alpha/cAMP signaling. J Endocr Soc 3, OR12-13.

Miller, C.L., Murakami, P., Ruczinski, I., Ross, R.G., Sinkus, M., Sullivan, B., Leonard, S., 2009. Two complex genotypes relevant to the kynurenine pathway and melanotropin function show association with schizophrenia and bipolar disorder. Schizophr Res 113, 259-267.

Millington, G.W.M., 2006. Proopiomelanocortin (POMC): the cutaneous roles of its melanocortin products and receptors. Clinical and Experimental Dermatology 31, 407-412.

Minokoshi, Y., Alquier, T., Furukawa, N., Kim, Y.B., Lee, A., Xue, B., Mu, J., Foufelle, F., Ferre, P., Birnbaum, M.J., Stuck, B.J., Kahn, B.B., 2004. AMP-kinase regulates food intake by responding to hormonal and nutrient signals in the hypothalamus. Nature 428, 569-574.

Mo, X.L., Yang, R., Tao, Y.X., 2012. Functions of transmembrane domain 3 of human melanocortin-4 receptor. J Mol Endocrinol 49, 221-235.

Møller, C.L., Pedersen, S.B., Richelsen, B., Conde-Frieboes, K.W., Raun, K., Grove, K.L., Wulff, B.S.J., 2015. Melanocortin agonists stimulate lipolysis in human adipose tissue explants but not in adipocytes. BMC Res Notes 8, 1-9.

Morgan, C., Cone, R.D., 2006. Melanocortin-5 receptor deficiency in mice blocks a novel pathway influencing pheromone-induced aggression. Behav Genet 36, 291-300.

Morgan, C., Thomas, R.E., Ma, W.D., Novotny, M.V., Cone, R.D., 2004. Melanocortin-5 receptor deficiency reduces a pheromonal signal for aggression in male mice. Chem Senses 29, 111-115.

Mountjoy, K.G., Jenny Wu, C.S., Dumont, L.M., Wild, J.M., 2003. Melanocortin-4 receptor messenger ribonucleic acid expression in rat cardiorespiratory, musculoskeletal, and integumentary systems. Endocrinology 144, 5488-5496.

Mountjoy, K.G., Mortrud, M.T., Low, M.J., Simerly, R.B., Cone, R.D., 1994. Localization of the melanocortin-4 receptor (MC4-R) in neuroendocrine and autonomic control circuits in the brain. Mol Endocrinol 8, 1298-1308.

Mountjoy, K.G., Robbins, L.S., Mortrud, M.T., Cone, R.D., 1992. The cloning of a family of genes that encode the melanocortin receptors. Science 257, 1248-1251.

Newman, E.A., Chai, B.X., Zhang, W., Li, J.Y., Ammori, J.B., Mulholland, M.W., 2006. Activation of the melanocortin-4 receptor mobilizes intracellular free calcium in immortalized hypothalamic neurons. J Surg Res 132, 201-207.

Nijenhuis, W.A., Oosterom, J., Adan, R.A., 2001. AgRP(83-132) acts as an inverse agonist on the human melanocortin-4 receptor. Mol Endocrinol 15, 164-171.

Nimura, M., Udagawa, J., Hatta, T., Hashimoto, R., Otani, H., 2006. Spatial and temporal patterns of expression of melanocortin type 2 and 5 receptors in the fetal mouse tissues and organs. Anat Embryol 211, 109-117.

Noon, L.A., Franklin, J.M., King, P.J., Goulding, N.J., Hunyady, L., Clark, A.J., 2002. Failed export of the adrenocorticotrophin receptor from the endoplasmic reticulum in non-adrenal cells: evidence in support of a requirement for a specific adrenal accessory factor. J Endocrinol 174, 17-25.

Nylander, J.A.A.M.v., 2004. MrAIC. pl. Program Distributed by the Author; Evolutionary

Biology Centre, Uppsala University: Uppsala, Sweden, 2004.

Ollmann, M.M., Wilson, B.D., Yang, Y.K., Kerns, J.A., Chen, Y., Gantz, I., Barsh, G.S., 1997. Antagonism of central melanocortin receptors in vitro and in vivo by agouti-related protein. Science 278, 135-138.

Palczewski, K., Kumasaka, T., Hori, T., Behnke, C.A., Motoshima, H., Fox, B.A., Le Trong, I., Teller, D.C., Okada, T., Stenkamp, R.E., 2000. Crystal structure of rhodopsin: a G protein-coupled receptor. Science 289, 739-745.

Podyma, B., Sun, H., Wilson, E.A., Carlson, B., Pritikin, E., Gavrilova, O., Weinstein, L.S., Chen, M., 2018. The stimulatory G protein Gsα is required in melanocortin 4 receptor–expressing cells for normal energy balance, thermogenesis, and glucose metabolism. J Biol Chem 293, 10993-11005.

Poggioli, R., Vergoni, A.V., Bertolini, A., 1986. ACTH-(1-24) and α-MSH antagonize feeding behavior stimulated by kappa opiate agonists. Peptides 7, 843-848.

Pritchard, L.E., Turnbull, A.V., White, A., 2002. Pro-opiomelanocortin processing in the hypothalamus: impact on melanocortin signalling and obesity. J Endocrinol 172, 411-421.

Rao, Y.Z., Chen, R., Zhang, Y., Tao, Y.X., 2019. Orange-spotted grouper melanocortin-4 receptor: modulation of signaling by MRAP2. Gen Comp Endocrinol 284, 113234.

Reinick, C.L., Liang, L., Angleson, J.K., Dores, R.M., 2012. Functional expression of *Squalus acanthias* melanocortin-5 receptor in CHO cells: ligand selectivity and interaction with MRAP. Eur J Pharmacol 680, 1-7.

Renquist, B.J., Zhang, C., Williams, S.Y., Cone, R.D., 2013. Development of an assay for high-throughput energy expenditure monitoring in the zebrafish. Zebrafish 10, 343-352.

Ringholm, A., Fredriksson, R., Poliakova, N., Yan, Y.L., Postlethwait, J.H., Larhammar, D., Schioth, H.B., 2002. One melanocortin 4 and two melanocortin 5 receptors from

zebrafish show remarkable conservation in structure and pharmacology. J Neurochem 82, 6-18.

Rodrigues, A.R., Almeida, H., Gouveia, A.M., 2013. α-MSH signalling via melanocortin 5 receptor promotes lipolysis and impairs re-esterification in adipocytes. Biochim Biophys Acta 1831, 1267-1275.

Rodrigues, A.R., Pignatelli, D., Almeida, H., Gouveia, A.M., 2009. Melanocortin 5 receptor activates ERK1/2 through a PI3K-regulated signaling mechanism. Mol Cell Endocrinol 303, 74-81.

Rossi, J., Balthasar, N., Olson, D., Scott, M., Berglund, E., Lee, C.E., Choi, M.J., Lauzon, D., Lowell, B.B., Elmquist, J.K., 2011. Melanocortin-4 receptors expressed by cholinergic neurons regulate energy balance and glucose homeostasis. Cell Metab 13, 195-204.

Rossi, M., Kim, M.S., Morgan, D.G., Small, C.J., Edwards, C.M., Sunter, D., Abusnana, S., Goldstone, A.P., Russell, S.H., Stanley, S.A., Smith, D.M., Yagaloff, K., Ghatei, M.A., Bloom, S.R., 1998. A C-terminal fragment of Agouti-related protein increases feeding and antagonizes the effect of alpha-melanocyte stimulating hormone *in vivo*. Endocrinology 139, 4428-4431.

Rouault, A.A.J., Lee, A.A., Sebag, J.A., 2017a. Regions of MRAP2 required for the inhibition of orexin and prokineticin receptor signaling. Biochim Biophys Acta 1864, 2322-2329.

Rouault, A.A.J., Srinivasan, D.K., Yin, T.C., Lee, A.A., Sebag, J.A., 2017b. Melanocortin receptor accessory proteins (MRAPs): functions in the melanocortin system and beyond. Biochim Biophys Acta 1863, 2462-2467.

Roy, S., Rached, M., Gallo-Payet, N., 2007. Differential regulation of the human adrenocorticotropin receptor [melanocortin-2 receptor (MC2R)] by human MC2R accessory protein isoforms α and β in isogenic human embryonic kidney 293 cells.

Mol Endocrinol 21, 1656-1669.

Saitou, N., Nei, M., 1987. The neighbor-joining method: a new method for reconstructing phylogenetic trees. Mol Biol Evol 4, 406-425.

Sánchez, E., Rubio, V.C., Cerdá-Reverter, J.M., 2009a. Characterization of the sea bass melanocortin 5 receptor: a putative role in hepatic lipid metabolism. J Exp Biol 212, 3901-3910.

Sánchez, E., Rubio, V.C., Thompson, D., Metz, J., Flik, G., Millhauser, G.L., Cerda-Reverter, J.M., 2009b. Phosphodiesterase inhibitor-dependent inverse agonism of agouti-related protein on melanocortin 4 receptor in sea bass (*Dicentrarchus labrax*). American Journal of Physiology, Regulatory, Integrative and Comparative Physiolology 296, R1293-R1306.

Sandrock, M., Schulz, A., Merkwitz, C., Schoneberg, T., Spanel-Borowski, K., Ricken, A., 2009. Reduction in corpora lutea number in obese melanocortin-4-receptor-deficient mice. Reprod Biol Endocrinol 7, 24.

Schjolden, J., Schioth, H.B., Larhammar, D., Winberg, S., Larson, E.T., 2009. Melanocortin peptides affect the motivation to feed in rainbow trout (*Oncorhynchus mykiss*). Gen Comp Endocrinol 160, 134-138.

Schonnop, L., Kleinau, G., Herrfurth, N., Volckmar, A.L., Cetindag, C., Muller, A., Peters, T., Herpertz, S., Antel, J., Hebebrand, J., Biebermann, H., Hinney, A., 2016. Decreased melanocortin-4 receptor function conferred by an infrequent variant at the human melanocortin receptor accessory protein 2 gene. Obesity (Silver Spring) 24, 1976-1982.

Sebag, J.A., Hinkle, P.M., 2007. Melanocortin-2 receptor accessory protein MRAP forms antiparallel homodimers. Proc Natl Acad Sci USA 104, 20244-20249.

Sebag, J.A., Hinkle, P.M., 2009a. Opposite effects of the melanocortin-2 (MC2) receptor accessory protein MRAP on MC2 and MC5 receptor dimerization and trafficking. J

Biol Chem 284, 22641-22648.

Sebag, J.A., Hinkle, P.M., 2009b. Regions of melanocortin 2 (MC2) receptor accessory protein necessary for dual topology and MC2 receptor trafficking and signaling. J Biol Chem 284, 610-618.

Sebag, J.A., Hinkle, P.M., 2010. Regulation of G protein-coupled receptor signaling: specific dominant-negative effects of melanocortin 2 receptor accessory protein 2. Sci Signal 3, ra28.

Sebag, J.A., Zhang, C., Hinkle, P.M., Bradshaw, A.M., Cone, R.D., 2013. Developmental control of the melanocortin-4 receptor by MRAP2 proteins in zebrafish. Science 341, 278-281.

Seifert, R., Wenzel-Seifert, K., 2002. Constitutive activity of G-protein-coupled receptors: cause of disease and common property of wild-type receptors. Naunyn Schmiedebergs Arch Pharmacol 366, 381-416.

Selkirk, J.V., Nottebaum, L.M., Lee, J., Yang, W., Foster, A.C., Lechner, S.M., 2007. Identification of differential melanocortin 4 receptor agonist profiles at natively expressed receptors in rat cortical astrocytes and recombinantly expressed receptors in human embryonic kidney cells. Neuropharmacology 52, 459-466.

Shenoy, S.K., Lefkowitz, R.J., 2011. β-Arrestin-mediated receptor trafficking and signal transduction. Trends Pharmacol Sci 32, 521-533.

Siljee, J.E., Unmehopa, U.A., Kalsbeek, A., Swaab, D.F., Fliers, E., Alkemade, A., 2013. Melanocortin 4 receptor distribution in the human hypothalamus. Eur J Endocrinol 168, 361-369.

Simamura, E., Arikawa, T., Ikeda, T., Shimada, H., Shoji, H., Masuta, H., Nakajima, Y., Otani, H., Yonekura, H., Hatta, T., 2015. Melanocortins contribute to sequential differentiation and enucleation of human erythroblasts via melanocortin receptors 1, 2 and 5. PLoS One 10, e0123232.

Smith, A.I., Funder, J.W., 1988. Proopiomelanocortin processing in the pituitary, central nervous system, and peripheral tissues. Endocr Rev 9, 159-179.

Soletto, L., Hernández-Balfagó, S., Rocha, A., Scheerer, P., Kleinau, G., Cerdá-Reverter, J.M., 2019. Melanocortin receptor accessory protein 2-induced adrenocorticotropic hormone response of human melanocortin 4 receptor. J Endocr Soc 3, 314-323.

Song, Y., Cone, R.D., 2007. Creation of a genetic model of obesity in a teleost. FASEB J 21, 2042-2049.

Spencer, J.D., Schallreuter, K.U., 2009. Regulation of pigmentation in human epidermal melanocytes by functional high-affinity β-melanocyte-stimulating hormone/melanocortin-4 receptor signaling. Endocrinology 150, 1250-1258.

Srinivasan, S., Lubrano-Berthelier, C., Govaerts, C., Picard, F., Santiago, P., Conklin, B.R., Vaisse, C., 2004. Constitutive activity of the melanocortin-4 receptor is maintained by its N-terminal domain and plays a role in energy homeostasis in humans. J Clin Invest 114, 1158-1164.

Srisai, D., Yin, T.C., Lee, A.A., Rouault, A.A.J., Pearson, N.A., Grobe, J.L., Sebag, J.A., 2017. MRAP2 regulates ghrelin receptor signaling and hunger sensing. Nat Commun 8, 1-10.

Steiner, A.L., Kipnis, D.M., Utiger, R., Parker, C., 1969. Radioimmunoassay for the measurement of adenosine 3',5'-cyclic phosphate. Proc Natl Acad Sci USA 64, 367-373.

Sutton, G.M., Duos, B., Patterson, L.M., Berthoud, H.R., 2005. Melanocortinergic modulation of cholecystokinin-induced suppression of feeding through extracellular signal-regulated kinase signaling in rat solitary nucleus. Endocrinology 146, 3739-3747.

Tao, M., Ji, R.L., Huang, L., Fan, S.Y., Liu, T., Liu, S.J., Tao, Y.X., 2020. Regulation of melanocortin-4 receptor pharmacology by two isoforms of melanocortin receptor

accessory protein 2 in topmouth culter (*Culter alburnus*). Front Endocrinol 11: 538.

Tao, Y.X., 2007. Functional characterization of novel melanocortin-3 receptor mutations identified from obese subjects. Biochim Biophys Acta 1772, 1167-1174.

Tao, Y.X., 2008. Constitutive activation of G protein-coupled receptors and diseases: Insights into mechanism of activation and therapeutics. Pharmacol Ther 120, 129-148.

Tao, Y.X., 2010. The melanocortin-4 receptor: physiology, pharmacology, and pathophysiology. Endocr Rev 31, 506-543.

Tao, Y.X., 2014. Constitutive activity in melanocortin-4 receptor: biased signaling of inverse agonists. Adv Pharmacol 70, 135-154.

Tao, Y.X., 2017. Melanocortin receptors. Biochim Biophys Acta 1863, 2411-2413.

Tao, Y.X., 2020. Molecular chaperones and G protein-coupled receptor maturation and pharmacology. Mol Cell Endocrinol 511, 110862.

Tao, Y.X., Conn, P.M., 2014. Chaperoning G protein-coupled receptors: From cell biology to therapeutics. Endocr Rev 35, 602-647.

Tao, Y.X., Huang, H., Wang, Z.Q., Yang, F., Williams, J.N., Nikiforovich, G.V., 2010. Constitutive activity of neural melanocortin receptors. Methods Enzymol 484, 267-279.

Tao, Y.X., Lin, H.R., Van Der Kraak, G., Peter, R.E., 1993. Hormonal induction of precocious sex reversal in ricefield eel, *Monopterus albus*. Aquaculture 118, 131-140.

Tao, Y.X., Segaloff, D.L., 2003. Functional characterization of melanocortin-4 receptor mutations associated with childhood obesity. Endocrinology 144, 4544-4551.

Taylor, A.W., Kitaichi, N., Biros, D., 2006. Melanocortin 5 receptor and ocular immunity. Cell Mol Biol 52, 53-59.

Thomas, A.L., Maekawa, F., Kawashima, T., Sakamoto, H., Sakamoto, T., Davis, P., Dores,

R.M., 2018. Analyzing the effects of co-expression of chick (*Gallus gallus*) melanocortin receptors with either chick MRAP1 or MRAP2 in CHO cells on sensitivity to ACTH (1-24) or ACTH (1-13) NH_2: Implications for the avian HPA axis and avian melanocortin circuits in the hypothalamus. Gen Comp Endocrinol 256, 50-56.

Trotta, M.C., Maisto, R., Alessio, N., Hermenean, A., D'Amico, M., Di Filippo, C., 2018. The melanocortin MC5R as a new target for treatment of high glucose-induced hypertrophy of the cardiac H9c2 cells. Frontiers in physiology 9, 1475.

Vaisse, C., Clement, K., Guy-Grand, B., Froguel, P., 1998. A frameshift mutation in human MC4R is associated with a dominant form of obesity. Nat Genet 20, 113-114.

Valen, R., Jordal, A.E., Murashita, K., Rønnestad, I., 2011. Postprandial effects on appetite-related neuropeptide expression in the brain of Atlantic salmon, *Salmo salar*. Gen Comp Endocrinol 171, 359-366.

Valli-Jaakola, K., Suviolahti, E., Schalin‐Jäntti, C., Ripatti, S., Silander, K., Oksanen, L., Salomaa, V., Peltonen, L., Kontula, K., 2008. Further evidence for the role of ENPP1 in obesity: association with morbid obesity in Finns. Obesity 16, 2113-2119.

Valverde, P., Healy, E., Jackson, I., Rees, J.L., Thody, A.J., 1995. Variants of the melanocyte-stimulating hormone receptor gene are associated with red hair and fair skin in humans. Nat Genet 11, 328-330.

Van der Ploeg, L.H., Martin, W.J., Howard, A.D., Nargund, R.P., Austin, C.P., Guan, X., Drisko, J., Cashen, D., Sebhat, I., Patchett, A.A., Figueroa, D.J., DiLella, A.G., Connolly, B.M., Weinberg, D.H., Tan, C.P., Palyha, O.C., Pong, S.S., MacNeil, T., Rosenblum, C., Vongs, A., Tang, R., Yu, H., Sailer, A.W., Fong, T.M., Huang, C., Tota, M.R., Chang, R.S., Stearns, R., Tamvakopoulos, C., Christ, G., Drazen, D.L., Spar, B.D., Nelson, R.J., MacIntyre, D.E., 2002. A role for the melanocortin 4 receptor in sexual function. Proc Natl Acad Sci USA 99, 11381-11386.

Vázquez-Moreno, M., Locia-Morales, D., Valladares-Salgado, A., Sharma, T., Wacher-Rodarte, N., Cruz, M., Meyre, D., 2021. Sex/gender modifies the association between the MC4R p. Ile269Asn mutation and type 2 diabetes in the Mexican population. J Clin Endocrinol Metab 106, e112-e117.

Vollbach, H., Brandt, S., Lahr, G., Denzer, C., Von Schnurbein, J., Debatin, K.M., Wabitsch, M., 2017. Prevalence and phenotypic characterization of MC4R variants in a large pediatric cohort. Int J Obes 41, 13-22.

Vongs, A., Lynn, N.M., Rosenblum, C.I., 2004. Activation of MAP kinase by MC4-R through PI3 kinase. Regul Pept 120, 113-118.

Wan, Y., Zhang, Y., Ji, P., Li, Y., Xu, P., Sun, X., 2012. Molecular characterization of CART, AgRP, and MC4R genes and their expression with fasting and re-feeding in common carp (*Cyprinus carpio)*. Mol Biol Rep 39, 2215-2223.

Wang, M., Chen, Y., Zhu, M., Xu, B., Guo, W., Lyu, Y., Zhang, C., 2019. Pharmacological modulation of melanocortin-4 receptor by melanocortin receptor accessory protein 2 in Nile tilapia. Gen Comp Endocrinol 282, 113219.

Wang, S.X., Fan, Z.C., Tao, Y.X., 2008. Functions of acidic transmembrane residues in human melanocortin-3 receptor binding and activation. Biochem Pharmacol 76, 520-530.

Webb, T.R., Clark, A.J., 2010. Minireview: the melanocortin 2 receptor accessory proteins. Mol Endocrinol 24, 475-484.

Wei, R., Yuan, D., Zhou, C., Wang, T., Lin, F., Chen, H., Wu, H., Xin, Z., Yang, S., Chen, D., Wang, Y., Liu, J., Gao, Y., Li, Z., 2013. Cloning, distribution and effects of fasting status of melanocortin 4 receptor (MC4R) in *Schizothorax prenanti*. Gene 532, 100-107.

Wen, Z., Li, Y., Bian, C., Shi, Q., Li, Y., 2020a. Characterization of two *kcnk3* genes in rabbitfish (*Siganus canaliculatus*): Molecular cloning, distribution patterns and their

potential roles in fatty acids metabolism and osmoregulation. Gen Comp Endocrinol 296, 113546.

Wen, Z.Y., Bian, C., You, X., Zhang, X., Li, J., Zhan, Q., Peng, Y., Li, Y.Y., Shi, Q., 2020b. Characterization of two *kcnk3* genes in Nile tilapia (*Oreochromis niloticus*): Molecular cloning, tissue distribution, and transcriptional changes in various salinity of seawater. Genomics 112, 2213-2222.

Wen, Z.Y., Liang, X.F., He, S., Li, L., Shen, D., Tao, Y.X., 2015. Molecular cloning and tissue expression of uncoupling protein 1, 2 and 3 genes in Chinese perch (*Siniperca chuatsi*). Comp Biochem Physiol Part B Biochem Mol Biol 185, 24-33.

Wen, Z.Y., Qin, C.J., Wang, J., He, Y., Li, H.T., Li, R., Wang, X.D., 2020c. Molecular characterization of two leptin genes and their transcriptional changes in response to fasting and refeeding in Northern snakehead (*Channa argus*). Gene 736, 144420.

Wen, Z.Y., Wang, J., Bian, C., Zhang, X., Li, J., Peng, Y., Zhan, Q., Shi, Q., Li, Y.Y., 2019. Molecular cloning of two *kcnk3* genes from the Northern snakehead (*Channa argus*) for quantification of their transcriptions in response to fasting and refeeding. Gen Comp Endocrinol 281, 49-57.

Wolverton, E.A., Wong, M.K., Davis, P.E., Hoglin, B., Braasch, I., Dores, R.M., 2019. Analyzing the signaling properties of gar (*Lepisosteus oculatus*) melanocortin receptors: Evaluating interactions with MRAP1 and MRAP2. Gen Comp Endocrinol 282, 113215.

Xu, A., Choi, K.L., Wang, Y., Permana, P.A., Xu, L.Y., Bogardus, C., Cooper, G.J., 2002. Identification of novel putative membrane proteins selectively expressed during adipose conversion of 3T3-L1 cells. Biochem Biophys Res Commun 293, 1161-1167.

Xu, J., Bian, C., Chen, K.C., Liu, G.M., Jiang, Y.L., Luo, Q., You, X.X., Peng, W.Z., Li, J.,

Huang, Y., 2017. Draft genome of the Northern snakehead, *Channa argus*. Giga Science 6, gix011.

Xu, Y.H., Guan, X.J., Zhou, R., Gong, R.J., 2020. Melanocortin 5 receptor signaling pathway in health and disease. Cell Mol Life Sci, 1-10.

Yang, L.K., Zhang, Z.R., Wen, H.S., Tao, Y.X., 2019. Characterization of channel catfish (*Ictalurus punctatus*) melanocortin-3 receptor reveals a potential network in regulation of energy homeostasis. Gen Comp Endocrinol 277, 90-103.

Yang, Z., Liang, X.F., Li, G.L., Tao, Y.X., 2020. Biased signaling in fish melanocortin-4 receptors (MC4Rs): Divergent pharmacology of four ligands on spotted scat (*Scatophagus argus*) and grass carp (*Ctenopharyngodon idella*) MC4Rs. Mol Cell Endocrinol, 110929.

Yang, Z., Tao, Y.X., 2016. Biased signaling initiated by agouti-related peptide through human melanocortin-3 and-4 receptors. Biochim Biophys Acta 1862, 1485-1494.

Yeo, G.S.H., Farooqi, I.S., Aminian, S., Halsall, D.J., Stanhope, R.G., O'Rahilly, S., 1998. A frameshift mutation in MC4R associated with dominantly inherited human obesity. Nat Genet 20, 111-112.

Yi, T.L., Yang, L.K., Ruan, G.L., Yang, D.Q., Tao, Y.X., 2018. Melanocortin-4 receptor in swamp eel (*Monopterus albus*): cloning, tissue distribution, and pharmacology. Gene 678, 79-89.

Yu, J., Gimenez, L.E., Hernandez, C.C., Wu, Y., Wein, A.H., Han, G.W., McClary, K., Mittal, S.R., Burdsall, K., Stauch, B., 2020. Determination of the melanocortin-4 receptor structure identifies Ca^{2+} as a cofactor for ligand binding. Science 368, 428-433.

Yun, C.W., Tamaki, H., Nakayama, R., Yamamoto, K., Kumagai, H., 1997. G-protein coupled receptor from yeast *Saccharomyces cerevisiae*. Biochem Biophys Res Commun 240, 287-292.

Zhang, J., Li, X., Zhou, Y., Cui, L., Li, J., Wu, C., Wan, Y., Li, J., Wang, Y., 2017. The

interaction of MC3R and MC4R with MRAP2, ACTH, α-MSH and AgRP in chickens. J Endocrinol 234, 155-174.

Zhang, K.Q., Hou, Z.S., Wen, H.S., Li, Y., Qi, X., Li, W.J., Tao, Y.X., 2019. Melanocortin-4 receptor in spotted sea bass, *Lateolabrax maculatus*: cloning, tissue distribution, physiology, and pharmacology. Front Endocrinol 10, 705.

Zhang, L., Li, W.H., Anthonavage, M., Eisinger, M., 2006. Melanocortin-5 receptor: a marker of human sebocyte differentiation. Peptides 27, 413-420.

Zhang, Y., Wen, H.S., Li, Y., Lyu, L.K., Zhang, Z.X., Wang, X.J., Li, J.S., Tao, Y.X., Qi, X., 2020. Melanocortin-4 receptor regulation of reproductive function in black rockfish (*Sebastes schlegelii*). Gene 741, 144541.

Zhu, M., Wang, M., Chen, Y.J., Zhang, C., 2019a. Pharmacological modulation of two melanocortin-5 receptors by MRAP2 proteins in zebrafish. J Mol Endocrinol 62, 27-36.

Zhu, M., Xu, B., Wang, M., Liu, S., Zhang, Y., Zhang, C., 2019b. Pharmacological modulation of MRAP2 protein on melanocortin receptors in the sea lamprey. Endocrine connections 8, 378-388.